

Cover Page



Universiteit Leiden



The handle <http://hdl.handle.net/1887/33100> holds various files of this Leiden University dissertation

Author: Dane, Martijn

Title: Structure and function of the endothelial glycocalyx in the microcirculation

Issue Date: 2015-06-02

Structure and Function of the Endothelial Glycocalyx in the Microcirculation

Martijn Dane

Structure and Function of the Endothelial Glycocalyx in the Microcirculation
Martijn Jacob Cornelis Dane, 2015

All rights are reserved. No part of this publication may be reproduced, stored, or transmitted in any form or by any means, without permission of the copyright owners.

ISBN: 978-94-6295-163-1
Cover: Martijn Dane
Layout: Martijn Dane
Printed by: Proefschriftmaken.nl || Uitgeverij BOXpress
Published by: Uitgeverij BOXpress, 's Hertogenbosch

The research presented in this thesis was performed at the department of Nephrology of the Leiden University Medical Center.

The research described in this thesis was supported by a grant from the Dutch Kidney Foundation (C08.2265). Financial support by the Dutch Kidney Foundation and the Dutch Heart Foundation for the publication of this thesis is gratefully acknowledged.

Publication of this thesis was further supported by Roche Nederland B.V., Sysmex Nederland B.V., ChipSoft and Greiner Bio-One.

Structure and Function of the Endothelial Glycocalyx in the Microcirculation

Proefschrift

ter verkrijging van
de graad van Doctor aan de Universiteit Leiden,
op gezag van Rector Magnificus prof. mr. C.J.J.M. Stolker,
volgens besluit van het College voor Promoties
te verdedigen op dinsdag 2 juni 2015
klokke 16.15 uur

door

Martijn Jacob Cornelis Dane

geboren te Roosendaal
in 1986

Promotiecommissie

Promotor: Prof. Dr. A.J. Rabelink

Co-promotores: Dr. B.M. van den Berg

Dr. H Vink

Overige leden: Prof. Dr. V.W.M. van Hinsbergh
*VU University Medical Centre,
Amsterdam, The Netherlands*

Dr. J. van der Vlag
*Radboud University Nijmegen Medical Centre,
Nijmegen, the Netherlands*

Prof. Dr. P. Reitsma

Prof. Dr. J.W. Jukema

Prof. Dr. ir. A.J. Koster

Contents

Chapter 1	General Introduction	7
Chapter 2	A microscopic view on the renal endothelial glycocalyx <i>Adapted from: Am J Physiol Renal Physiol 00532 02014, 2015</i>	29
Chapter 3	Prolonged shear stress modifies the composition of the endothelial glycocalyx <i>In preparation</i>	49
Chapter 4	Glomerular endothelial surface layer acts as a barrier against albumin filtration <i>Am J Pathol 182: 1532-1540, 2013</i>	69
Chapter 5	Association of kidney function with changes in the endothelial surface layer <i>CJASN 9: 698-704, 2014</i>	95
Chapter 6	Deeper penetration of erythrocytes into the endothelial glycocalyx is associated with impaired microvascular perfusion <i>PloS One 9: e96477,2014</i>	117
Chapter 7	General discussion and summary	137
Chapter 8	Nederlandse samenvatting Curriculum Vitae List of publications Dankwoord	151

1

Introduction and outline

*Published as part of:
Am J Physiol Renal Physiol ajprenal 00532 02014, 2015.*

Martijn J.C. Dane¹, Bernard M. van den Berg¹, Dae Hyun Lee¹, Margien G.S. Boels¹, Gesa L. Tiemeier¹, M. Cristina Avramut², Anton Jan van Zonneveld¹, Johan van der Vlag³, Hans Vink⁴, Ton J. Rabelink¹

¹*Department of Nephrology, Einthoven laboratory for Vascular Medicine, LUMC, Leiden University Medical Center, The Netherlands* ²*Department of Molecular Cell Biology, Section Electron Microscopy LUMC, Leiden University Medical Center, The Netherlands* ³*Department of Nephrology, Radboud Institute for Molecular Life Sciences, Radboud University Medical Center, Nijmegen, the Netherlands* ⁴*Department of Physiology, Maastricht University Medical Center, Maastricht, the Netherlands*

The endothelial glycocalyx

The endothelial glycocalyx or endothelial surface layer (EG), is a negatively charged gel-like surface structure of proteoglycans with their covalently bound polysaccharide chains called glycosaminoglycans (GAGs), glycoproteins and glycolipids. Its main carbohydrate constituents are heparan sulfate (HS), chondroitin sulfate (CS) and hyaluronan (HA). The endothelial glycocalyx governs transcapillary fluid exchange and acts as biomechanical sensor to confer shear to the endothelium (EC) [1-3]. Glycosaminoglycans within the glycocalyx function as a molecular scaffold that facilitates protein binding in a very selective manner. In this way, circulating proteins, such as growth factors and chemokines are concentrated and spatially organized in gradients at the endothelial surface [4,5]. The proteins that bind to the glycocalyx include proteins involved in cell attachment, migration, differentiation, morphogenesis, blood coagulation, lipid metabolism, and inflammation, thus putting the endothelial surface layer at the very center of the pathophysiology of cardiovascular and renal disease (**figure 1**). However, despite its pivotal role in endothelial cell biology, glycocalyx function has proven to be hard to study due to its complex carbohydrate chemistry and the difficulties in interrogating its function in vivo and in vitro. Here we will describe the structure and main biological functions of the endothelial glycocalyx in the kidney and an give an outline of this thesis.

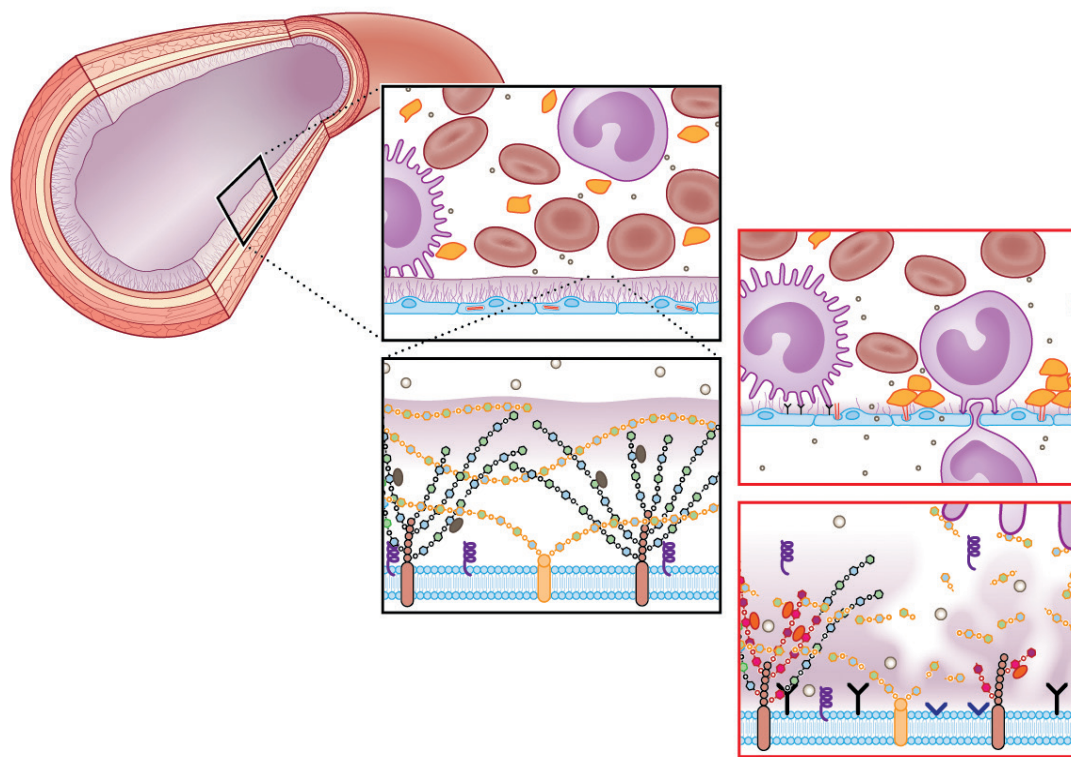


Figure 1: Schematic overview of the endothelial glycocalyx in a healthy and diseased condition.
 Left: In a physiological state, the endothelial glycocalyx protects against protein leakage, inflammation and coagulation. Heparan sulfates, bound to a heparan sulfate core protein, and hyaluronan, bound to e.g. CD44, are the main constituents of the endothelial glycocalyx (EG). Order and modification of disaccharide repeats within HS determine the binding site for specific proteins.
 Right: Upon endothelial activation, heparan sulfate disaccharide modification occurs, resulting in a change in protein binding sites. During a chronic disease condition, the EG gets damaged, mainly due to up regulation of degrading enzymes such as hyaluronidase, heparanase and proteinases. Both HS modification and EG degradation result in inflammation, coagulation and protein leakage.

Biochemical structure of the endothelial glycocalyx

The membrane bound part of the endothelial glycocalyx consists of proteoglycans, glycosaminoglycans, glycoproteins and glycolipids. Proteoglycans with their bound GAGs are the main contributors to the EG structure and function[6]. Of these GAGs, heparan sulfate and hyaluronan constitute up to 90% [7-9].

Heparan sulfate is a linear polysaccharide which consists of the repeating disaccharide β 1-4-linked D-glucuronic acid (GlcA) and α 1-4-linked N-acetyl-D-glucosamine (GlcNAc). This polymer is covalently attached to a limited number of core proteins at cell surface, called heparan sulfate proteoglycans (HSPGs). The proteoglycans found on the luminal endothelial side are syndecans 1 and 4, glypican 1, versican and thrombomodulin. HS chains are processed in the Golgi apparatus where they undergo a series of modifications in which subsets of glucosamine residues can become N-deacetylated and N-sulfated and where glucuronic acids may undergo epimerization to L-iduronic acid (IdoA). In particular, C2 of uronic acid and C6 (and rarely C3) of glucosamine residues may become sulfated [10]. After intracellular processing, further extracellular modification can occur. Heparanase (HPSE1) and endosulfatases (SULF1,2) can cleave the HS chain or further modify the sulfate groups within HS, respectively [11]. **(figure 2)** Although they do attribute to a wide variety of specific HS binding sites for protein interactions that determine endothelial cell biology, regulation of these modifications is still not well understood. While the core proteins can function independently of the HS chains they carry, the HS chains predominantly dictate ligand-binding capability and therefore the biological roles of HSPG. Some examples are discussed in the next section. HS is structurally related to heparin, a highly sulfated GAG [10-12].

Hyaluronan lacks the complex chemical editing of HS. It is a nonsulfated glycosaminoglycan composed of repeating polymeric disaccharides D-glucuronic acid and N-acetyl-D-glucosamine linked by a glucuronidic bond [2,3]. Under physiologic conditions, hyaluronan is synthesized by membrane bound synthases (HAS1, 2 and 3) as a macromolecule of 105–107 Da. Following its synthesis, hyaluronan is directed to the cell surface where it interacts with hyaluronan binding surface proteins (hyaladherins) such as CD44, or is assembled into the pericellular extracellular matrix [1]. The repeating nature of the polysaccharide and hence its protein binding sites, has been suggested to confer structural periodicity to the endothelial surface layer [13]. The main modifiers of hyaluronan are hyaluronidases, enzymes that cleave high molecular weight (HMW) hyaluronan chains into smaller low molecular weight hyaluronan fragments.

Function of the endothelial glycocalyx

Biomechanical properties

The endothelial glycocalyx is believed to be the primary molecular sieve for plasma proteins and, therefore, the origin of the oncotic forces that control transcapillary fluid exchange. This has led to a revised Starling principle in which the capillary filtration equilibrium is generated over the glycocalyx, rather than across the entire endothelial layer as had been widely assumed [14]. Within the glycocalyx, hyaluronan is a key determinant of many biomechanical and hydrodynamic properties such as its function in fluid exchange and shear sensing properties [15-19]. In particular, its physical properties in solution contribute to the function of hyaluronan [2,20,21]. Even small amounts of hyaluronan can bind large amounts of water molecules, forming a gel-like structure. Small molecules like water, electrolytes and nutrients can freely diffuse through the solvent. In contrast, large molecules, such as proteins, are excluded because of their hydrodynamic sizes in solution. In this way, hyaluronan contributes to the barrier function of the endothelial glycocalyx. The negative charge of the sulfated heparan groups in HS chains further adds to the barrier function of the glycocalyx, by repelling negatively charged circulating proteins like albumin.

An intact glycocalyx also serves as the primary sensor of shear stress on ECs. Hydrodynamic drag arising from flowing plasma through this layer transmits fluid shear stress through the thin sub-layer where proteoglycans, glycoproteins and glycolipids are directly linked to the endothelial cytoskeleton [22]. Both, the presence of hyaluronan, possibly by linking to the epithelial sodium channel (ENaC) in the endothelium, and HS appear to be critical for this function [23]. For example, enzymatic removal of hyaluronan or HS from the glycocalyx results in reduced nitric oxide (NO) release during shear [17]. Heparinase III, a bacterial enzyme that cleaves HS proteoglycans, has a dramatic effect on the ECs' ability to produce NO to shear stress and transfer shear forces to the actin cytoskeleton [8,24]. Interestingly, the enzyme chondroitinase, employed to selectively degrade CS, did not affect shear-induced NO production, underpinning the importance of HS for the biomechanical properties of the endothelial glycocalyx [25].

Inflammation

The gel-like anti-adhesive properties of the endothelial glycocalyx preclude direct leukocyte interaction with adhesion molecules on the endothelial surface. However, during their passage through the capillaries the leukocytes will compress the endothelial glycocalyx thus allowing for engagement of the microvilli of the leukocyte with the GAGs in the glycocalyx. For example, HS on the endothelium acts as a direct ligand for L-selectin [26,27]. Interestingly, this interaction is modulated by very specific HS sulfation patterning. Endothelial deletion of the biosynthetic enzyme, N-acetylglucosamine N-deacetylase-N-sulfotransferase-1 (NDST1) which leads to decreased sulfation of the HS chains in the endothelium, reduces the binding of L-selectin, and leads to an increase in neutrophil rolling velocity [28]. Inflammatory stimuli, such as TNF- α , induce



NDST1 which results in expression of HS domains on glomerular endothelium that are associated with inflammation [29,30]. In agreement, we recently showed that endothelial deletion of NDST1 results in reduced leukocyte extravasation in experimental anti-GBM glomerulonephritis [30].

The migration of leukocytes across the endothelium occurs along chemoattractant gradients composed of chemokines that have bound to the endothelium [5]. Nearly all members of the chemokine family bind to HS by way of a positively charged C-terminal domain. Again, this binding may be modified by chemical editing of HS chains. For example, changing the domain structure of HS by inactivation of HS2ST (which causes a compensatory increase in glucosamine N-sulfation and 6-O-sulfation) results in enhanced binding of IL-8 to the endothelium and increases inflammation [31].

Endothelial HS has also been shown to be critical for the function of the complement system. The function of many of the components of the complement system, including C1, C1q, C1 inhibitor, C2, C4, C4b, FactorB, FactorD, FactorH, Properdin, and complement receptors CR3(CD11b/CD18) (24) and CR4 (CD11c/CD18) is dependent upon binding to specific glycosaminoglycan domains [32-34]. The clinical importance and the specificity of these interactions are illustrated by patients with mutations in the short consensus repeats 19 and 20 of the complement inhibitor, factor H. These mutations result in impaired binding of factor H to the glomerular endothelium, but not to other endothelial beds. Upon a trigger that activates the complement system this may result in glomerular endothelial injury and presents itself clinically as atypical hemolytic uremic syndrome [35].

In addition to HS, hyaluronan has also been demonstrated to modulate inflammatory processes. The HMW form of hyaluronan possesses anti-inflammatory, anti-angiogenic, and immunosuppressive properties and protects cells from injury, and leukocyte adhesion [36]. In part this is related to its gel-like physical properties. In addition, binding of tumor necrosis factor (TNF)-stimulated gene 6 (TSG-6) to hyaluronan inhibits chemokine-stimulated trans-endothelial migration of neutrophils via a direct interaction between TSG-6 and the glycosaminoglycan-binding site of CXCL8 [37]. However, during tissue injury and inflammatory processes hyaluronan can become depolymerized through oxidative stress and enzymatic cleavage by hyaluronidases. This results in the formation of low molecular weight (LMW) hyaluronan fragments [38]. Removal of LMW hyaluronan from sites of injury is dependent on their interaction with CD44, and the associated downstream signaling events have been implicated in cell proliferation, migration and activation. LMW hyaluronan also has been demonstrated to interact with Toll-like receptors enabling hyaluronan signaling in inflammatory cells [38,39].

Anticoagulation

Both the biomechanical properties as well as glycocalyx-protein interactions play a prominent role in preventing the blood from clotting. The gel-like properties of the glycocalyx prevent platelets from accessing the endothelium [40]. HS in the glycocalyx is required to activate antithrombin, a serine protease that inhibits thrombin and thus the conversion of fibrinogen to fibrin. By acting as a scaffold and simultaneously binding to both enzyme and substrate, HS greatly increases engagement of thrombin with antithrombin [41,42]. This interaction depends upon a specific pentasaccharide, an insight that led to the clinical development of fondaparinux. By binding the plasma protein Heparin cofactor II (HCII), heparan sulfate repeats in the glycocalyx further inhibit the pro-coagulant activity of thrombin. The latter pathway has been shown to counteract thrombus formation in the presence of endothelial injury [43].

A key regulator of the natural anticoagulant system is the endothelial glycocalyx protein thrombomodulin. Upon binding of thrombin it generates activated protein C (APC). APC regulates blood coagulation by cleaving and inhibiting two cofactors, activated factor V (FVa) and activated factor VIII (FVIIIa), which serve as phospholipid- membrane-bound cofactors to factor Xa (FXa) and factor IXa (FIXa), respectively. APC not only has anticoagulant properties, but also through PAR signaling induces a quiescent phenotype in the endothelium [44,45]. Activation of this pathway could prevent the development of diabetic nephropathy, underscoring the importance of APC formation in prevention of kidney disease [45]. Finally, thrombomodulin-thrombin binding activates thrombin-activatable fibrinolysis inhibitor (TAFI) thus suppressing fibrinolysis at the same time. This system is intensively modulated by interactions with glycosaminoglycans. First, thrombomodulin can bind chondroitin sulfate, greatly facilitating the interaction with thrombin and the formation of APC [46,47]. The activity of APC and thrombin in their turn are negatively regulated by protein C inhibitor which form together with different HS repeats ternary complexes [48]. While very complex and still only partially understood the intricate interaction of the coagulation system with the glycocalyx demonstrates the importance of the latter as a molecular scaffold.



Risk factors for endothelial glycocalyx degradation

The EG has a vulnerable location between the endothelium and flowing blood which might contain circulating risk factors such as glucose, lipids and inflammatory intermediates. In patients, acute hyperglycemia is associated with perturbation of EG and vascular permeability [49]. In diabetes mellitus type 1 (DM1) patients, increased levels of circulating hyaluronidase were observed [50]. In vitro, both an upregulation of the EG degrading enzyme heparanase [51] and a marked reduction in the biosynthesis of GAGs was observed upon high glucose stimuli in glomerular endothelial cells (GEnCs) [52]. An association between plasma LDL cholesterol levels, reduced expression of endothelial GAGs and increased wall thickness at carotid lesion-prone sites was observed in previous studies, suggesting glycocalyx damage during hyperlipidemia [53,54]. These data concur with a study that demonstrates partial restoration of endothelial glycocalyx volume upon normalization of LDL levels [55]. Another type of risk factors affecting the endothelial glycocalyx are inflammatory mediators. For example, TNF α increases permeation of macromolecules into the ESL in hamsters and also LPS administration results in an induced dysfunction of the microcirculation accompanied by glycocalyx degradation [56]. Also, TNF α stimulation has been demonstrated to change expression of HS modifying enzymes and increase inflammatory epitopes within GEnC HS [29]. Endothelial damage upon stimulation with risk factors can occur both directly, such as by oxygen radicals produced during cellular stress that alter the composition of the EG [57-59], as well as indirectly through chronic stimulation resulting in changes in production and modification of GAGs by changing the expression of the involved synthesizing- and or degrading enzymes such as hyaluronidase and heparanase [50,58].

Current treatment options to stabilize the endothelial glycocalyx

The proposed role of the EG as target for cardiovascular risk factors implies that the EG could be an interesting target for therapies against the development of vasculature-born pathologies. First of all, as endothelial dysfunction seems to be closely associated with endothelial glycocalyx loss, current medication based on improving vascular or endothelial function will most likely also affect the endothelial glycocalyx. Stabilizing the endothelium, for example with angiotensin II receptor antagonist (AngII), has been shown to enhance glycocalyx thickness in frog mesenteric cells and increase GAG production in human microvascular endothelium [60].

In contrast to these indirect effects, several options have been proposed to directly influence endothelial glycocalyx. This is done by GAG supplementation. One of the most well studied glycosaminoglycan supplements is sulodexide; a highly purified mixture of low molecular weight heparin (80%) and dermatan sulfate (20%). Although its function has been prescribed to different mechanisms over the past years, its anti-albuminuric effect has been demonstrated in several studies [61-63]. For example, in male participants with type 2 diabetes (T2D), sulodexide administration led to an increase in systemic glycocalyx thickness. It showed a reduction in plasma hyaluronidase, as well as a trend towards the normalization of systemic albumin clearance [64]. Although a recent study showed that sulodexide failed to demonstrate renoprotection in overt type 2 diabetic nephropathy patients [65], this can most likely be explained by the progression of type 2 diabetes. Restoring the EG has the most significant effects during the early stages of the disease, before irreversible morphological changes within the kidney occur. Indeed, animal studies showed that sulodexide ameliorates only early disease in models of radiation nephropathy and diabetic nephropathy in rats [66]. Nonetheless, the disadvantage of sulodexide is the heterogeneity of the composition, which might also explain the diversity in study results.

To solve this heterogeneity problem, a purified glycosaminoglycan should be produced. This targeting of specific heparan sulfate modification patterns seems to be a promising upcoming field. Several oligosaccharides and single chain antibodies directed against specific oligosaccharide compositions are being screened for their potential to block the HS moieties that initiate inflammation and angiogenesis on the endothelial surface [67-70]. The other way around, small peptides that resemble the HS binding region within a specific protein, might be developed to block the HS binding site. Furthermore, since increased amounts of heparanase and hyaluronidase are associated with a high variety of diseases, inhibiting such glycocalyx degrading enzymes might be interesting for future studies [71].

The endothelial glycocalyx in the glomerular filtration barrier

The kidney

In addition to the general composition and function of the endothelial glycocalyx in the vasculature, we studied the role of the endothelial glycocalyx in renal filtration. The human kidney contains approximately $0.8-1.5 \times 10^6$ nephrons, which are the functional units of the kidney. The normal glomerular filtration rate ranges from 130-180 liters per day [72]. Circulating blood enters the glomerulus via the afferent arterioles. In the glomerulus ultrafiltration takes place (**figure 3**). Here, water and small solutes, like salts, can pass through the glomerular filtration barrier, while larger molecular like proteins and cells are retained within the circulation.

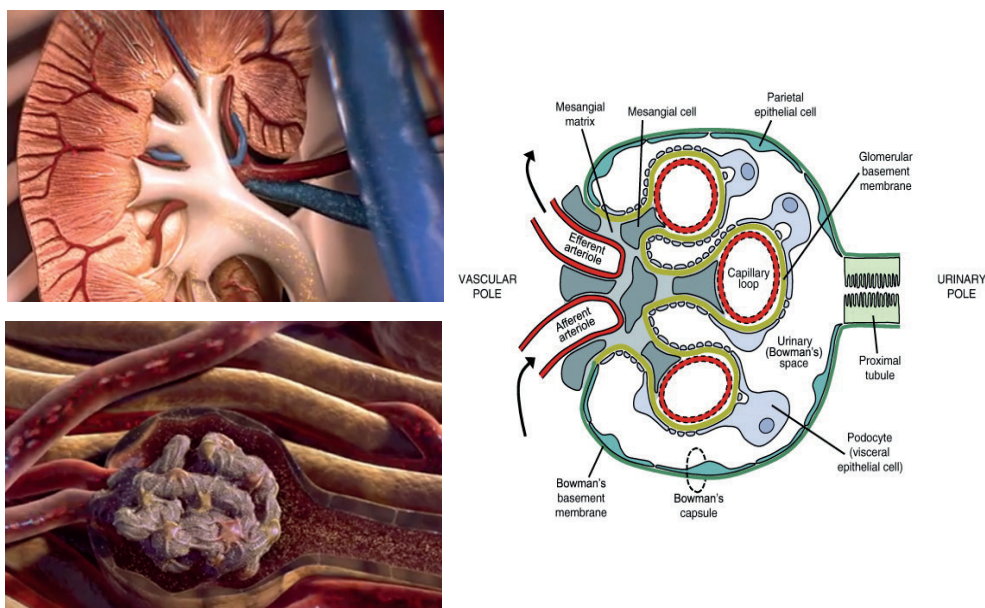


Figure 3: Structure and function of the kidney and glomerulus. One of the main functions of the kidney is glomerular filtration. Blood enters the kidney (top left) and flows through the afferent artery into the glomerulus (bottom left). Here the blood is filtered: fluid containing small solutes passes the filtration barrier, while bigger components, such as proteins are maintained within the vasculature. The glomerular stalk (right) consists of mesangial cells, endothelial cells, glomerular basement membrane and podocytes. The combination of these cells is necessary to maintain the structure and function of the glomerulus. The filtration barrier, better shown in figure 4, is responsible for the filtration within the glomerulus. The bowman's space, where the filtrate is collected, is lined by parietal epithelial cells. From here, the filtrate goes through the tubuli, where reabsorption of essential components such as glucose and sodium takes place.

Barrier function in the glomerulus

Although still under some debate [73], most evidence points towards the glomerular filtration barrier (GFB) as the main site of filtration. Farquhar demonstrated, using electron microscopy, that in intact glomeruli only about 0.06% of plasma albumin gets filtrated [74,75]. Although tubular reabsorption may play a role in fine-tuning the leakage of albumin, the GFB is assumed to play the key role in filtration. This filtration function of the GFB is maintained by the three layers of the filtration barrier: endothelium, glomerular basement membrane (GBM) and podocytes. Together with the mesangium, these components form the glomerulus: a unique non-clogging filter that can endure the filtration for over a lifetime. Although all layers and its specific roles within the GFB are often studied separately, it should always be taken into account that all these layers depend on each other's structure and function to form this highly specialized glomerular filtration barrier. For example, disturbed VEGF signaling from the podocytes affects endothelial health [76], and perturbed PDGF signaling from the endothelium affects the mesangium [77].

Until recently, it was reasoned that the endothelial layer could not contribute to the filtration barrier because of its large fenestrae. These fenestrae lack a diaphragm and can therefore be considered as holes of about 60-80 nanometer [78]. These holes support the passage of high volumes of water, but are also large enough to allow proteins like albumin to pass the endothelial layer. Consequently, most studies focused on the GBM and podocytes as main components of the filtration barrier. However, recently Weil et al. showed that changes in the endothelial layer were associated with glomerular filtration rate and albumin-creatinine ratio in T2D patients [79,80].

A role for the endothelium in the filtration barrier is further supported by the little variation in reflection coefficient between fenestrated and continuous capillary beds [81,82]. Ryan et al. demonstrated that under physiological conditions hardly any albumin is observed in the GBM or underlying podocytes [83]. This can be explained by the observation that endothelial fenestrae are filled with endothelial glycocalyx [84,85]. Consequently, the endothelial glycocalyx within the fenestrae was proposed to be the first barrier within the GFB that excludes proteins [86]. Glycosaminoglycan-degrading enzymes such as chondroitinase and heparinase have been shown to alter the charge selectivity of the glomerular filter [87,88]. In addition, even local displacement of only the non-covalently bound components of the renal glycocalyx has been demonstrated to result in a 12-fold increase in fractional albumin clearance [89]. This indicates that besides GAGs, the loosely bound plasma proteins are also essential for the structure of the endothelial glycocalyx and for the barrier function of the glomerulus.

Although these data clearly indicate a role for the endothelial glycocalyx as filtration barrier, the exact mechanism is yet unknown. It has been postulated that glycocalyx polyanions such as heparan sulfate and sialated proteins on the surface of the endothelium and podocytes, as well as in the glomerular basement membrane would electrically repel



the negatively charged albumin [90,91]. Although this is supported by data with non-metabolizable negatively charged probes that would support that electric charge would modify filtration of albumin [92,93], this concept has been challenged by *in vivo* studies of the fractional clearance of negatively charged Ficoll as compared with Ficoll where negative charge selectivity did not exist [94,95].

Irrespective of the debate about charge exclusion, it is very plausible that the glycocalyx acts as a size barrier to albumin filtration. The glycocalyx basically functions as a hydrogel where glycosaminoglycans, i.e. heparan-, chondroitin sulfate and hyaluronan, constitute a fiber mesh with pores [20,96,97]. Plasma proteins bind multivalent to these glycosaminoglycans, thus creating steric hindrance to protein filtration. This barrier function will be further modified by the fluid drag through the glycocalyx which allows for dynamic equilibrium with glycocalyx-bound and free circulating proteins [98]. Such a size barrier function of the endothelial glycocalyx has in fact also been suggested from observations in the microcirculation in general, where the hydrostatic and osmotic forces that determine fluid filtration were shown to exist only across the glycocalyx and not across the endothelial cell towards the interstitium [99]. It is of interest that elongated molecules, such as bikunin and hyaluronan have >100-fold higher glomerular sieving coefficients than albumin, despite similar molecular weights and charges [100]. While such experiments may be challenged by confounding factors due to metabolism of albumin by the proximal tubulus [101], they can also be interpreted to demonstrate the importance of pore characteristics in relationship to the molecular conformation of the protein sieved. The latter is further supported by recent observations that large straight nanotubes (200-300 nm) may be filtered by the glomerulus similarly to small molecules [102].

Scope of this thesis

In the introduction we described a role for the EG in the onset of development in several vasculature-related pathologies like cardiovascular a disease, diabetes, but also renal failure. In this thesis the structure and function of the EG and its components in the vasculature in general and in the glomerular capillaries have been studied. In addition, methods to determine changes in the EG and the relation with known vascular damage markers in healthy and diseased subjects have been newly developed.

In **Chapter 2**, we mainly focus on the challenges in visualization and quantification of the endothelial glycocalyx. Here, the different methods to study ESL thickness and composition, both in vitro and in vivo, are discussed.

Because it has been demonstrated that EG is absent in vitro, we hypothesized that mimicking the in vivo situation by subjecting the cells to prolonged shear stress would change the endothelial glycocalyx dimensions and composition. This will be further discussed in **chapter 3**.

The EG contributes to the permeability function of the endothelium throughout the whole vasculature. In the fenestrated endothelium of the kidney, the EG is also present within the fenestrae, suggesting a role for the EG in glomerular filtration. The main EG component that contributes to endothelial permeability has been proposed to be HA. In **chapter 4** we studied the role of the EG, and specifically HA, in the filtration barrier. Therefore, we systemically removed HA with hyaluronidase and examined the effects on the function of the filtration barrier.

In **chapter 5**, we used a novel method to measure changes in the EG in end stage renal disease patients. Using SDF imaging of the sublingual microvasculature, we looked into variations in the width of the RBC column as a measure for changes in the EG. In addition, we looked into endothelial activation and glycocalyx shedding to determine the association between renal function, endothelial dysfunction and glycocalyx shedding. Finally we studied the ability of the EG to recover after successful kidney transplantation.

In **chapter 6** we studied the EG in a cohort of healthy but obese participants. Here we demonstrated the relation between microvascular perfusion and EG thickness. Furthermore, these participants have a higher risk for the development of cardiovascular disease. Therefore this study functions as baseline measurement for future follow-up studies. Consequently the question whether early changes in EG predict cardiovascular events will be studied.

Finally, in **chapter 7** this thesis is summarized and the relevance of these results in combination with the current knowledge in literature is discussed. Furthermore, some future perspectives are proposed.



References

1. Lennon FE, Singleton PA (2011) Hyaluronan regulation of vascular integrity. *Am J Cardiovasc Dis* 1: 200-213.
2. Laurent TC, Fraser JR (1992) Hyaluronan. *FASEB J* 6: 2397-2404.
3. Laurent T (1989) The biology of hyaluronan. Introduction. *Ciba Found Symp* 143: 1-20.
4. Rops AL, van der Vlag J, Lensen JF, Wijnhoven TJ, van den Heuvel LP, et al. (2004) Heparan sulfate proteoglycans in glomerular inflammation. *Kidney Int* 65: 768-785.
5. Massena S, Christoffersson G, Hjertstrom E, Zcharia E, Vlodavsky I, et al. (2010) A chemotactic gradient sequestered on endothelial heparan sulfate induces directional intraluminal crawling of neutrophils. *Blood* 116: 1924-1931.
6. Reitsma S, Slaaf DW, Vink H, van Zandvoort MA, oude Egbrink MG (2007) The endothelial glycocalyx: composition, functions, and visualization. *Pflugers Arch* 454: 345-359.
7. Oohira A, Wight TN, Bornstein P (1983) Sulfated proteoglycans synthesized by vascular endothelial cells in culture. *J Biol Chem* 258: 2014-2021.
8. Florian JA, Kosky JR, Ainslie K, Pang Z, Dull RO, et al. (2003) Heparan sulfate proteoglycan is a mechanosensor on endothelial cells. *Circ Res* 93: e136-142.
9. Rix DA, Douglas MS, Talbot D, Dark JH, Kirby JA (1996) Role of glycosaminoglycans (GAGs) in regulation of the immunogenicity of human vascular endothelial cells. *Clin Exp Immunol* 104:60-65.
10. Esko JD, Lindahl U (2001) Molecular diversity of heparan sulfate. *J Clin Invest* 108: 169-173.
11. Esko JD, Selleck SB (2002) Order out of chaos: assembly of ligand binding sites in heparan sulfate. *Annu Rev Biochem* 71: 435-471.
12. Casu B, Lindahl U (2001) Structure and biological interactions of heparin and heparan sulfate. *Adv Carbohydr Chem Biochem* 57: 159-206.
13. Day AJ, Sheehan JK (2001) Hyaluronan: polysaccharide chaos to protein organisation. *Curr Opin Struct Biol* 11: 617-622.
14. Levick JR, Michel CC (2010) Microvascular fluid exchange and the revised Starling principle. *Cardiovasc Res* 87: 198-210.
15. van den Berg BM, Vink H, Spaan JA (2003) The endothelial glycocalyx protects against myocardial edema. *Circ Res* 92: 592-594.
16. van den Berg BM, Spaan JA, Vink H (2009) Impaired glycocalyx barrier properties contribute to enhanced intimal low-density lipoprotein accumulation at the carotid artery bifurcation in mice. *Pflugers Arch* 457: 1199-1206.
17. Mochizuki S, Vink H, Hiramatsu O, Kajita T, Shigeto F, et al. (2003) Role of hyaluronic acid glycosaminoglycans in shear-induced endothelium-derived nitric oxide release. *Am J Physiol Heart Circ Physiol* 285: H722-726.
18. Henderson-Toth CE, Jahnsen ED, Jamarani R, Al-Roubaie S, Jones EA (2012) The glycocalyx is present as soon as blood flow is initiated and is required for normal vascular development. *Dev Biol* 369: 330-339.

19. Nagy N, Freudenberger T, Melchior-Becker A, Rock K, Ter Braak M, et al. (2010) Inhibition of hyaluronan synthesis accelerates murine atherosclerosis: novel insights into the role of hyaluronan synthesis. *Circulation* 122: 2313-2322.
20. Laurent TC, Laurent UB, Fraser JR (1995) Functions of hyaluronan. *Ann Rheum Dis* 54: 429-432.
21. Laurent TC, Laurent UB, Fraser JR (1996) The structure and function of hyaluronan: An overview. *Immunol Cell Biol* 74: A1-7.
22. Weinbaum S, Tarbell JM, Damiano ER (2007) The structure and function of the endothelial glycocalyx layer. *Annu Rev Biomed Eng* 9: 121-167.
23. Ramiro-Diaz J, Barajas-Espinosa A, Chi-Ahumada E, Perez-Aguilar S, Torres-Tirado D, et al. (2010) Luminal endothelial lectins with affinity for N-acetylglucosamine determine flow-induced cardiac and vascular paracrine-dependent responses. *Am J Physiol Heart Circ Physiol* 299: H743-751.
24. Thi MM, Tarbell JM, Weinbaum S, Spray DC (2004) The role of the glycocalyx in reorganization of the actin cytoskeleton under fluid shear stress: a “bumper-car” model. *Proc Natl Acad Sci U S A* 101: 16483-16488.
25. Pahakis MY, Kosky JR, Dull RO, Tarbell JM (2007) The role of endothelial glycocalyx components in mechanotransduction of fluid shear stress. *Biochem Biophys Res Commun* 355: 228-233.
26. Norgard-Sumnicht K, Varki A (1995) Endothelial heparan sulfate proteoglycans that bind to L-selectin have glucosamine residues with unsubstituted amino groups. *J Biol Chem* 270: 12012-12024.
27. Norgard-Sumnicht KE, Varki NM, Varki A (1993) Calcium-dependent heparin-like ligands for L-selectin in nonlymphoid endothelial cells. *Science* 261: 480-483.
28. Wang L, Fuster M, Sriramarao P, Esko JD (2005) Endothelial heparan sulfate deficiency impairs L-selectin- and chemokine-mediated neutrophil trafficking during inflammatory responses. *Nat Immunol* 6: 902-910.
29. Rops AL, van den Hoven MJ, Baselmans MM, Lensen JF, Wijnhoven TJ, et al. (2008) Heparan sulfate domains on cultured activated glomerular endothelial cells mediate leukocyte trafficking. *Kidney Int* 73: 52-62.
30. Rops AL, Loeven MA, van Gemst JJ, Eversen I, Van Wijk XM, et al. (2014) Modulation of heparan sulfate in the glomerular endothelial glycocalyx decreases leukocyte influx during experimental glomerulonephritis. *Kidney Int* 86: 932-942
31. Axelsson J, Xu D, Kang BN, Nussbacher JK, Handel TM, et al. (2012) Inactivation of heparan sulfate 2-O-sulfotransferase accentuates neutrophil infiltration during acute inflammation in mice. *Blood* 120: 1742-1751.
32. Wuillemin WA, te Velthuis H, Lubbers YT, de Ruig CP, Eldering E, et al. (1997) Potentiation of C1 inhibitor by glycosaminoglycans: dextran sulfate species are effective inhibitors of in vitro complement activation in plasma. *J Immunol* 159: 1953-1960.
33. Sahu A, Pangburn MK (1993) Identification of multiple sites of interaction between heparin and the complement system. *Mol Immunol* 30: 679-684.



34. Presanis JS, Hajela K, Ambrus G, Gal P, Sim RB (2004) Differential substrate and inhibitor profiles for human MASP-1 and MASP-2. *Mol Immunol* 40: 921-929.
35. Boels MG, Lee DH, van den Berg BM, Dane MJ, van der Vlag J, et al. (2013) The endothelial glycocalyx as a potential modifier of the hemolytic uremic syndrome. *Eur J Intern Med* 24: 503-509.
36. Yung S, Thomas GJ, Davies M (2000) Induction of hyaluronan metabolism after mechanical injury of human peritoneal mesothelial cells in vitro. *Kidney Int* 58: 1953-1962.
37. Dyer DP, Thomson JM, Hermant A, Jowitt TA, Handel TM, et al. (2014) TSG-6 Inhibits Neutrophil Migration via Direct Interaction with the Chemokine CXCL8. *J Immunol* 192: 2177-2185.
38. Jiang D, Liang J, Noble PW (2011) Hyaluronan as an immune regulator in human diseases. *Physiol Rev* 91: 221-264.
39. Kim MY, Muto J, Gallo RL (2013) Hyaluronic acid oligosaccharides suppress TLR3-dependent cytokine expression in a TLR4-dependent manner. *PLoS One* 8: e72421.
40. Reitsma S, Oude Egbrink MG, Heijnen VV, Megens RT, Engels W, et al. (2011) Endothelial glycocalyx thickness and platelet-vessel wall interactions during atherogenesis. *Thromb Haemost* 106: 939-946.
41. Olson ST, Bjork I (1991) Predominant contribution of surface approximation to the mechanism of heparin acceleration of the antithrombin-thrombin reaction. Elucidation from salt concentration effects. *J Biol Chem* 266: 6353-6364.
42. Li W, Johnson DJ, Esmo CT, Huntington JA (2004) Structure of the antithrombin-thrombin-heparin ternary complex reveals the antithrombotic mechanism of heparin. *Nat Struct Mol Biol* 11: 857-862.
43. He L, Vicente CP, Westrick RJ, Eitzman DT, Tollefsen DM (2002) Heparin cofactor II inhibits arterial thrombosis after endothelial injury. *J Clin Invest* 109: 213-219.
44. Parkinson JF, Vlahos CJ, Yan SC, Bang NU (1992) Recombinant human thrombomodulin. Regulation of cofactor activity and anticoagulant function by a glycosaminoglycan side chain. *Biochem J* 283 (Pt 1): 151-157.
45. Isermann B, Vinnikov IA, Madhusudhan T, Herzog S, Kashif M, et al. (2007) Activated protein C protects against diabetic nephropathy by inhibiting endothelial and podocyte apoptosis. *Nat Med* 13: 1349-1358.
46. Ye J, Esmo CT, Johnson AE (1993) The chondroitin sulfate moiety of thrombomodulin binds a second molecule of thrombin. *J Biol Chem* 268: 2373-2379.
47. Lin JH, McLean K, Morser J, Young TA, Wydro RM, et al. (1994) Modulation of glycosaminoglycan addition in naturally expressed and recombinant human thrombomodulin. *J Biol Chem* 269: 25021-25030.
48. Li W, Huntington JA (2008) The heparin binding site of protein C inhibitor is protease-dependent. *J Biol Chem* 283: 36039-36045.
49. Broekhuizen LN, Mooij HL, Kastelein JJ, Stroses ES, Vink H, et al. (2009) Endothelial glycocalyx as potential diagnostic and therapeutic target in cardiovascular disease. *Curr Opin Lipidol* 20: 57-62.

Introduction and outline

50. Nieuwdorp M, Mooij HL, Kroon J, Atasever B, Spaan JA, et al. (2006) Endothelial glycocalyx damage coincides with microalbuminuria in type 1 diabetes. *Diabetes* 55: 1127-1132.
51. Han J, Woytowich AE, Mandal AK, Hiebert LM (2007) Heparanase upregulation in high glucose-treated endothelial cells is prevented by insulin and heparin. *Exp Biol Med (Maywood)* 232: 927-934.
52. Singh A, Friden V, Dasgupta I, Foster RR, Welsh GI, et al. (2011) High glucose causes dysfunction of the human glomerular endothelial glycocalyx. *Am J Physiol Renal Physiol* 300: F40-48.
53. van den Berg BM, Spaan JA, Rolf TM, Vink H (2006) Atherogenic region and diet diminish glycocalyx dimension and increase intima-to-media ratios at murine carotid artery bifurcation. *Am J Physiol Heart Circ Physiol* 290: H915-920.
54. Meuwese MC, Broekhuizen LN, Kuikhoven M, Heeneman S, Lutgens E, et al. (2010) Endothelial surface layer degradation by chronic hyaluronidase infusion induces proteinuria in apolipoprotein E-deficient mice. *PLoS One* 5: e14262.
55. Meuwese MC, Mooij HL, Nieuwdorp M, van Lith B, Marck R, et al. (2009) Partial recovery of the endothelial glycocalyx upon rosuvastatin therapy in patients with heterozygous familial hypercholesterolemia. *J Lipid Res* 50: 148-153.
56. Chappell D, Hofmann-Kiefer K, Jacob M, Rehm M, Briegel J, et al. (2009) TNF-alpha induced shedding of the endothelial glycocalyx is prevented by hydrocortisone and antithrombin. *Basic Res Cardiol* 104: 78-89.
57. Czarnowska E, Karwatowska-Prokopczuk E (1995) Ultrastructural demonstration of endothelial glycocalyx disruption in the reperfused rat heart. Involvement of oxygen free radicals. *Basic Res Cardiol* 90: 357-364.
58. Nieuwdorp M (2006) Loss of endothelial glycocalyx during acute hyperglycemia coincides with endothelial dysfunction and coagulation activation in vivo. *Diabetes* 55:480-486.
59. Girish KS, Kemparaju K (2007) The magic glue hyaluronan and its eraser hyaluronidase: a biological overview. *Life Sci* 80: 1921-1943.
60. Salmon AH, Neal CR, Sage LM, Glass CA, Harper SJ, et al. (2009) Angiopoietin-1 alters microvascular permeability coefficients in vivo via modification of endothelial glycocalyx. *Cardiovasc Res* 83: 24-33.
61. Gaddi AV, Cicero AF, Gambaro G (2010) Nephroprotective action of glycosaminoglycans: why the pharmacological properties of sulodexide might be reconsidered. *Int J Nephrol Renovasc Dis* 3: 99-105.
62. Gambaro G, Kinalska I, Oksa A, Pont'uch P, Hertlová M, et al. (2002) Oral Sulodexide Reduces Albuminuria in Microalbuminuric and Macroalbuminuric Type 1 and Type 2 Diabetic Patients: The Di.N.A.S. Randomized Trial. *Journal of the American Society of Nephrology* 13: 1615-1625.
63. Bang K, Chin HJ, Chae DW, Joo KW, Kim YS, et al. (2011) Anti-proteinuric effect of sulodexide in immunoglobulin a nephropathy. *Yonsei Med J* 52: 588-594.



64. Broekhuizen LN, Lemkes BA, Mooij HL, Meuwese MC, Verberne H, et al. (2010) Effect of sulodexide on endothelial glycocalyx and vascular permeability in patients with type 2 diabetes mellitus. *Diabetologia* 53: 2646-2655.
65. Packham DK, Wolfe R, Reutens AT, Berl T, Heerspink HL, et al. (2012) Sulodexide Fails to Demonstrate Renoprotection in Overt Type 2 Diabetic Nephropathy. *Journal of the American Society of Nephrology* 23: 123-130.
66. Rossini M, Naito T, Yang H, Freeman M, Donnert E, et al. (2010) Sulodexide ameliorates early but not late kidney disease in models of radiation nephropathy and diabetic nephropathy. *Nephrol Dial Transplant* 25: 1803-1810.
67. Parish CR, Freeman C, Brown KJ, Francis DJ, Cowden WB (1999) Identification of sulfated oligosaccharide-based inhibitors of tumor growth and metastasis using novel in vitro assays for angiogenesis and heparanase activity. *Cancer Res* 59: 3433-3441.
68. van Kuppevelt TH, Jenniskens GJ, Veerkamp JH, ten Dam GB, Dennissen MA (2001) Phage display technology to obtain antiheparan sulfate antibodies. *Methods Mol Biol* 171: 519-534.
69. Ikeda Y, Charef S, Ouidja MO, Barbier-Chassefiere V, Sineriz F, et al. (2011) Synthesis and biological activities of a library of glycosaminoglycans mimetic oligosaccharides. *Biomaterials* 32: 769-776.
70. Lensen JF, Rops AL, Wijnhoven TJ, Hafmans T, Feitz WF, et al. (2005) Localization and functional characterization of glycosaminoglycan domains in the normal human kidney as revealed by phage display-derived single chain antibodies. *J Am Soc Nephrol* 16: 1279-1288.
71. Gil N, Goldberg R, Neuman T, Garsen M, Zcharia E, et al. (2012) Heparanase is essential for the development of diabetic nephropathy in mice. *Diabetes* 61: 208-216.
72. Silverthorn DU (2004) The kidneys. *Human physiology*. third edition ed: Pearson education. pp. 598-624.
73. Comper WD, Haraldsson B, Deen WM (2008) Resolved: normal glomeruli filter nephrotic levels of albumin. *J Am Soc Nephrol* 19: 427-432.
74. Farquhar MG, Palade GE (1961) Glomerular permeability. II. Ferritin transfer across the glomerular capillary wall in nephrotic rats. *JExpMed* 114: 699-716.
75. Farquhar MG, Wissig SL, Palade GE (1961) Glomerular permeability. I. Ferritin transfer across the normal glomerular capillary wall. *JExpMed* 113: 47-66.
76. Eremina V, Sood M, Haigh J, Nagy A, Lajoie G, et al. (2003) Glomerular-specific alterations of VEGF-A expression lead to distinct congenital and acquired renal diseases. *JClinInvest* 111: 707-716.
77. Schlondorff D, Banas B (2009) The mesangial cell revisited: no cell is an island. *J Am Soc Nephrol* 20: 1179-1187.
78. Harvey SJ, Zheng K, Sado Y, Naito I, Ninomiya Y, et al. (1998) Role of distinct type IV collagen networks in glomerular development and function. *Kidney Int* 54: 1857-1866.

79. Weil EJ, Lemley KV, Mason CC, Yee B, Jones LI, et al. (2012) Podocyte detachment and reduced glomerular capillary endothelial fenestration promote kidney disease in type 2 diabetic nephropathy. *Kidney Int* 82: 1010-1017.
80. Satchell SC (2012) The glomerular endothelium emerges as a key player in diabetic nephropathy. *Kidney Int* 82: 949-951.
81. Levick JR, Smaje LH (1987) An analysis of the permeability of a fenestra. *Microvasc Res* 33: 233-256.
82. Michel CC, Curry FE (1999) Microvascular permeability. *Physiol Rev* 79: 703-761.
83. Ryan GB, Karnovsky MJ (1976) Distribution of endogenous albumin in the rat glomerulus: role of hemodynamic factors in glomerular barrier function. *Kidney Int* 9:36-45.
84. Rostgaard J, Qvortrup K (1997) Electron microscopic demonstrations of filamentous molecular sieve plugs in capillary fenestrae. *Microvasc Res* 53: 1-13.
85. Avasthi PS, Koshy V (1988) The anionic matrix at the rat glomerular endothelial surface. *Anat Rec* 220: 258-266.
86. Salmon AH, Satchell SC (2012) Endothelial glycocalyx dysfunction in disease: albuminuria and increased microvascular permeability. *J Pathol* 226: 562-574.
87. Jeansson M, Haraldsson B (2003) Glomerular size and charge selectivity in the mouse after exposure to glucosaminoglycan-degrading enzymes. *J Am Soc Nephrol* 14: 1756-1765.
88. Jeansson M, Haraldsson B (2006) Morphological and functional evidence for an important role of the endothelial cell glycocalyx in the glomerular barrier. *Am J Physiol Renal Physiol* 290: F111-116.
89. Friden V, Oveland E, Tenstad O, Ebefors K, Nystrom J, et al. (2011) The glomerular endothelial cell coat is essential for glomerular filtration. *Kidney Int* 79: 1322-1330.
90. Chang RL, Deen WM, Robertson CR, Brenner BM (1975) Permselectivity of the glomerular capillary wall: III. Restricted transport of polyanions. *Kidney Int* 8: 212-218.
91. Chang RL, Ueki IF, Troy JL, Deen WM, Robertson CR, et al. (1975) Permselectivity of the glomerular capillary wall to macromolecules. II. Experimental studies in rats using neutral dextran. *Biophys J* 15: 887-906.
92. Ohlson M, Sorensson J, Haraldsson B (2000) Glomerular size and charge selectivity in the rat as revealed by FITC-ficoll and albumin. *Am J Physiol Renal Physiol* 279: F84-91.
93. Bhalla G, Deen WM (2009) Effects of charge on osmotic reflection coefficients of macromolecules in fibrous membranes. *Biophys J* 97: 1595-1605.
94. Guimaraes MA, Nikolovski J, Pratt LM, Greive K, Comper WD (2003) Anomalous fractional clearance of negatively charged Ficoll relative to uncharged Ficoll. *Am J Physiol Renal Physiol* 285: F1118-1124.
95. Miner JH (2008) Glomerular filtration: the charge debate charges ahead. *Kidney Int* 74:259-261.



96. Arkill KP, Knupp C, Michel CC, Neal CR, Qvortrup K, et al. (2011) Similar endothelial glycocalyx structures in microvessels from a range of mammalian tissues: evidence for a common filtering mechanism? *Biophys J* 101: 1046-1056.
97. Comper WD, Laurent TC (1978) Physiological function of connective tissue polysaccharides. *Physiol Rev* 58: 255-315.
98. Weinbaum S, Zhang X, Han Y, Vink H, Cowin SC (2003) Mechanotransduction and flow across the endothelial glycocalyx. *Proc Natl Acad Sci U S A* 100: 7988-7995.
99. Adamson RH, Lenz JF, Zhang X, Adamson GN, Weinbaum S, et al. (2004) Oncotic pressures opposing filtration across non-fenestrated rat microvessels. *J Physiol* 557: 889-907.
100. Lindstrom KE, Blom A, Johnsson E, Haraldsson B, Fries E (1997) High glomerular permeability of bikunin despite similarity in charge and hydrodynamic size to serum albumin. *Kidney Int* 51: 1053-1058.
101. Comper WD (2014) Albuminuria is controlled primarily by proximal tubules. *Nat Rev Nephrol* 10: 180.
102. Ruggiero A, Villa CH, Bander E, Rey DA, Bergkvist M, et al. (2010) Paradoxical glomerular filtration of carbon nanotubes. *Proc Natl Acad Sci U S A* 107: 12369-12374.

2

A microscopic view on the renal endothelial glycocalyx

*Published as part of:
Am J Physiol Renal Physiol ajprenal 00532 02014, 2015.*

Martijn J.C. Dane¹, Bernard M. van den Berg¹, Dae Hyun Lee¹, Margien G.S. Boels¹, Gesa L. Tiemeier¹, M. Cristina Avramut², Anton Jan van Zonneveld¹, Johan van der Vlag³, Hans Vink⁴, Ton J. Rabelink¹

¹*Department of Nephrology, Einthoven laboratory for Vascular Medicine, LUMC, Leiden University Medical Center, The Netherlands* ²*Department of Molecular Cell Biology, Section Electron Microscopy LUMC, Leiden University Medical Center, The Netherlands* ³*Department of Nephrology, Radboud Institute for Molecular Life Sciences, Radboud University Medical Center, Nijmegen, the Netherlands* ⁴*Department of Physiology, Maastricht University Medical Center, Maastricht, the Netherlands*

Introduction

Endothelial cells perform key homeostatic functions such as regulating blood flow and permeability, preventing leukocyte activation, and aiding immune surveillance for pathogens. Endothelial activation therefore has been identified as an important effector mechanism in progression of renal disease as well as the associated development of cardiovascular disease. The primary interface between blood and the endothelium is the glycocalyx. This carbohydrate-rich gel-like structure mediates most of the regulatory functions of the endothelium. Because the endothelial glycocalyx is a highly dynamic and fragile structure *ex-vivo*, studying its dimensions and function has been proven to be a challenge. Tissue processing for staining and perfusion-fixation, usually will result in a partial or complete loss of the glycocalyx. Consequently, its functions and its potential as a therapeutic target have often been underappreciated. Here we will outline the different techniques to visualize structure function relationships in kidney and vasculature.

Imaging the endothelial glycocalyx

Endothelial activation has been shown to be a central mediator in the development of cardiovascular and kidney disease [1,2]. Because the endothelial glycocalyx is the primary interface for interaction of blood with the vessel wall, it can be postulated that endothelial activation in fact is primarily mediated through changes in EG function or composition. Well known risk factors for the development for cardiovascular and renal disease such as diabetes have been associated with both upregulation of heparanase and hyaluronidase [3,4], resulting in degradation or loss of glycocalyx. For example, increased activity of heparanase has been demonstrated in both circulating mononuclear cells as well as the plasma of hemodialysis patients and linked to the presence of atherosclerotic lesions [5]. Because the EG is a highly dynamic and fragile structure, it is unstable when taken out of its *in vivo* environment. Consequently, bound plasma components and GAGs can be lost during fixation, dehydration, sectioning and staining procedures. As a result, only membrane bound parts of the glycocalyx will remain. Avoiding this loss of the EG is one of the biggest challenges in EG visualization. Attempts to visualize changes in EG composition and thickness, have led to imaging techniques based on different characteristics of the EG.

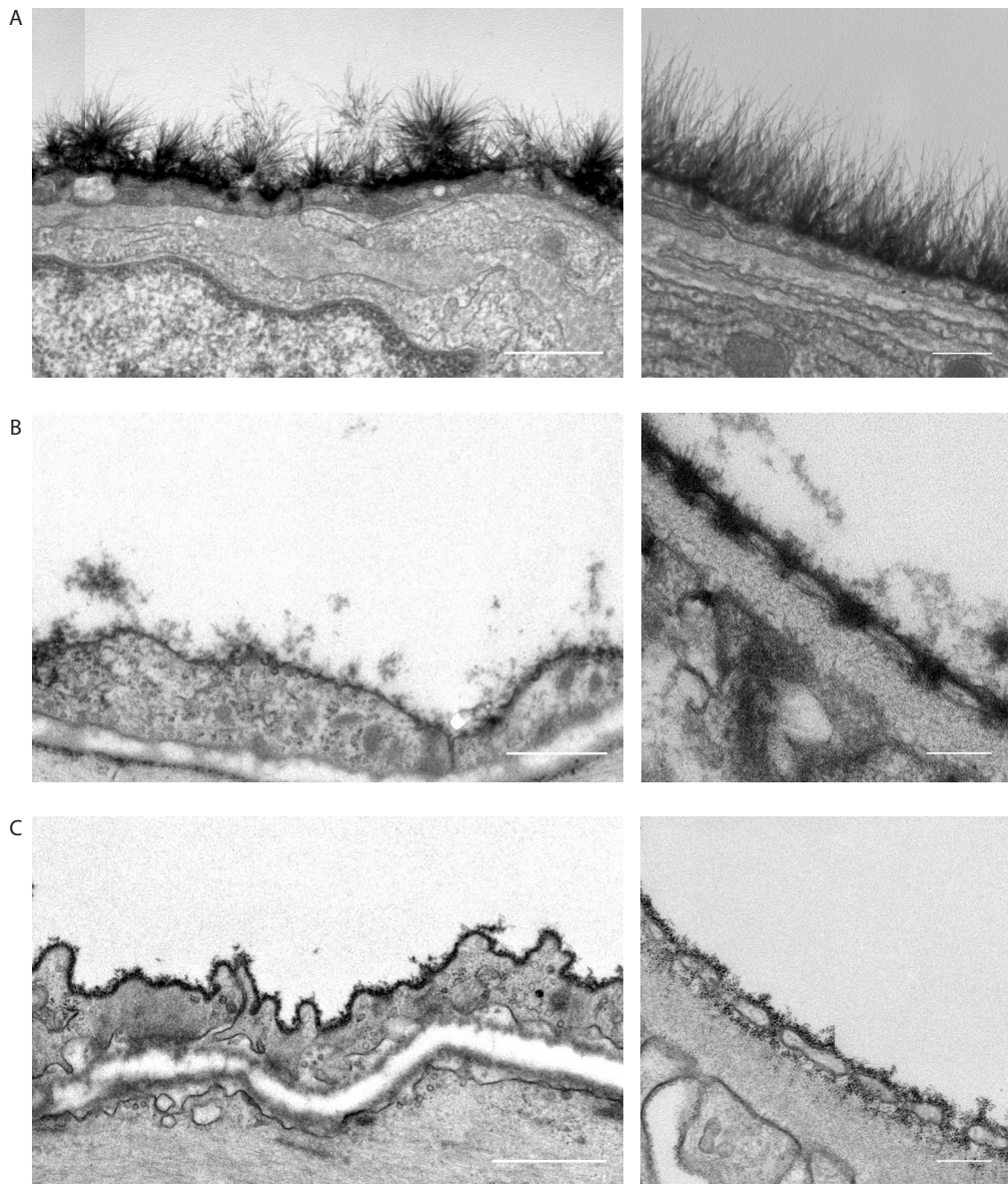


Figure 1: Three methods to stabilize and stain the endothelial glycocalyx for electron microscopy. A) Alcian Blue 8X stained artery (left) and detailed image of an Alcian Blue 8x stained myocardial capillary. B) Cupromeronic Blue stained vein (left) and detailed image of glomerular capillary (right). C) Cationic Ferritin stained vein (left) and detailed image of glomerular capillary (right). Scale bars represent 500 nm (left) and 200 nm (right)

Electron microscopy

Preserving and staining the EG for EM

The high polysaccharide content of the EG interacts poorly with the commonly used post-fixation stains. As a result, the EG scatters few electrons and is indistinguishable from its environment in conventionally processed samples for TEM [6]. Thus, even if the pre-treatment of the sample maintains the structural integrity of the endothelial glycocalyx, an additional staining or preservation is required for visualization of the EG in TEM. This explains the absence of visible EG structures in almost all tissues that are conventionally processed for TEM. The first to succeed in staining the EG for electron microscopy was Luft in 1966, who used ruthenium red, or ammoniated ruthenium oxychloride, which stains the aldehyde fixed mucopolysaccharides in the EG and generates an electron dense stain in the presence of osmium tetroxide [7].

The presence of the luminal EG has subsequently been shown using TEM in combination with a variety of staining and preservation techniques such as ruthenium red, ferritin, and lanthanum. Most of these agents cationic dyes bind to the negative charge of the sulfated GAGs and form an electron dense contrast together with osmium tetroxide, to enable visualization [8-12]. Using alcian blue 8GX, van den Berg et al. were the first to be able to better stabilize the anionic carbohydrate structures in myocardial capillaries, thereby visualizing an impressive EG of up to 500 nm thick [13]. The saccharine nature of these visualized structures was confirmed by perfusion of gold-labelled lectins before the staining procedure. Recently, we were able to visualize the EG in the renal glomerulus using cupromeronic blue, a chemically more stable cationic dye resembling some alcian blue properties [14]. This revealed a staining of matrix polysaccharides on the luminal surface of the glomerular endothelial membranes and a dense staining of polysaccharide matrix within the fenestrae. Examples of the described staining procedures are shown in **figure 1**.

High pressure freezing

Because optimal preservation of the EG and its visualization requires the use of perfusion fixation techniques, it has not been possible to reliably image the EG in patient biopsy material. Although not yet used for this purpose, a combination of rapid freezing and freeze substitution of the tissue might be an interesting way to preserve the EG. With a combination of instantaneous high pressure and a rapid decrease in temperature, high-pressure freezing preserves the tissue while reducing the formation of ice crystals. In a frozen state water can be replaced and tissue can be stained at the same time. This way molecules can be fixated in plastic, while preserving their native structure as much as possible. Results of this procedure are shown in the example of a high pressure frozen mouse renal sample which is stained during freeze substitution with acridine orange and uranyl (**figure 2**). Although further optimization is necessary, it does appear to be a promising technique that might pave the way for studying changes in the local EG in patients.

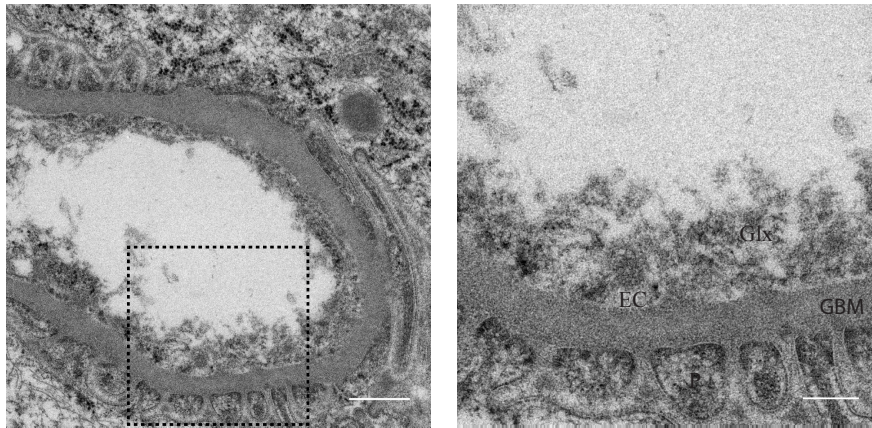


Figure 2: EG in a glomerular capillary of a high pressure frozen kidney section. EG was stained with acridin orange and uranyl during the freeze substitution stage. Overview (left) and detailed image of the glycocalyx on top of the glomerular filtration barrier (right). EC: endothelial cell, GBM: glomerular basement membrane, P: Podocytes, Glx: Glycocalyx. Scale bars represent 500 nm (left) and 200 nm (right).

3-Dimensional EM imaging

Over the recent years some interesting developments took the field of electron microscopy to a next level. These new methods might be used to better and more reliably study the EG. In regular EM imaging techniques, the highly detailed 2-dimensional EM images are prone to selection bias, as only a small area of interest is shown. To avoid this operator introduced selection bias, Faas et al. developed a method which provides high resolution and high detailed images while maintaining the lower resolution overview of the cellular context [15]. Examples of images in which virtual zooming was used on a stitch of a Cupromeronic blue stained glomerulus are shown in **figure 3**.

Interestingly, within one stitch of a mouse glomerulus different structural organizations of the EG can be observed, depending on its location (figure 3B non-fenestrated (top) vs fenestrated (bottom) endothelium). In addition 3D imaging can also be used to decrease bias and obtain more insight in the imaged structures. Based on earlier publications where bacterial flagellae were imaged [16], Arkill et al. succeeded to make a 3D reconstruction of the EG using 3D electron tomography. In electron tomography, an electron beam passes through the sample which is tilted after every image so that images can be taken at different angles. By reconstructing these images, a 3D image of the sample can be produced [17]. Although not used for EG imaging yet, some newer techniques, like SEM with a built-in microtome and focused ion beam scanning electron microscopy (FIB-SEM), will make the 3D analysis in electron microscopy even more detailed [18].

A microscopic view on the renal endothelial glycocalyx

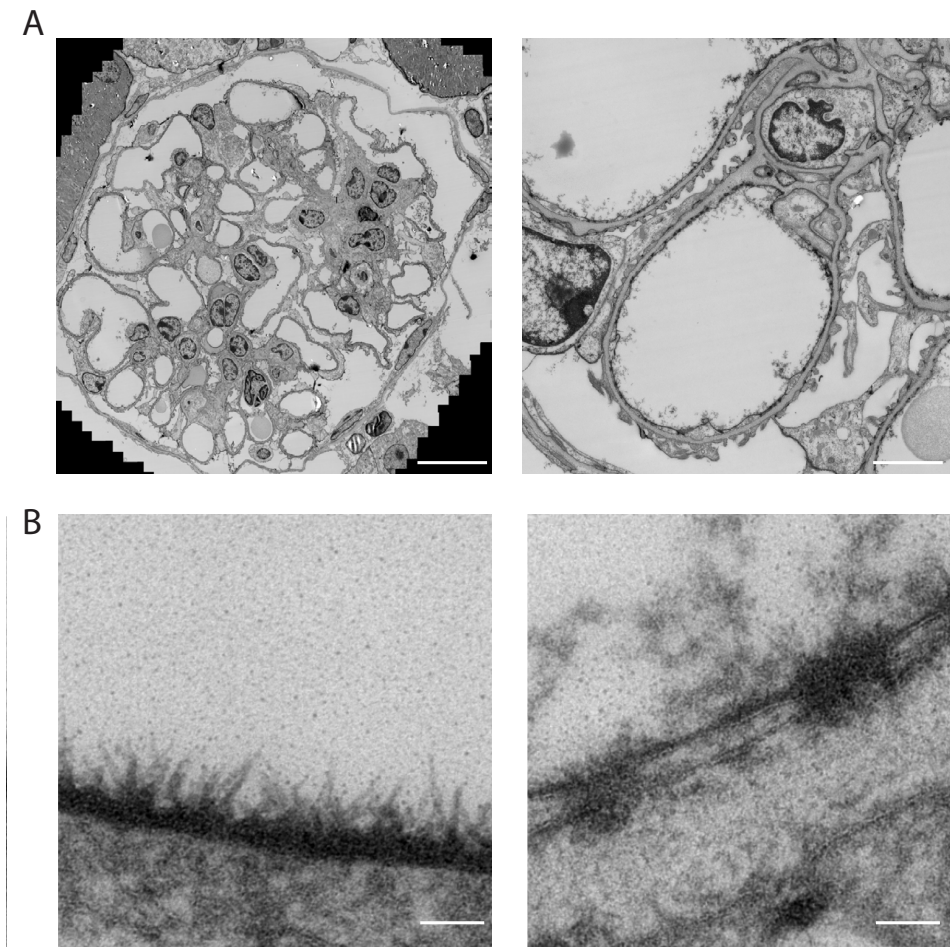


Figure 3: Transmission electron microscopic images of a cupromeronic blue stained glomerulus. A) Overview (left) and virtual zoom (right) of a stitch of a mouse glomerulus. B) Virtual zoom with maximal detail showing different structures of the endothelial glycocalyx on top of continuous endothelium (left) and fenestrated endothelium (right). Scale bars represent 10 μm (left) and 1 μm (right) (A) and 100 nm (B).

Fluorescence microscopy

Staining and imaging specific EG components

The carbohydrates within the EG have been imaged using specific lectins, mostly in combination with fluorescence microscopy. Lectins are carbohydrate binding proteins that recognize specific sugar moieties and 3D configurations. One of the most commonly used lectins is wheat germ agglutinin (WGA). Although lectin staining of the EG can be used to study changes in dimensions, they do not allow to determine changes in the specific composition of different GAGs. Consequently, antibodies are needed to more specifically determine compositional changes within the EG.

Over the recent years several antibodies have been obtained against specific carbohydrate domains within heparan sulfates (e.g. JM403, 10E4 and HEPSS1), hyaluronan and chondroitin sulfates or against the proteoglycan core proteins such as syndecan, glypican or perlecan [19-24]. Chondroitin sulfate and hyaluronan have been shown to be present on the endothelium, using an anti-CS antibody and by capitalizing on the protein binding properties of HA with a fluorescent hyaluronan binding protein (HABP), respectively [24-26]. Although all these techniques have shown the presence of glycocalyx components on the endothelial cells, a considerable part of these studies have been performed using epi-fluorescence microscopy, which has major limitations with respect to optical spatial resolution necessary for imaging the luminal endothelial glycocalyx.

With the development of confocal and two photon laser scanning microscopy (TPLSM), fluorescence microscopy has been improved in such a way that the resolution is high enough to be used for detailed EG imaging in situ. Examples of in situ stained mouse glomerulus and WGA perfused isolated carotid arteries, imaged with multiphoton microscopy are shown in **figure 4**. The so-called super-resolution microscopy, such as stimulation emission depletion (STED), ground state depletion (GSD) and saturated structured illumination microscopy (SSIM) even enables higher detailed imaging than the conventional confocal microscopy.



A microscopic view on the renal endothelial glycocalyx

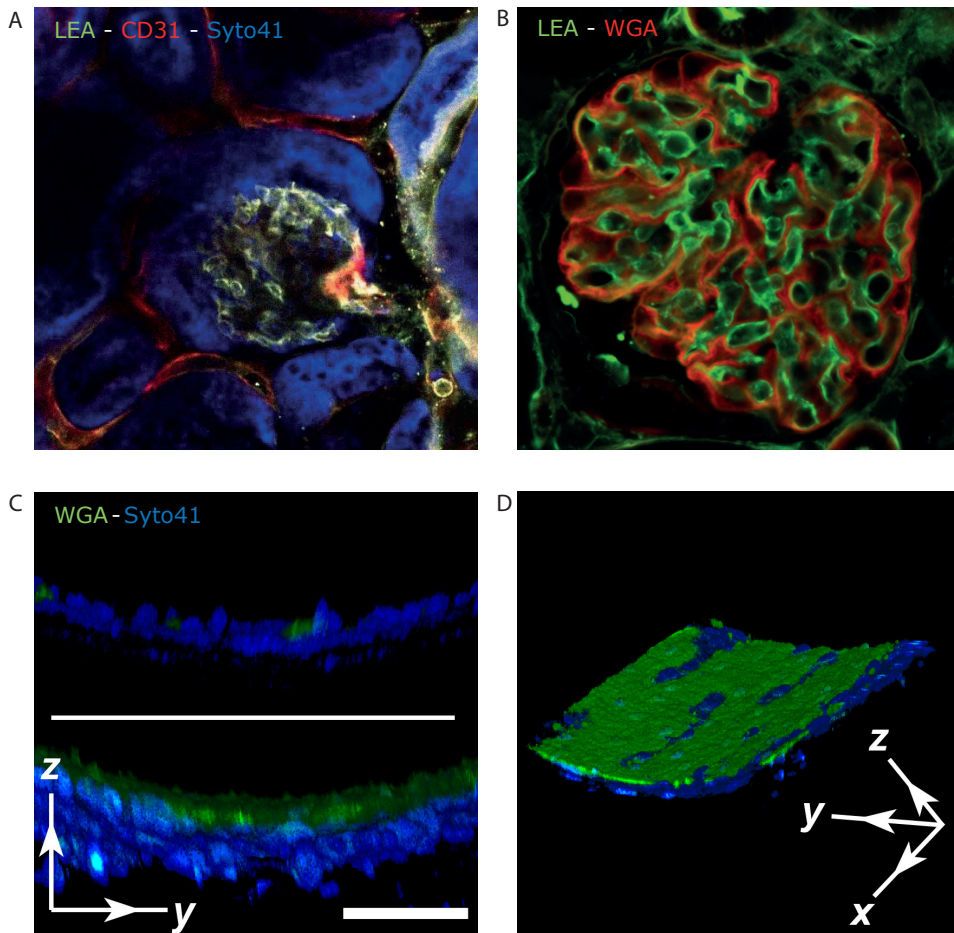


Figure 4: Endothelial glycocalyx imaged ex vivo with confocal- or multiphoton imaging techniques. A) Mouse glomerulus visualised with anti-CD31 antibodies and TRITC-labeled conjugate for endothelium (red), syto41 for nuclei (blue) and lycopersicon esculentum (LEA) for EG (green). B) Mouse glomerulus visualised with LEA (green) and wheat-germ agglutinin WGA (Red). C-D) Mouse common carotid artery images obtained with two-photon laser scanning microscopy showing part of the vessel wall. Vessel was perfused with FITC-labeled WGA (green) and SYTO 41 (blue). Endothelial glycocalyx is almost inaccessible to WGA in normal situations (C, upper part) and becomes visible after exposure to a small air bubble (C, lower part). 3D reconstruction shows that the endothelial glycocalyx stained by WGA covers the endothelium (D) Bar represents 50 μm . The arrows indicate the direction of the X, Y, and Z axis.

New labels for imaging the EG: Single chain antibodies

A complex but promising field for studying heparan sulfates within the EG is the use of single chain antibodies. For the selection of these single chain antibodies, a synthetic single-chain variable fragment library is used. Out of these single chain variable fragments, specific antibodies can be selected. In this way, antibodies against tissue specific modified HS domains can be produced. This method has been used previously to study heparan sulfate domains present in the basement membrane [27]. Although the same principle is used to study the role of heparan sulfates present on glomerular endothelial cells [28], it has never been used to image these heparan sulfates specifically on the luminal endothelial surface. Therefore, the use of single chain antibodies in conditions that allow for EG staining might be interesting to obtain more insight in the complexity of the different subcomponents within the EG. This promises to be an interesting field for the development of new antibodies specific for certain GAG domains within the luminal EG.



Measuring and imaging structural characteristics

Circulating markers of the glycocalyx

In response to reactive oxygen species (ROS) or other inflammatory mediators, both single GAGs and proteoglycans can be shed from the endothelium [29-31]. This has been suggested to be mediated by endoglycosidases such as heparanase and hyaluronidase, or proteases such as matrix metalloproteases [30,32,33]. Consequently, measuring shed glycocalyx components might be used as a marker for endothelial glycocalyx stability. For example, syndecan-1 and heparan sulfate are released from the tissue and can be detected in the circulating blood of patients with perioperative global or regional ischemia [34,35]. The glycocalyx core protein syndecan-1 acts as negative regulator of endothelial activation [36] and has been shown to be critical for processing and inactivation of heparanase on the cell surface [37]. In addition, release of the endothelium specific proteoglycan thrombomodulin has been shown to coincide with diabetes and diabetic nephropathy [38,39]. We demonstrated that patients with renal failure have increased circulating levels of syndecan-1 and thrombomodulin, which was reversed by kidney transplantation [40]. Furthermore, renal failure was shown to correlate with increased concentrations of shed HA [41]. Altogether, while several glycocalyx components are shed upon endothelial activation, the exact location, mechanism and timing of shedding is complex and mostly unknown. Interpreting the results is still challenging.

Atomic Force microscopy

To determine the elastic properties of the EG, atomic force microscopy (AFM), has been shown to be a valuable tool. An AFM consists of a cantilever with a spherical tip which can scan the surface of the specimen. Reaching close contact with the specimen, forces between the tip and sample will result in deflection of this cantilever, that can be detected by changes in reflection of a laser spot. This technique has been previously used to measure mechanical stiffness in endothelial cells. However, by comparing endothelial cell layers with and without removal of the EG, the presence and stiffness of the EG could also be measured. This resulted in an estimated thickness of 400 nm of the EG on cultured endothelial cells, with a 50% EG thickness reduction after heparinase treatment [42]. Changes in the endothelial surface layer stiffness and thickness were associated with both endothelial activation and shedding of syndecan-1 and HA in renal failure patients and in animals [43].

Exclusion of macromolecules

Using intravital microscopy, a luminal microdomain that is inaccessible for erythrocytes, leukocytes and macromolecules (e.g. 70 kDa dextran, dex70) can be demonstrated. For small molecules however, this microdomain is still accessible. When damaging this layer, using a 1-2 minute light-dye treatment, erythrocytes and dex70 are able to enter this microdomain (**figure 5A,B**) [44]. In addition to the demonstration of size exclusion, this technique can also be used to show the charge exclusion properties of the EG (**figure 5C**) [45].

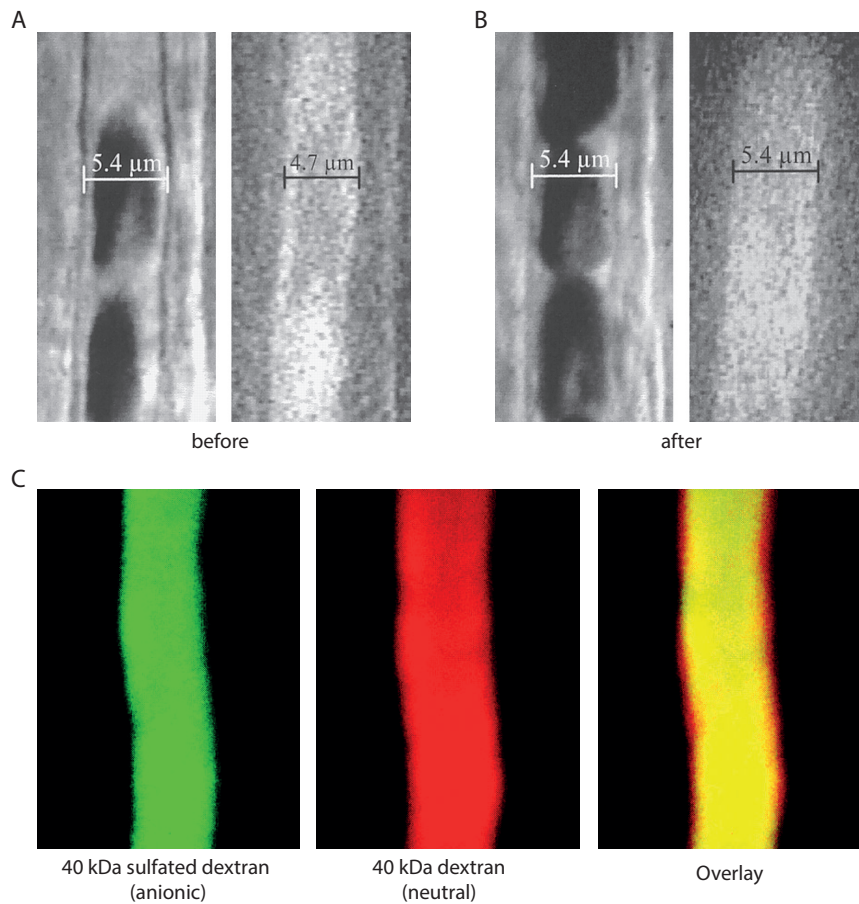


Figure 5: Exclusion properties of the endothelial surface layer in vivo. A) Intravital microscopic image a hamster cremaster muscle capillary. The anatomical diameter of $5.4 \mu\text{m}$ is clearly larger than the red blood cell column width (left pane) or the plasma column width (right pane) labelled with fluorescent dextran (70 kD). This is caused by the endothelial glycocalyx (EG), as it is impermeable for Dex70 and RBCs. B) Image of the same hamster cremaster muscle capillary after light dye treatment (for methodology see ref [44]). The anatomical diameter of $5.4 \mu\text{m}$ is the same as the red blood cell column width (left pane) or the plasma column width (right pane) labelled with fluorescent dextran (70 kD), suggesting a destruction of the EG. C) Anionic sulfated 40 kDa dextran (green, left) and neutral 40 kDa dextran (red, middle) in mouse cremaster tissue capillaries. Difference in distribution within the same capillary (overlay, right), shows the charge-based exclusion of the anionic dextran from the endothelial surface layer.

Most of the techniques developed to estimate the changes in EG are based on this principle. Haraldsson et al. used Intralipid, a chylomicron-like suspension of purified soybean oil, egg-yolk phospholipids, glycerol, and water to use the physical exclusion properties of the EG for determining the EG thickness in TEM. After making electron micrographs of capillaries, the location of the lipid drop was identified as central or peripheral (being within 200 nm from the luminal endothelial surface) [46]. By comparing the distribution of these lipid particles before and after for example adriamycin treatment, changes in EG thickness could be estimated [47]. In vivo, a theoretically comparable method was used by Smith et al., who looked into the location of flowing microspheres. Using dual-flash epi-illumination, the velocity of infused fluorescently labelled microspheres was estimated in the near wall plasma-rich region of venules before and after light-dye treatment to degrade the EG. Using this technique, the theoretically suggested hydraulic resistivity of the surface layer was demonstrated [48]. Also, the EG thickness was estimated to be 0.33-0.44 μm , which confirms the measurements by Vink and Duling [44].

Tracer dilution technique

Based on their in vivo observations in mice, the group of Vink et al. has mainly focused on the development of a method to measure changes in EG in patients. The tracer dilution technique was the first technique to estimate the glycocalyx volume. By comparing the circulating blood volume, using a glycocalyx impermeable tracer, and the total intravascular volume, using a glycocalyx permeable tracer, the total glycocalyx volume could be estimated. This concept was first applied when Nieuwdorp et al. showed that both acute hyperglycemia and type 1 diabetes mellitus coincided with a reduction of the estimated EG volume [49,50]. Unfortunately this technique has the disadvantage that it is very time-consuming and invasive to infuse labelled RBCs and Dex40.

RBC-EC gap and SDF imaging

Based on previous observations of the RBC exclusion zone in animal models, the presence of an RBC exclusion zone between the RBC column and the endothelium was demonstrated in trans-illuminated hamster cremaster muscle capillaries [51,52]. More recently we tested the hypothesis that the EG occupies this RBC-EC gap. When comparing the width of the RBC column with the internal anatomical vessel diameter as defined by the position of the fluorescent endothelium a decreased RBC-EC gap was observed after degradation of the EG with hyaluronidase [41].

In addition, Han et al. demonstrated a decrease in this RBC-EC gap when a leukocyte was passing through the capillary. Based on earlier data and a rapid recovery of the RBC-EC gap, it was concluded that the passing leukocyte temporarily compresses the EG [53]. Consequently, the local EG thickness can be estimated in vivo by measuring the difference of the RBC column width before and directly after the passing of a leukocyte. This hypothesis was validated when the EG was degraded by oxidized LDL after which no change in RBC-EC gap could be observed before and after leukocyte passage [54].

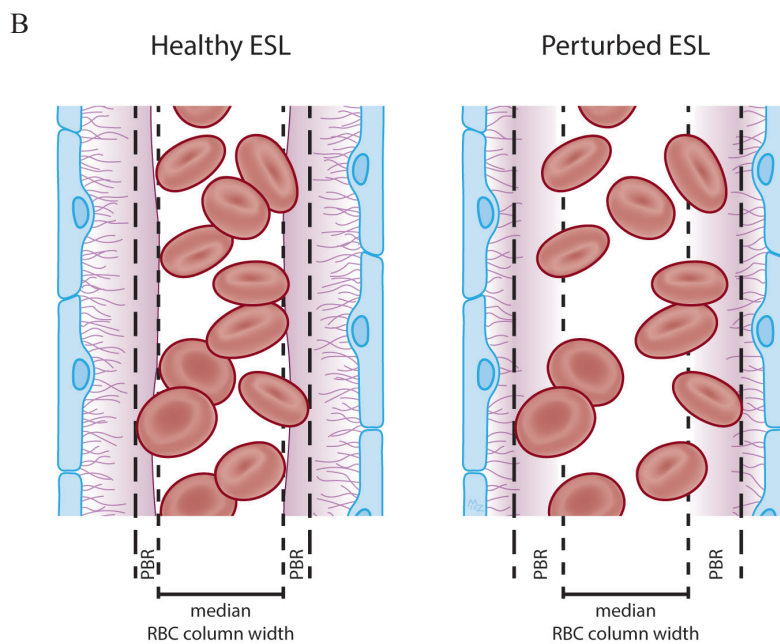
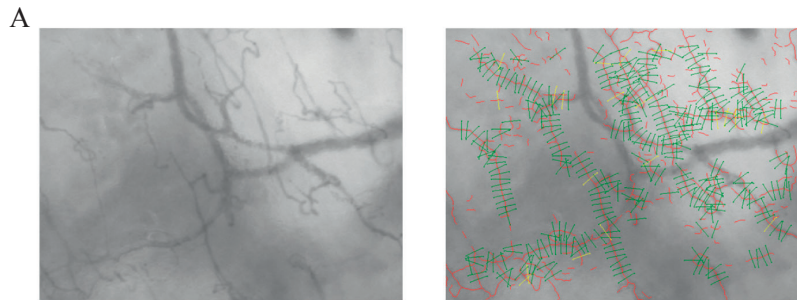


Figure 6: Sidestream darkfield (SDF) imaging to measure the perfused boundary region (PBR) in the sublingual capillary bed. A) Recordings from the sublingual capillary bed made with the SDF camera (left). Capillaries are automatically recognized and analysed after various quality checks (right). Based on the shift in RBC column width in time, the PBR can be calculated. B) Model of a blood vessel showing the PBR in a healthy situation (left) the endothelial glycocalyx prevents the RBC to approach the endothelial cell, thus a small PBR is measured. In a disease situation (right) (40, 55, 57, 60), or after enzymatical endothelial glycocalyx (EG) breakdown in an animal-model,(41) the damaged EG allows the RBCs to approach the endothelium more often. This results in a higher variation in RBC column width reflected by a high PBR. ESL: endothelial surface layer/ glycocalyx.

Using side stream darkfield (SDF) imaging the ability of the RBC to access the EG in the microcirculation can be measured. The technique uses light with a wavelength within the absorption spectrum of hemoglobin. A connected video camera visualizes the scattered light from the illuminated tissue [55]. Using this wavelength, the RBC column of the superficial microvasculature can be imaged *in vivo*. Based on the concept that an RBC can penetrate deeper into an instable or damaged EG, variations in RBC column width in time can be measured and taken as a proxy for EG accessibility. The intraluminal RBC perfused region that is situated in between the median RBC column width and unperfused domain of glycocalyx, has been coined the perfused boundary region (PBR) (**figure 6**). Deeper penetration of RBCs into the compromised glycocalyx results in increased dimension of PBR. We and others have used this technique to determine changes in EG in patients compared to control participants. In these studies, the PBR was demonstrated to be associated with microvascular perfusion and to be increased in patients with coronary artery disease, sepsis and renal failure [40,56-58]. In addition, PBR was also associated with microvascular changes in the retinal vascular bed [59]. A recent study, however, failed to demonstrate a distinction between the PBR of a pooled group of participants with a variable increased cardiovascular risk profile, stressing the need for a better understanding of PBR profiles in different patient subclasses based on gender and e.g. ethnic background [60]. Nonetheless, patient studies and the validation studies in animal models suggest that measuring the PBR to estimate microvascular risk is a promising concept.

Summary and conclusion

The endothelial glycocalyx is proposed to mediate almost all of the endothelial functions and structural or compositional perturbation of this glycocalyx associates with a variety of vasculature related pathologies. However, monitoring the EG is challenging, since the stability of the layer highly depends on its environment (e.g. blood pressure, loosely bound plasma proteins and water). Nevertheless, several imaging methods have been developed to study the endothelial glycocalyx over the last decades. Using electron microscopy, the presence of the endothelial glycocalyx has been observed in vascular tissue. An important remaining future challenge for imaging with electron microscopy (but also for other visualization techniques) is the preservation of the EG without using stabilizing perfusion fixation techniques. This would allow staining and dimensional quantification of the EG in conventionally processed patient biopsies.

To study compositional changes in the glycocalyx, at least 3D imaging should be used. Nonetheless, to study the exact (compositional) changes within the endothelial glycocalyx in more detail, future development of new techniques to analyse GAG sequence and modifications is of crucial importance. For patient studies, non-invasively measuring changes in the EG using SDF imaging is an interesting new field. With the current techniques changes in EG in severely diseased patients can be detected noninvasively. However, further validation and optimization of this technique in healthy and diseased situations is needed to clear the way for measuring changes in EG as a risk factor for the development of vascular diseases



References

1. Rabelink TJ, de Boer HC, van Zonneveld AJ (2010) Endothelial activation and circulating markers of endothelial activation in kidney disease. *Nat Rev Nephrol* 6: 404-414.
2. Deanfield JE, Halcox JP, Rabelink TJ (2007) Endothelial function and dysfunction: testing and clinical relevance. *Circulation* 115: 1285-1295.
3. Ikegami-Kawai M, Suzuki A, Karita I, Takahashi T (2003) Increased hyaluronidase activity in the kidney of streptozotocin-induced diabetic rats. *J Biochem* 134: 875-880.
4. Wijnhoven TJ, van den Hoven MJ, Ding H, van Kuppevelt TH, van der Vlag J, et al. (2008) Heparanase induces a differential loss of heparan sulphate domains in overt diabetic nephropathy. *Diabetologia* 51: 372-382.
5. Cohen-Mazor M, Sela S, Mazor R, Ilan N, Vlodaysky I, et al. (2008) Are primed polymorphonuclear leukocytes contributors to the high heparanase levels in hemodialysis patients? *Am J Physiol Heart Circ Physiol* 294: H651-658.
6. Erlandsen SL, Kristich CJ, Dunny GM, Wells CL (2004) High-resolution visualization of the microbial glycocalyx with low-voltage scanning electron microscopy: dependence on cationic dyes. *J Histochem Cytochem* 52: 1427-1435.
7. Luft JH (1966) Fine structures of capillary and endocapillary layer as revealed by ruthenium red. *Fed Proc* 25: 1773-1783.
8. Bruegger D, Jacob M, Rehm M, Loetsch M, Welsch U, et al. (2005) Atrial natriuretic peptide induces shedding of endothelial glycocalyx in coronary vascular bed of guinea pig hearts. *Am J Physiol Heart Circ Physiol* 289: H1993-1999.
9. Jacob M, Bruegger D, Rehm M, Welsch U, Conzen P, et al. (2006) Contrasting effects of colloid and crystalloid resuscitation fluids on cardiac vascular permeability. *Anesthesiology* 104: 1223-1231.
10. Chappell D, Jacob M, Paul O, Rehm M, Welsch U, et al. (2009) The glycocalyx of the human umbilical vein endothelial cell: an impressive structure ex vivo but not in culture. *Circ Res* 104: 1313-1317.
11. Becker BF, Chappell D, Jacob M (2010) Endothelial glycocalyx and coronary vascular permeability: the fringe benefit. *Basic Res Cardiol* 105: 687-701.
12. Vogel J, Sperandio M, Pries AR, Linderkamp O, Gaehtgens P, et al. (2000) Influence of the endothelial glycocalyx on cerebral blood flow in mice. *J Cereb Blood Flow Metab* 20: 1571-1578.
13. van den Berg BM, Vink H, Spaan JA (2003) The endothelial glycocalyx protects against myocardial edema. *Circ Res* 92: 592-594.
14. Dane MJ, van den Berg BM, Avramut MC, Faas FG, van der Vlag J, et al. (2013) Glomerular endothelial surface layer acts as a barrier against albumin filtration. *Am J Pathol* 182: 1532-1540.
15. Faas FG, Avramut MC, van den Berg BM, Mommaas AM, Koster AJ, et al. (2012) Virtual nanoscopy: generation of ultra-large high resolution electron microscopy maps. *J Cell Biol* 198: 457-469.

16. Pigino G, Geimer S, Lanzavecchia S, Paccagnini E, Cantele F, et al. (2009) Electron-tomographic analysis of intraflagellar transport particle trains in situ. *J Cell Biol* 187: 135-148.
17. Arkill KP, Neal CR, Mantell JM, Michel CC, Qvortrup K, et al. (2012) 3D reconstruction of the glycocalyx structure in mammalian capillaries using electron tomography. *Microcirculation* 19: 343-351.
18. Kizilyaprak C, Bittermann AG, Daraspe J, Humbel BM (2014) FIB-SEM Tomography in Biology. *Methods Mol Biol* 1117: 541-558.
19. Zeng Y, Waters M, Andrews A, Honarmandi P, Ebong EE, et al. (2013) Fluid shear stress induces the clustering of heparan sulfate via mobility of glypican-1 in lipid rafts. *Am J Physiol Heart Circ Physiol* 305: H811-820.
20. Giantsos-Adams KM, Koo AJ, Song S, Sakai J, Sankaran J, et al. (2013) Heparan Sulfate Regrowth Profiles Under Laminar Shear Flow Following Enzymatic Degradation. *Cell Mol Bioeng* 6: 160-174.
21. Singh A, Ramnath RD, Foster RR, Wylie EC, Friden V, et al. (2013) Reactive oxygen species modulate the barrier function of the human glomerular endothelial glycocalyx. *PLoS One* 8: e55852.
22. Singh A, Friden V, Dasgupta I, Foster RR, Welsh GI, et al. (2011) High glucose causes dysfunction of the human glomerular endothelial glycocalyx. *Am J Physiol Renal Physiol* 300: F40-48.
23. Singh A, Satchell SC, Neal CR, McKenzie EA, Tooke JE, et al. (2007) Glomerular endothelial glycocalyx constitutes a barrier to protein permeability. *J Am Soc Nephrol* 18: 2885-2893.
24. Zeng Y, Ebong EE, Fu BM, Tarbell JM (2012) The structural stability of the endothelial glycocalyx after enzymatic removal of glycosaminoglycans. *PLoS One* 7: e43168.
25. Lopez-Quintero SV, Cancel LM, Pierides A, Antonetti D, Spray DC, et al. (2013) High glucose attenuates shear-induced changes in endothelial hydraulic conductivity by degrading the glycocalyx. *PLoS One* 8: e78954.
26. Foster RR, Armstrong L, Baker S, Wong DW, Wylie EC, et al. (2013) Glycosaminoglycan Regulation by VEGFA and VEGFC of the Glomerular Microvascular Endothelial Cell Glycocalyx in Vitro. *Am J Pathol* 183: 604-616.
27. van den Hoven MJ, Wijnhoven TJ, Li JP, Zcharia E, Dijkman HB, et al. (2008) Reduction of anionic sites in the glomerular basement membrane by heparanase does not lead to proteinuria. *Kidney Int* 73: 278-287.
28. Rops AL, van den Hoven MJ, Baselmans MM, Lensen JF, Wijnhoven TJ, et al. (2008) Heparan sulfate domains on cultured activated glomerular endothelial cells mediate leukocyte trafficking. *Kidney Int* 73: 52-62.
29. Mulivor AW, Lipowsky HH (2004) Inflammation- and ischemia-induced shedding of venular glycocalyx. *Am J Physiol Heart Circ Physiol* 286: H1672-1680.
30. Lipowsky HH, Lescanic A (2013) The effect of doxycycline on shedding of the glycocalyx due to reactive oxygen species. *Microvasc Res* 90: 80-85.



31. Kliment CR, Tobolewski JM, Manni ML, Tan RJ, Enghild J, et al. (2008) Extracellular superoxide dismutase protects against matrix degradation of heparan sulfate in the lung. *Antioxid Redox Signal* 10: 261-268.
32. Lipowsky HH, Gao L, Lescanic A (2011) Shedding of the endothelial glycocalyx in arterioles, capillaries, and venules and its effect on capillary hemodynamics during inflammation. *Am J Physiol Heart Circ Physiol* 301: H2235-2245.
33. Mulivor AW, Lipowsky HH (2009) Inhibition of glycan shedding and leukocyte-endothelial adhesion in postcapillary venules by suppression of matrixmetalloprotease activity with doxycycline. *Microcirculation* 16: 657-666.
34. Rehm M, Bruegger D, Christ F, Conzen P, Thiel M, et al. (2007) Shedding of the endothelial glycocalyx in patients undergoing major vascular surgery with global and regional ischemia. *Circulation* 116: 1896-1906.
35. Snoeijns MG, Vink H, Voesten N, Christiaans MH, Daemen JW, et al. (2010) Acute ischemic injury to the renal microvasculature in human kidney transplantation. *Am J Physiol Renal Physiol* 299: F1134-1140.
36. Voyvodic PL, Min D, Liu R, Williams E, Chitalia V, et al. (2014) Loss of syndecan-1 induces a pro-inflammatory phenotype in endothelial cells with a dysregulated response to atheroprotective flow. *J Biol Chem* 289: 9547-9559.
37. Shteingauz A, Ilan N, Vlodayvsky I (2014) Processing of heparanase is mediated by syndecan-1 cytoplasmic domain and involves syntenin and alpha-actinin. *Cell Mol Life Sci*.
38. Iwashima Y, Sato T, Watanabe K, Ooshima E, Hiraishi S, et al. (1990) Elevation of plasma thrombomodulin level in diabetic patients with early diabetic nephropathy. *Diabetes* 39: 983-988.
39. Oida K, Takai H, Maeda H, Takahashi S, Tamai T, et al. (1990) Plasma thrombomodulin concentration in diabetes mellitus. *Diabetes Res Clin Pract* 10: 193-196.
40. Vlahu CA, Lemkes BA, Struijk DG, Koopman MG, Krediet RT, et al. (2012) Damage of the endothelial glycocalyx in dialysis patients. *J Am Soc Nephrol* 23: 1900-1908.
41. Dane MJ, Khairoun M, Lee DH, van den Berg BM, Eskens BJ, et al. (2014) Association of kidney function with changes in the endothelial surface layer. *Clin J Am Soc Nephrol* 9: 698-704.
42. Oberleithner H, Peters W, Kusche-Vihrog K, Korte S, Schillers H, et al. (2011) Salt overload damages the glycocalyx sodium barrier of vascular endothelium. *Pflügers Arch* 462: 519-528.
43. Padberg J-S, Wiesinger A, Marco GSd, Reuter S, Grabner A, et al. (2014) Damage of the endothelial glycocalyx in chronic kidney disease. *Atherosclerosis* in press.
44. Vink H, and Duling BR. (2014) Identification of distinct luminal domains for macromolecules, erythrocytes, and leukocytes within mammalian capillaries. *Circ Res* 79: 581-589
45. van den Berg BM, Nieuwdorp M, Stroes ES, Vink H (2006) Glycocalyx and endothelial (dys) function: from mice to men. *Pharmacol Rep* 58 Suppl: 75-80.

46. Hjalmarsson C, Johansson BR, Haraldsson B (2004) Electron microscopic evaluation of the endothelial surface layer of glomerular capillaries. *Microvasc Res* 67: 9-17.
47. Jeansson M, Bjorck K, Tenstad O, Haraldsson B (2009) Adriamycin alters glomerular endothelium to induce proteinuria. *J Am Soc Nephrol* 20: 114-122.
48. Smith ML, Long DS, Damiano ER, Ley K (2003) Near-wall micro-PIV reveals a hydrodynamically relevant endothelial surface layer in venules in vivo. *Biophys J* 85: 637-645.
49. Nieuwdorp M, Mooij HL, Kroon J, Atasever B, Spaan JA, et al. (2006) Endothelial glycocalyx damage coincides with microalbuminuria in type 1 diabetes. *Diabetes* 55: 1127-1132.
50. Nieuwdorp M, van Haeften TW, Gouverneur MC, Mooij HL, van Lieshout MH, et al. (2006) Loss of endothelial glycocalyx during acute hyperglycemia coincides with endothelial dysfunction and coagulation activation in vivo. *Diabetes* 55: 480-486.
51. Vink H, Constantinescu AA, Spaan JA (2000) Oxidized lipoproteins degrade the endothelial surface layer : implications for platelet-endothelial cell adhesion. *Circulation* 101: 1500-1502.
52. Constantinescu AA, Vink H, Spaan JA (2001) Elevated capillary tube hematocrit reflects degradation of endothelial cell glycocalyx by oxidized LDL. *Am J Physiol Heart Circ Physiol* 280: H1051-1057.
53. Han Y, Weinbaum S, Spaan JA, Vink H (2006) Large-deformation analysis of the elastic recoil of fibre layers in a Brinkman medium with application to the endothelial glycocalyx. *J Fluid Mech* 554: 217-235.
54. Nieuwdorp M, Meuwese MC, Mooij HL, Ince C, Broekhuizen LN, et al. (2008) Measuring endothelial glycocalyx dimensions in humans: a potential novel tool to monitor vascular vulnerability. *J Appl Physiol* (1985) 104: 845-852.
55. Groner W, Winkelmann JW, Harris AG, Ince C, Bouma GJ, et al. (1999) Orthogonal polarization spectral imaging: a new method for study of the microcirculation. *Nat Med* 5: 1209-1212.
56. Donati A, Damiani E, Domizi R, Romano R, Adrario E, et al. (2013) Alteration of the sublingual microvascular glycocalyx in critically ill patients. *Microvasc Res*.
57. Mulders TA, Nieuwdorp M, Stroes ES, Vink H, Pinto-Sietsma SJ (2013) Non-invasive assessment of microvascular dysfunction in families with premature coronary artery disease. *Int J Cardiol*.
58. Lee DH, Dane MJ, van den Berg BM, Boels MG, van Teeffelen JW, et al. (2014) Deeper penetration of erythrocytes into the endothelial glycocalyx is associated with impaired microvascular perfusion. *PLoS One* 9: e96477.
59. Broekhuizen LN, Lemkes BA, Mooij HL, Meuwese MC, Verberne H, et al. (2010) Effect of sulodexide on endothelial glycocalyx and vascular permeability in patients with type 2 diabetes mellitus. *Diabetologia* 53: 2646-2655.
60. Amraoui F, Olde Engberink RH, van Gorp J, Ramdani A, Vogt L, et al. (2014) Microvascular Glycocalyx Dimension Estimated by Automated SDF Imaging is not Related to Cardiovascular Disease. *Microcirculation* 21: 499-505.



3

Prolonged shear stress modifies the composition of the endothelial glycocalyx

In preparation

Martijn JC Dane¹ & Dae Hyun Lee¹, Bernard M. van den Berg¹, Margien GS Boels¹,
Johan van der Vlag², Anton Jan van Zonneveld¹, Ton. J. Rabelink¹

¹*Department of Nephrology, Eindhoven laboratory for Vascular Medicine, LUMC,
Leiden University Medical Centre, The Netherlands* ²*Department of Nephrology, Radboud
Institute for Molecular Life Sciences, Radboud University Medical Center, Nijmegen, the
Netherlands*

Abstract

Throughout the vasculature a gel-like layer consisting of proteoglycans, glycosaminoglycans, glycoproteins and adsorbed plasma molecules covers the endothelium. Within the endothelial glycocalyx (EG) heparan sulfates and hyaluronan have been proposed to be the most important functional components. The EG has been demonstrated to regulate vascular permeability, transduce shear stress and bind chemokines and growth factors. Glycocalyx dimension and composition both have been shown to be crucial for endothelial function. We hypothesized that long-term continuous laminar shear stress induces changes in the EG composition. For this purpose, human umbilical vein endothelial cells (HUVECs) were cultured under flow for 7 days. Using wheat germ agglutinin (WGA) and the carbohydrate specific antibodies 10E4 and JM403, we observed an increased density and thickness of carbohydrates on top of the endothelium and a change in heparan sulfate composition within the endothelial glycocalyx. Furthermore, by blocking the JM403 epitope within HS in static conditions, we observed a reduction of THP-1 monocyte adhesion upon TNF- α stimulation, confirming the predicted pro-inflammatory role of the JM403 binding epitope. Consequently, the observed reduction in JM403 epitope expression within heparan sulfate suggests that long-term shear stress leads to a glycocalyx with anti-inflammatory properties.

Introduction

Throughout the vasculature, the endothelium is covered by a membrane-bound glycocalyx with adsorbed plasma proteins [1,2]. The membrane bound part of the glycocalyx contains glycoproteins, glycosaminoglycans and proteoglycans (PG), i.e. core proteins with long side-branches that consist of repeated disaccharide glycosaminoglycans (GAGs). Examples of GAGs present in the endothelial glycocalyx are heparan sulfate (HS), hyaluronan (HA) and chondroitin sulfate (CS) [2].

Heparan sulfate is attached to membrane bound core-proteins such as syndecans 1 and -4, glypican-1 and versican, forming proteoglycans. Starting with glycosylation at serine residues on a core protein, HS and CS GAGs are produced in the Golgi apparatus. Here, especially HS is extensively modified. N-Deacetylase/N-Sulfotransferase (NDST) modifies the N-acetylglucosamine by N-deacetylation or subsequent N-sulfation, while some glucuronic acids are epimerized to L-iduronic acid (IdoA). Hereafter, the sulfation pattern of the HS chain is modified by several sulfotransferases, which sulfates C2 of the uronic acids and C6 (and rarely C3) of the glucosamine residues. After modification, the HSPG is transported to the membrane where it can be modified again by endosulfatases (SULF1 and SULF2) and heparanases. In contrast to heparan sulfates, hyaluronan is not directly attached to the membrane via a core-protein, but can be bound to hyaluronan synthase, CD44, or hyaluronidase. Hyaluronan can also be cross-linked by various hyaluronan binding proteins, such as versican, aggrecan, neurocan and tumor necrosis factor-stimulated gene 6 (TSG-6), some of which are also able to bind HS [3,4]. This interconnected matrix of carbohydrates has been proposed to be involved in almost all functions of the endothelial layer, such as inflammation, coagulation, permeability, shear sensing and regulation of perfusion [2,5,6]. Perturbation of this layer has been associated with cardiovascular disease, sepsis, renal failure and diabetes [5].

While HS functions as an interactive matrix for protein interaction, the GAG composition is critical for the function of the EG and the underlying endothelium. In particular, variation in HS disaccharide sequence and sulfation patterns determines binding properties for circulating proteins [7,8]. Binding of growth factors, such as FGF-2 and VEGF, or cytokines have been shown to be critically dependent on binding to specific sulfated HS moieties, generating gradients (e.g. chemokines) over the endothelium to guide cells towards the underlying tissue or concentrate factors near their receptor (e.g. growth factors) [9-11]. HS are made up of up to 150 modified disaccharide units, which allow for a high variety in binding sites for different proteins [7,9,12]. Consequently, HS are involved in many cellular processes such as attachment, migration, differentiation, blood coagulation, lipid metabolism, and inflammation [7]. Because the production of HS is continuously ongoing and the sulfation pattern can be rapidly modified by enzymes such as sulfotransferases and sulfatases, protein binding specificity can be rapidly adjusted upon changes in the environment [13,14].



In vitro, the endothelial surface layer lacks most of its barrier function in cultured HUVECs when compared to the in vivo situation [15,16]. In addition, the endothelial glycocalyx dimensions observed in vitro are reduced [17]. One of the explanations for these differences between in vivo and in vitro is lack of a proper endothelial environment during culture [18-20]. Especially, shear stress has been shown to be involved in glycocalyx production and function. For example, shear stress has been shown to result in incorporation of hyaluronan within the endothelial glycocalyx [21]. In vivo, perturbation of the endothelial glycocalyx was observed in areas of disturbed flow, areas that are also vulnerable for development of atherosclerosis [22-24]. These findings have been also demonstrated in cultured endothelial cells through the exposure to either atheroprone or atheroprotective waveforms during prolonged culture and suggest that uniform laminar shear stress is beneficial for presence of a healthy endothelial glycocalyx [25].

In this study we hypothesized that prolonged laminar shear stress leads to compositional, dimensional and consequently also functional changes within the endothelial glycocalyx. To study this, primary isolated human umbilical vein endothelial cells (HUVECs) were cultured under continuous laminar flow (shear stress is 10 dyne/cm²) for 7 days. Wheat germ agglutinin (WGA) was used to quantify the total amount of carbohydrates on top of the endothelial cell. Compositional changes were studied using antibodies against different HS moieties (domains). For this we used HS antibodies 10E4 and JM403, since the cell-associated HS-epitope necessary for binding is known for both of these antibodies: 10E4 mainly binds to mixed HS domains, containing both N-acetylated and N-sulfated disaccharide units [26], whereas JM403 binding depends on the presence of N-unsubstituted glucosamine [27]. Functional changes within the glycocalyx were examined by analyzing the role of the JM403 binding epitope in monocytic THP-1 cell adhesion.

Material and methods

Cells

HUVECs were isolated from umbilical cords by perfusion, and 20 minutes incubation, with trypsin at 37°C. Freshly isolated HUVECs were cultured on 0.5% gelatin coated 75 cm² flasks (Greiner Bio-one) in EGM2 medium (Lonza, Basel, Switzerland) supplemented with antibiotics/antimycotics (Life technology, Carlsbad, California, USA) and used for experiments at passage 1-3.

Flow experiments

Flow experiments were performed using an ibidi flow system (Ibidi, Martinsried, Germany). HUVECs were seeded into closed perfusion chambers (ibiTreat 0.4 µ-Slide I or VI, Luer) at a concentration of 1.5x10⁶ cells per mL. Cells were allowed to adhere for 3 hours. Hereafter, the chamber was connected to a computer-controlled air pressure pump and a fluidic unit with a two-way switching valve. The pump setup allowed pumping of 16 mL cell culture medium from two reservoirs in a unidirectional way through the flow channel over the monolayer of endothelial cells at a constant shear stress of 10 dyne/cm². Medium was refreshed after 1 and 4 days of culture. The chamber and the reservoirs containing the medium were kept in an incubator at 37°C and 5% CO₂. RNA was isolated from cells subjected to shear stress in a 0.4 µ-Slide I Luer flow chamber, while the 6 lanes of a 0.4 µ-Slide VI Luer were used for immunofluorescent staining experiments.

RNA Isolation and qRT-PCR

Total RNA was isolated from HUVECs cultured in a µ-Slide using Trizol reagent (Life Technologies, Carlsbad, California, USA) and isolation kit (Qiagen, Hilden, Germany). Reverse transcription was performed using a 5 minute 65°C incubation of 500 ng total RNA with deoxyribonucleotide triphosphates (Life Technologies) and oligo(dT) (Life Technologies), cDNA was synthesized using M-MLV First-Strand Synthesis (Life Technologies), and detection was carried out using SYBR Green Master Mix (Life technologies). Levels of expression were determined by normalizing to GAPDH levels.

Cell culture and confocal immunofluorescence microscopy

After static culture (24 hours) or exposure to flow (24 hours or 7 days), HUVECs were fixed in freshly made 4% paraformaldehyde in HBSS for 10 minutes, washed twice with HBSS (life technologies) and blocked for 30 minutes with 3% normal goat serum (NGS) in HBSS. Cells were incubated overnight (16 hours) at 4°C with 10 µg/mL TRITC-labeled wheat germ agglutinin (WGA) (Sigma-Aldrich, St Louis, MA, USA), Hoechst 33528 (Sigma-Aldrich, 1:5000) and one of the primary antibodies (at 10 µg/mL): 10E4 (Amsbio), JM403 (kind gift of dr. van der Vlag, Radboud University Medical Centre, Nijmegen, The Netherlands), eNOS (BD bioscience), VE-cadherin (BD bioscience), phalloidin-rhodamine (Sigma-Aldrich), or the appropriate control IgM or IgG isotype antibodies diluted in HBSS. After washing three times with HBSS, cells were incubated with a secondary antibody for 1 hour (2 µg/mL of anti-mouse IgM-Alexa488 or anti-mouse IgG-



Alexa488). Cells were again washed for three times with HBSS and imaged using a Leica SP5 confocal microscope and a 63x (N.A. 1.4) objective.

Mononuclear cell adhesion assays

Mononuclear THP-1 cell adhesion assay was performed as published previously with some modifications [28]. In short, HUVECs (1.5×10^6 cells/mL in EGM2 medium) were seeded into closed perfusion chambers (ibiTreat 0.4 μ -Slide VI Luer). After 24 hours of static culture the monolayer of endothelial cells was stimulated with TNF- α (10 ng/ml) for 5 hours. Cells were washed with HBSS containing 1% BSA cells and incubated with either JM403 or IgM isotype control (both 10 μ g/mL) for 1 hour at room temperature. Next, flow chambers were positioned on an inverted microscope (Leica AF6000) and attached to a syringe pump to perfuse the endothelial monolayer with THP-1 monocytes (5×10^5 cells/mL in HBSS + 1% BSA). THP-1 cells were perfused over the EC layer for 5 minutes at 0.5 dyne/cm² after which the monolayer was washed with HBSS + 1% BSA for 5 minutes. Flow chambers were imaged at 10 different locations. All images were taken at the centerline of the flow chamber. The number of adherent cells per field of view was quantified using the public domain National Institutes of Health IMAGE program (ImageJ, available at <http://rsb.info.nih.gov/nih-image>).

CLSM image analysis and quantification

Confocal 12-bit gray-scale axial image stacks (xyz dimensions, $0.08 \times 0.08 \times 0.13$ μ m) that covered 6724 μ m² of surface area per image and a height of 5 to 10 μ m above the EC nuclear plane were recorded using LAS-AF image software (Leica). The image stacks were analyzed using ImageJ software. For the luminal endothelial glycocalyx quantification, first the nuclear and peri-nuclear area was selected, to exclude the cell area in which the cell thickness was too thin to differentiate between luminal and abluminal staining. Thickness of the WGA stained layer was estimated within this area of interest, between the peak nuclear (Hoechst) signal and the luminal end of WGA fluorescence, designated as twice the background signal. Next, total luminal WGA signal of the 3 dimensional area of interest was calculated from the sum of average fluorescence in every z-plane within this area. In addition, heterogeneity in WGA distribution was determined by calculating the coefficient of variance between these planes. To quantify specific staining for the HS moiety antibodies, total isotype control (IgM) signal was subtracted from the total $10E4$ or JM403 signal. A visualization of this method is shown in **figure 1**.

Statistical analyses

Data are presented as mean \pm SEM, unless stated otherwise. To exclude variations due to technical differences between the experiments, fold change of staining intensity and coefficient of variances were shown relative to the static control group. Differences between the groups were tested by analysis of variance (ANOVA). Differences were considered statistically significant if $p < 0.05$. Data analysis was performed using SPSS version 20.0 (SPSS Inc, Chicago, IL) and GraphPad Prism, version 5.0 (GraphPad Prism Software Inc, San Diego, CA).

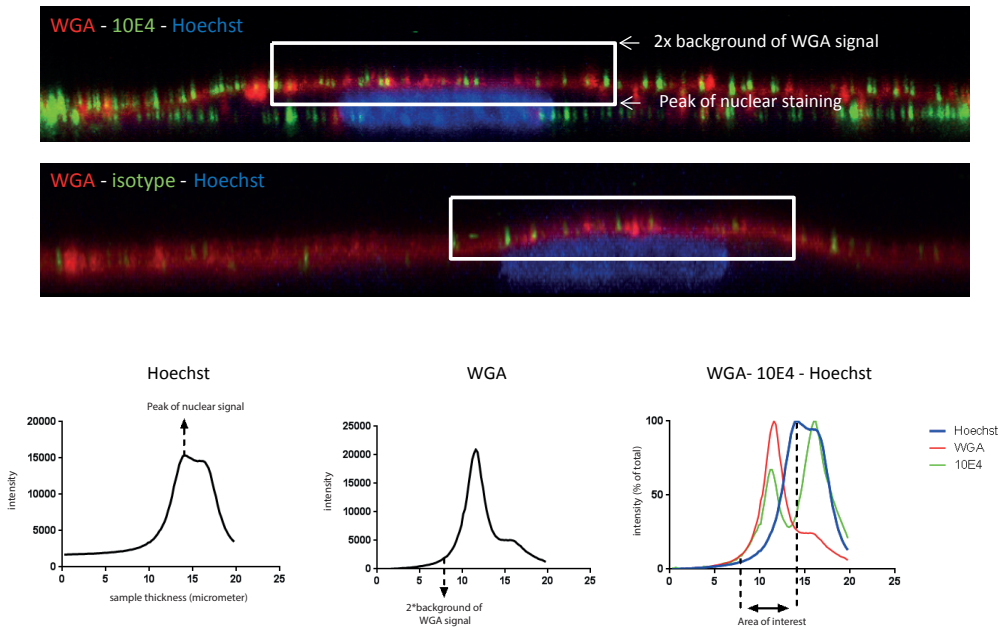


Figure 1: Methods to quantify the luminal endothelial glycocalyx stainings. A) Method to quantify the luminal glycocalyx. Example of endothelial glycocalyx stained with wheat germ agglutinin (WGA), 10E4 and Hoechst. White box shows the area of interest which should be quantified (upper). B) Example of endothelial glycocalyx stained with wheat germ agglutinin (WGA), IgM isotype control and Hoechst. Total signal within the white box was subtracted from total signal of the HS staining to control for non-specific staining. C) Example of quantification method. Peak of Hoechst signal determines the lower border of the area of interest (left). 2x WGA background signal is used to determine the upper border of the area of interest (middle). Total area under the curve of the area of interest is used to determine the total luminal signal. Thickness of area of interest is used to determine dimensions of WGA signal.



Results

Prolonged laminar flow leads to a quiescent monolayer of HUVECs

HUVECs were cultured under a laminar flow of 10 dyne/cm² for 7 days to confirm the ability to induce a quiescent endothelial phenotype.(20) First, the effect of prolonged shear stress on endothelium was tested by analyzing cell morphology and expression of shear responsive genes and proteins. After 7 days at 10 dyne/cm², shear stress sensitive genes Krüppel-like Factor 2 (KLF2) and endothelial nitric oxide synthase (NOS3) were up regulated compared to static cultured cells (14.1% to 1.7%, p<0.05 for KLF2 and 8.9% to 2.3%, p<0.01 for eNOS, relative to GAPDH expression respectively). In contrast, gene expression of the inflammatory markers E-selectin and IL-8 decreased after 7 days of flow culture (**figure 2**). The inflammatory marker IL-8, however, dramatically increased after 24 hours of culture under flow (0.2% to 24.2% of GAPDH expression levels, static vs. flow 24hrs, respectively), which confirms previous data showing an acute inflammatory response upon short-term exposure to shear stress [29].

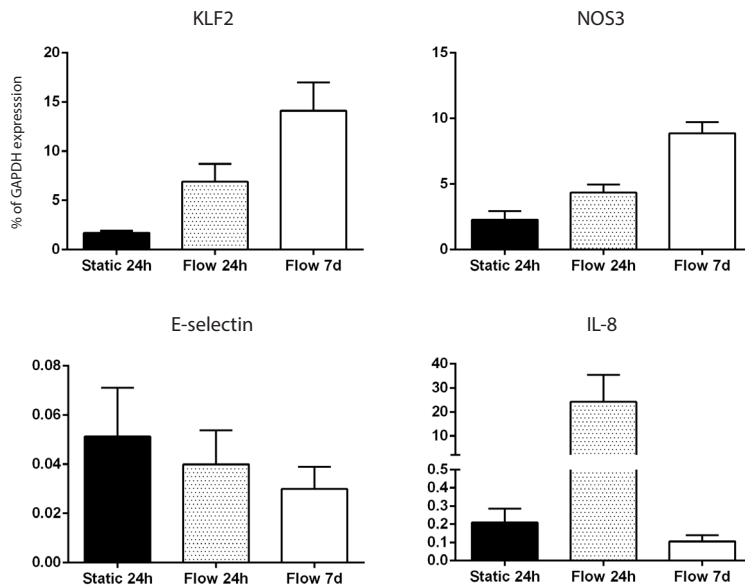


Figure 2: Effects of prolonged shear stress on gene expression of shear responsive genes. Gene expression as percentage of GAPDH expression after static, 1 day flow and 7 days of flow culture for KLF2, eNOS, E-selectin and IL-8.

In addition, typical short F-actin shear fibers and alignment to the direction of the flow was observed after the prolonged shear culture [30] and VE-cadherin and eNOS expression both were increased and robustly expressed at the cell-cell contacts (**figure 3**).

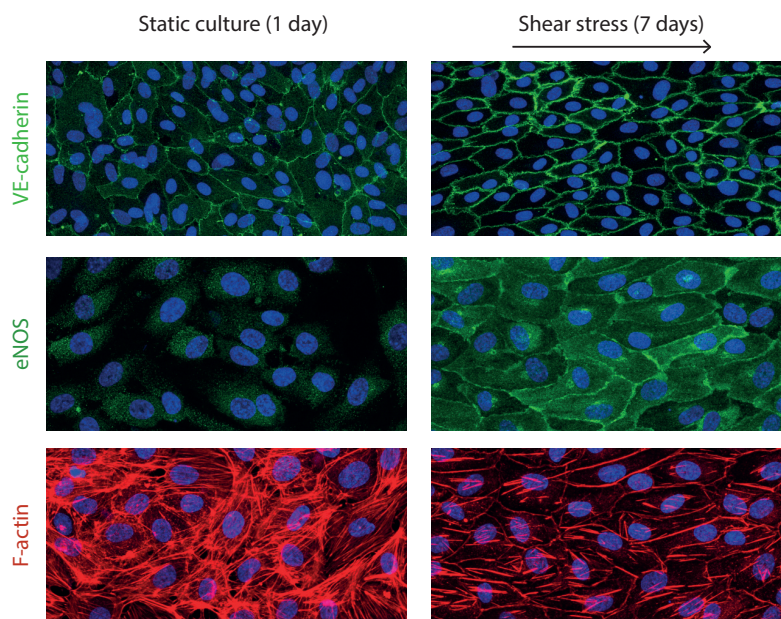


Figure 3: Cells change upon prolonged shear stress culture. HUVECs are stained with antibodies against VE-cadherin (upper) and eNOS (middle) and the F-actin binding phalloidin-rhodamine (lower) to visualize endothelial phenotypic changes. Static cultured HUVECs (left) were compared to HUVECs cultured for 7 days at a shear stress of 10 dynes/cm².

Laminar shear stress induces a thicker glycocalyx

Next, we tested our hypothesis that this prolonged exposure leads to changes in endothelial glycocalyx production and composition. For this, we stained the EC after indicated time periods with the N-acetylneuraminic acid and N-acetyl- β -D-glucosamine binding lectin WGA and the specific HS-binding antibodies 10E4 and JM403. After 7 days of exposure to 10 dyne/cm² shear stress, total intensity of WGA staining was significantly increased compared to static conditions (1.49 fold increase, $p < 0.05$) (**figure 4**). EG thickness was also increased after 7 days of shear stress compared to both 24hrs of static culture and 24hrs of shear stress (3.10 vs 2.52 and 2.61 μm respectively, $p < 0.01$ and $p < 0.05$). Besides this notable increase in WGA intensity and thickness, a more homogeneously distributed layer was observed (reflected by the lowest coefficient of variance: 0.84 fold change compared to 24hrs of static culture, $p < 0.05$).

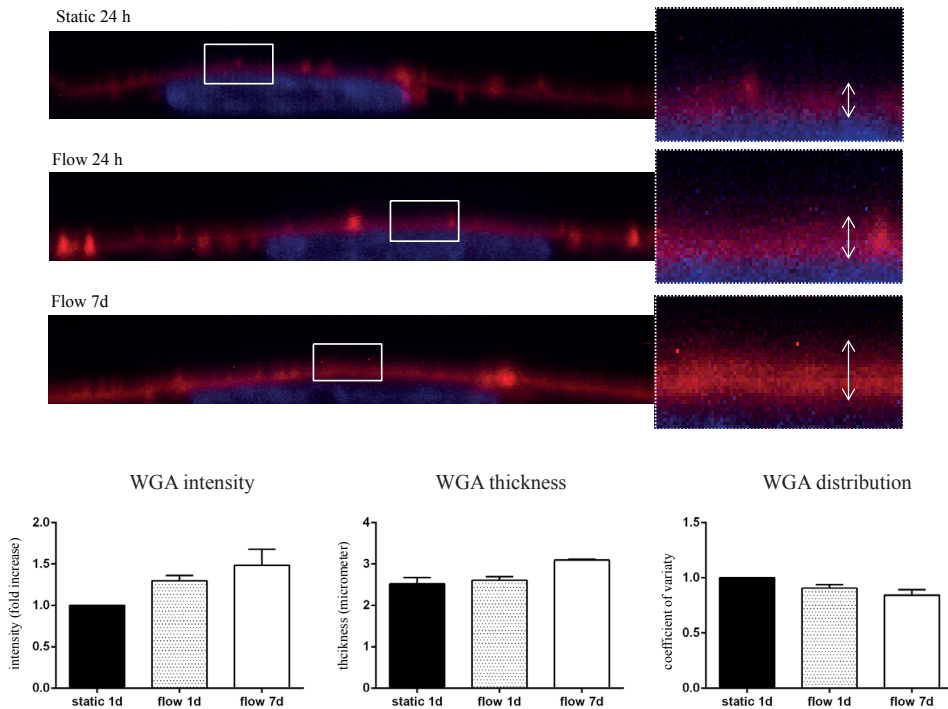


Figure 4: Prolonged shear stress increases WGA thickness and density on top of HUVECs. A) Representative examples of WGA staining on top of the endothelial cells. White box shows the zoomed area (right). B) Quantification method described in figure 2 was used for the stainings in A). Within the area of interest the total intensity (left), thickness of the stained area (middle) and distribution on top of the endothelium (right) was measured.

Laminar shear stress induces a change in enzymes involved in glycocalyx modification.

Production and composition of the endothelial glycocalyx are determined by the presence and activity of several enzymes. Changes in each of these enzymes can result in functional changes of the endothelial glycocalyx. To determine whether the composition of heparan sulfates within the endothelial glycocalyx could be changed by changes in gene expression upon shear stress, gene expression levels of enzymes involved in HS sulfation pattern modification were studied. Seven days of flow exposure did not alter N-deacetylase/N-sulfotransferase-1 and -2 (NDST1, NDST2) expression (data not shown).

Nevertheless, the intracellular HS-chain modifying heparan sulfate sulfotransferases (HS2ST1, HS3ST1 and HS6ST1) were variably changed upon shear stress stimulation. In addition, the extracellular modifying enzymes 6-O-endosulfatase 1 and 2 (SULF1, SULF2) and heparanase (HPSE1) were all increased upon 7 days of shear stress (figure 5). Next to enzymes involved in heparan sulfate production, the gene expression of the hyaluronan synthesizing enzyme HAS2 was increased after prolonged shear stress (no changes were observed for HAS1 or HAS3) and was accompanied by an increase in the hyaluronan degrading enzyme hyaluronidase 2 (HYAL2) gene expression.

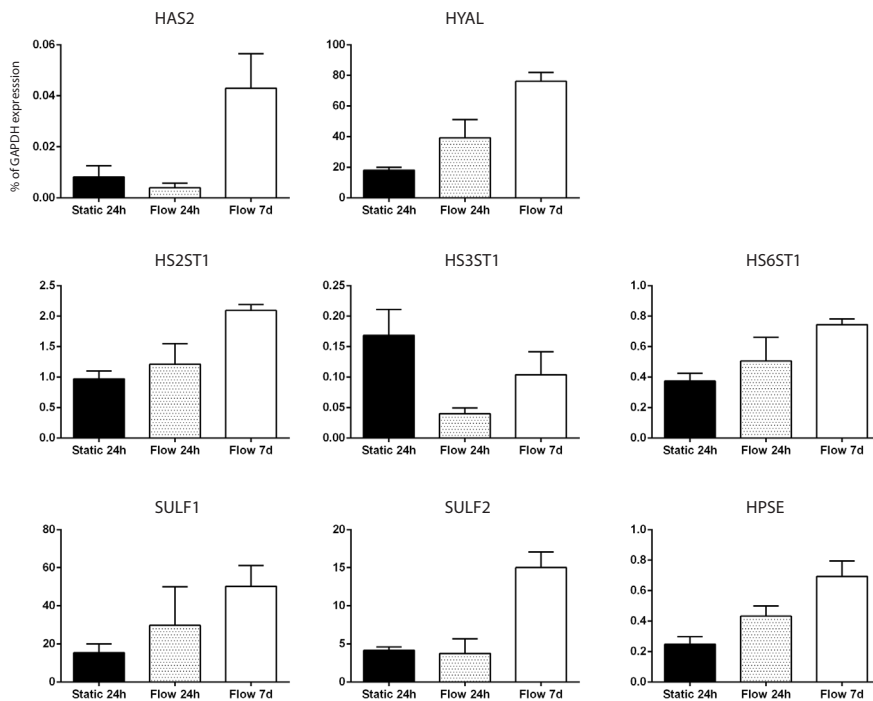


Figure 5: Prolonged shear stress alters gene expression of enzymes involved in HS and HA production and modification. Gene expressions as percentage of GAPDH expression after static, 1 day flow and 7 days of flow culture for the genes coding for enzymes involved in HA production (HAS2) and breakdown (HYAL) and HS sulfation pattern modification (HS2ST1, HS3ST1, HS6ST1, SULF1, SULF2) and breakdown (HPSE).

Prolonged Shear stress induces changes in luminal heparan sulfate composition

The HS modifying enzyme gene expression indicates that the chain is compositionally altered upon prolonged shear stress. This was tested further using binding of antibodies against two different HS domains. The expression of specific HS domains was studied after 1 and 7 days of shear stress and was compared to static control conditions. For this purpose, two antibodies against HS domains (JM403, 10E4) were used. Interestingly, total JM403 signal was significantly increased after 1 day of culture under shear stress (total signal intensity of 72290 ± 19400 vs 34928 ± 11937 in static culture, $p < 0.05$) (figure 6).

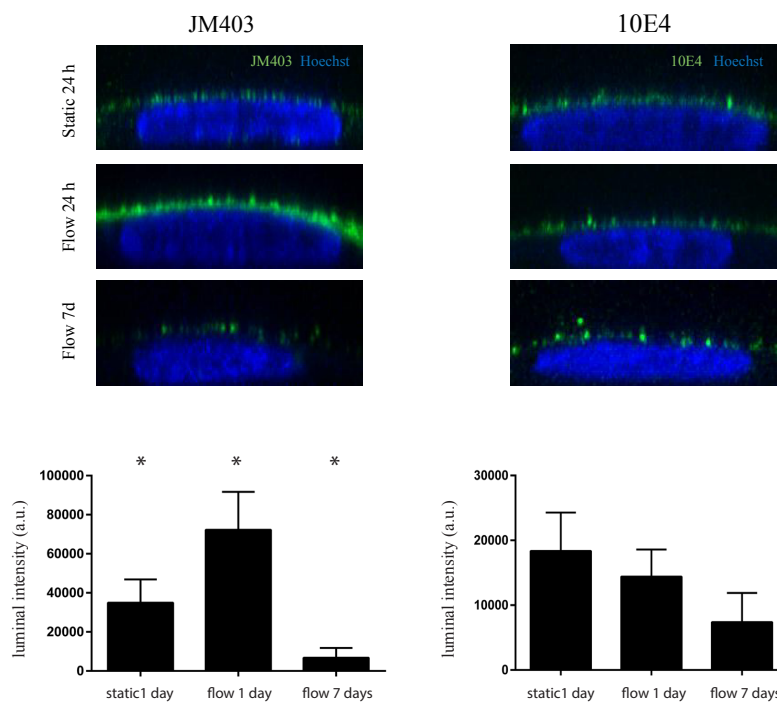


Figure 6: Prolonged shear stress alters the expression of heparan sulfate domains. A) Representative examples of HS staining on top of the endothelial cells with JM403 (left) and 10E4 (right) after static, 1 day flow and 7 days of flow culture. B) Quantification of staining with specific HS-domain antibodies JM403 (left) and 10E4 (right). For quantification, isotype control staining is subtracted from the stainings shown in figure 6A.

However, after 7 days of flow the total luminal staining signal was markedly reduced for JM403 compared to both static culture and 1 day shear stress (total signal intensity of 6786 ± 5022 , $p < 0.05$) (**figure 6**). In contrast, total 10E4 signal was not significantly changed, although a trend towards a reduction could be observed during 7 days of flow. Both antibody expression levels thereby suggest that exposure to shear stress results in the modification of the luminal heparan sulfate composition in HUVECs bearing less N-substituted residues

Laminar shear stress induces an anti-inflammatory glycocalyx

Both JM403 and L-selectin have been previously shown to require the presence of N-unsubstituted glucosamine residues to bind to HS [27,31]. Consequently, we predicted that the JM403 epitope could be a pro-inflammatory HS domain. In our study, this would imply that the increase in JM403 after 24 hours and the decrease after 7 days flow, reflect a pro- and anti-inflammatory phenotype, respectively. To study this hypothesis, the capacity of the JM403 epitope to mediate monocyte recruiting and adhesion was tested. For this purpose, static cultured HUVECS were stimulated with TNF- α to enable inflammatory cell adhesion. Consequently, these cells were perfused with THP-1 monocytes. To determine the role of the JM403 epitope in adhesion, the assay was performed after blocking the epitope with JM403 antibodies or an appropriate isotype control. Blocking the JM403 domain on the endothelial cell surface with JM403 antibody specifically reduced adhesion of the mononuclear THP-1 cells (71.7% of control adhesion, $p < 0.01$) (**figure 7**).



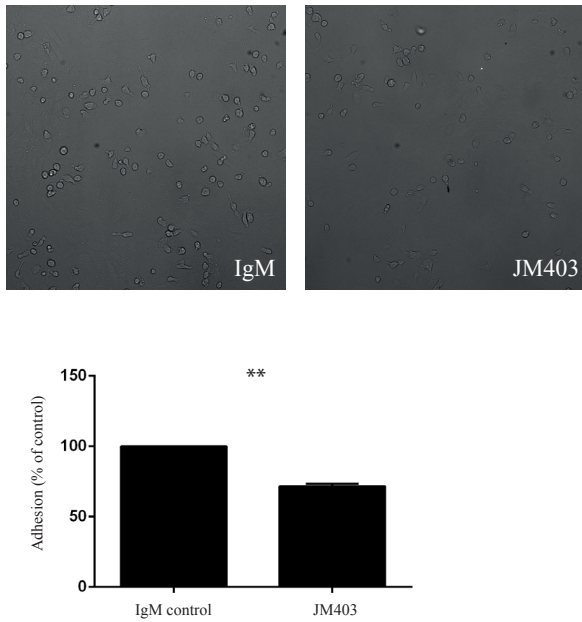


Figure 7: Monocyte adhesion after blocking the JM403 epitope in cultured HUVECs. A) Examples of monocytes adhered to the endothelial layer after blocking with JM403 (right) and a control IgM antibody (left). B) Quantification of A. Number of adhered monocytes where corrected after blocking for JM403 were corrected for the number adhered in the control situation.

Discussion:

Changing the endothelial environment in vitro through exposing the cells to a prolonged uniform laminar shear stress not only induces a more homogeneously distributed and thicker glycocalyx but also changes heparan sulfate composition of surface expressed HSPG leading to a non-inflammatory, non-adhering phenotype.

While previous studies already have suggested a role for shear stress in expression and function of an endothelial glycocalyx [21,25,32,33], we focused in this study on the compositional and functional changes in the luminal endothelial glycocalyx upon exposure to long-term shear stress. To quantify the luminal stained endothelial glycocalyx we reconstructed this layer to a 3-dimensional image to properly distinct luminal from abluminal staining. In contrast to the observed effects of long-term shear stress exposure, we confirmed with the observed increase in IL-8 levels after 24 hours of shear stress previous data that short-term exposure to high laminar shear stress evokes a profound inflammatory response in endothelial cells instead of inducing a quiescent phenotype [29]. Furthermore, the subsequent decrease in IL-8 after 7 days reveals that prolonged exposure to such shear stress induces the quiescent phenotype, as exemplified by induction of the well-known shear-responsive genes, such as KLF2 and eNOS. Together, with rearranging of VE-cadherin and eNOS proteins into cell-cell contacts and the appearance of typical short stranded f-actin filaments at the abluminal endothelial domain.

After subjecting the cells to shear stress we observed an increase in WGA staining intensity and thickness after 7 days. WGA binds N-acetyl-D-glucosamine which enables us to estimate changes in the endothelial glycocalyx dimensions, since this carbohydrate is present in most of the glycocalyx components (except for chondroitin and dermatan sulfate). Interestingly we also observed a more homogeneous distribution of the WGA staining on top of the endothelial layer. Previously a decrease of WGA staining was observed upon stimulating endothelial cells with ROS [34]. Furthermore, WGA staining on endothelial cells in rat glomeruli was decreased in a model of spontaneous kidney failure in aged rats [35].

Since WGA stains most of the subcomponents of the endothelial glycocalyx, the biochemical composition of the glycocalyx cannot be studied directly using this lectin. Since the specific composition could be crucial for endothelial cell function we used the following HS-domain specific antibodies 10E4 and JM403. While 10E4 mainly recognizes mixed HS domains that contains both N-acetylated and N-sulfated disaccharide units [26], JM403 typically needs the relatively rare N-unsubstituted glucosamine residues within the HS chain to be able to bind [27]. The presence of this N-unsubstituted domain within the HS sequence mostly likely depends on the activity and efficiency of the NDST enzymes. These enzymes modify the HS sequence during the modification process by substituting the acetyl group from glucosamine residues with sulfate, via an N-unsubstituted intermediate. However, sometimes this modification is partial, which then results in N-unsubstituted



domains in mature HS [36-38]. Since under normal, healthy, circumstances this domain occurs relatively rare, it has been proposed that due to pathological processes this domain contributes to selective protein, and or receptor binding [39].

To the best of our knowledge, we are the first to study the specifically luminal expressed JM403 epitope in HS, since most studies only investigated JM403 binding within the ECM. Interestingly, JM403 staining was significantly increased after 24 hours. After 7 days of shear culture, hardly any JM403 staining was observed. The observed increase after 1 day coincided with a pro-inflammatory phenotype, since IL-8 expression was 100-fold increased. This might imply a relation between the JM403 epitope within HS and a pro-inflammatory endothelial phenotype. The observation that this epitope for JM403 binding, a domain with N-unsubstituted glucosamine residues, is involved in THP-1 adhesion further supports this hypothesis. Since it has been shown that endothelial HS that are able to bind L-selectin are enriched for N-unsubstituted glucosamine residues [31], the observed reduction in monocyte adhesion might be L-selectin dependent. In addition to the quiescent endothelial phenotype, this indicates that prolonged shear stress induces an anti-inflammatory HS modification. In contrast, a short period of shear stress leads to a pro-inflammatory phenotype of the cell (high IL-8 gene expression) and glycocalyx (high JM403 staining).

Although the changes in EG are clearly observed after 7 days of shear stress culture, we cannot be sure that shear stress is the single responsible stimulus. Prolonged culture of endothelial cells under static conditions has been shown previously to also induce endothelial glycocalyx growth [40]. However, when endothelial cells were cultured under static conditions for 7 days, they slowly continued to proliferate and eventually formed several cell layers without any organization. This made it practically impossible to compare the glycocalyx on top of 7 days cultured cells in static conditions with the monolayer in flow conditions (data not shown).

Altogether we demonstrated that prolonged fluid shear stress alters the composition and structure of the endothelial glycocalyx. Shear stress induces the production of a thicker and more homogeneously distributed layer which. Furthermore, the altered HS composition results in the decrease of the epitope for JM403 binding, which is indicative for a more anti-inflammatory endothelial glycocalyx upon prolonged shear stress stimulation.

Acknowledgements:

Financial Support by the Dutch Kidney Foundation grants C08.2265 & C09.03.

References

1. Weinbaum S, Tarbell JM, Damiano ER (2007) The structure and function of the endothelial glycocalyx layer. *Annu Rev Biomed Eng* 9: 121-167.
2. Reitsma S, Slaaf DW, Vink H, van Zandvoort MA, oude Egbrink MG (2007) The endothelial glycocalyx: composition, functions, and visualization. *Pflugers Arch* 454: 345-359.
3. Wheeler-Jones CP, Farrar CE, Pitsillides AA (2010) Targeting hyaluronan of the endothelial glycocalyx for therapeutic intervention. *Curr Opin Investig Drugs* 11: 997-1006.
4. Lennon FE, Singleton PA (2011) Hyaluronan regulation of vascular integrity. *Am J Cardiovasc Dis* 1: 200-213.
5. Broekhuizen LN, Mooij HL, Kastelein JJ, Stroes ES, Vink H, et al. (2009) Endothelial glycocalyx as potential diagnostic and therapeutic target in cardiovascular disease. *Curr Opin Lipidol* 20: 57-62.
6. Lee DH, Dane MJ, van den Berg BM, Boels MG, van Teeffelen JW, et al. (2014) Deeper penetration of erythrocytes into the endothelial glycocalyx is associated with impaired microvascular perfusion. *PLoS One* 9: e96477.
7. Esko JD, Selleck SB (2002) Order out of chaos: assembly of ligand binding sites in heparan sulfate. *Annu Rev Biochem* 71: 435-471.
8. Rops AL, Jacobs CW, Linssen PC, Boezeman JB, Lensen JE, et al. (2007) Heparan sulfate on activated glomerular endothelial cells and exogenous heparinoids influence the rolling and adhesion of leucocytes. *Nephrol Dial Transplant* 22: 1070-1077.
9. Esko JD, Lindahl U (2001) Molecular diversity of heparan sulfate. *J Clin Invest* 108: 169-173.
10. Quarto N, Amalric F (1994) Heparan sulfate proteoglycans as transducers of FGF-2 signalling. *J Cell Sci* 107 (Pt 11): 3201-3212.
11. Yayon A, Klagsbrun M, Esko JD, Leder P, Ornitz DM (1991) Cell surface, heparin-like molecules are required for binding of basic fibroblast growth factor to its high affinity receptor. *Cell* 64: 841-848.
12. Lindahl U, Kusche-Gullberg M, Kjellen L (1998) Regulated diversity of heparan sulfate. *J Biol Chem* 273: 24979-24982.
13. Kolset SO, Reinholt FP, Jenssen T (2012) Diabetic nephropathy and extracellular matrix. *J Histochem Cytochem* 60: 976-986.
14. Uchimura K, Lemjabbar-Alaoui H, van Kuppevelt TH, Rosen SD (2010) Use of a phage display antibody to measure the enzymatic activity of the Sulfs. *Methods Enzymol* 480: 51-64.
15. Potter DR, Damiano ER (2008) The hydrodynamically relevant endothelial cell glycocalyx observed in vivo is absent in vitro. *Circ Res* 102: 770-776.
16. Smith ML, Long DS, Damiano ER, Ley K (2003) Near-wall micro-PIV reveals a hydrodynamically relevant endothelial surface layer in venules in vivo. *Biophys J* 85: 637-645.
17. Chappell D, Jacob M, Paul O, Rehm M, Welsch U, et al. (2009) The glycocalyx of the



- human umbilical vein endothelial cell: an impressive structure *ex vivo* but not in culture. *Circ Res* 104: 1313-1317.
18. van Thienen JV, Fledderus JO, Dekker RJ, Rohlena J, van Ijzendoorn GA, et al. (2006) Shear stress sustains atheroprotective endothelial KLF2 expression more potently than statins through mRNA stabilization. *Cardiovasc Res* 72: 231-240.
 19. Dekker RJ, van Thienen JV, Rohlena J, de Jager SC, Elderkamp YW, et al. (2005) Endothelial KLF2 links local arterial shear stress levels to the expression of vascular tone-regulating genes. *Am J Pathol* 167: 609-618.
 20. Dekker RJ, van Soest S, Fontijn RD, Salamanca S, de Groot PG, et al. (2002) Prolonged fluid shear stress induces a distinct set of endothelial cell genes, most specifically lung Kruppel-like factor (KLF2). *Blood* 100: 1689-1698.
 21. Gouverneur M, Spaan JA, Pannekoek H, Fontijn RD, Vink H (2006) Fluid shear stress stimulates incorporation of hyaluronan into endothelial cell glycocalyx. *Am J Physiol Heart Circ Physiol* 290: H458-452.
 22. Gouverneur M, Berg B, Nieuwdorp M, Stroes E, Vink H (2006) Vasculoprotective properties of the endothelial glycocalyx: effects of fluid shear stress. *J Intern Med* 259: 393-400.
 23. van den Berg BM, Spaan JA, Vink H (2009) Impaired glycocalyx barrier properties contribute to enhanced intimal low-density lipoprotein accumulation at the carotid artery bifurcation in mice. *Pflugers Arch* 457: 1199-1206.
 24. van den Berg BM, Spaan JA, Rolf TM, Vink H (2006) Atherogenic region and diet diminish glycocalyx dimension and increase intima-to-media ratios at murine carotid artery bifurcation. *Am J Physiol Heart Circ Physiol* 290: H915-920.
 25. Koo A, Dewey CF, Jr., Garcia-Cardena G (2013) Hemodynamic shear stress characteristic of atherosclerosis-resistant regions promotes glycocalyx formation in cultured endothelial cells. *Am J Physiol Cell Physiol* 304: C137-146.
 26. van den Born J, Salmivirta K, Henttinen T, Ostman N, Ishimaru T, et al. (2005) Novel heparan sulfate structures revealed by monoclonal antibodies. *J Biol Chem* 280: 20516-20523.
 27. van den Born J, Gunnarsson K, Bakker MA, Kjellen L, Kusche-Gullberg M, et al. (1995) Presence of N-unsubstituted glucosamine units in native heparan sulfate revealed by a monoclonal antibody. *J Biol Chem* 270: 31303-31309.
 28. Voyvodic PL, Min D, Liu R, Williams E, Chitalia V, et al. (2014) Loss of Syndecan-1 Induces a Pro-inflammatory Phenotype in Endothelial Cells with a Dysregulated Response to Atheroprotective Flow*. *Journal of Biological Chemistry* 289: 9547-9559.
 29. Boon RA, Horrevoets AJ (2009) Key transcriptional regulators of the vasoprotective effects of shear stress. *Hamostaseologie* 29: 39-40, 41-33.
 30. Boon RA, Leyen TA, Fontijn RD, Fledderus JO, Baggen JM, et al. (2010) KLF2-induced actin shear fibers control both alignment to flow and JNK signaling in vascular endothelium. *Blood* 115: 2533-2542.
 31. Norgard-Sumnicht K, Varki A (1995) Endothelial heparan sulfate proteoglycans that bind to L-selectin have glucosamine residues with unsubstituted amino groups. *J Biol Chem* 270: 12012-12024.

32. Ebong EE, Lopez-Quintero SV, Rizzo V, Spray DC, Tarbell JM (2014) Shear-induced endothelial NOS activation and remodeling via heparan sulfate, glypican-1, and syndecan-1. *Integr Biol (Camb)* 6: 338-347.
33. Bai K, Wang W (2013) Shear stress-induced redistribution of the glycocalyx on endothelial cells in vitro. *Biomech Model Mechanobiol*.
34. Singh A, Ramnath RD, Foster RR, Wylie EC, Friden V, et al. (2013) Reactive oxygen species modulate the barrier function of the human glomerular endothelial glycocalyx. *PLoS One* 8: e55852.
35. Salmon AH, Ferguson JK, Burford JL, Gevorgyan H, Nakano D, et al. (2012) Loss of the endothelial glycocalyx links albuminuria and vascular dysfunction. *J Am Soc Nephrol* 23: 1339-1350.
36. Toida T, Yoshida H, Toyoda H, Koshiishi I, Imanari T, et al. (1997) Structural differences and the presence of unsubstituted amino groups in heparan sulphates from different tissues and species. *Biochem J* 322 (Pt 2): 499-506.
37. Westling C, Lindahl U (2002) Location of N-unsubstituted glucosamine residues in heparan sulfate. *J Biol Chem* 277: 49247-49255.
38. Vanpouille C, Deligny A, Delehedde M, Denys A, Melchior A, et al. (2007) The heparin/heparan sulfate sequence that interacts with cyclophilin B contains a 3-O-sulfated N-unsubstituted glucosamine residue. *J Biol Chem* 282: 24416-24429.
39. Wei Z, Deakin JA, Blaum BS, Uhrin D, Gallagher JT, et al. (2011) Preparation of heparin/heparan sulfate oligosaccharides with internal N-unsubstituted glucosamine residues for functional studies. *Glycoconj J* 28: 525-535.
40. Bai K, Wang W (2012) Spatio-temporal development of the endothelial glycocalyx layer and its mechanical property in vitro. *J R Soc Interface* 9: 2290-2298.



4

The glomerular endothelial surface layer acts as a barrier against albumin filtration

Am J Pathol 182: 1532-1540, 2013.

Martijn J.C. Dane^{1,4}, Bernard M. van den Berg¹, M. Cristina Avramut¹, Frank G.A. Faas², Johan van der Vlag³, Angeliqne L.W.M.M. Rops³, Raimond B.G. Ravelli², A.J. Koster², Anton Jan van Zonneveld¹, Hans Vink⁴, Ton J. Rabelink¹

¹*Department of Nephrology, Eindhoven laboratory for Vascular Medicine, Leiden University Medical Center, the Netherlands* ²*Department of Molecular Cell Biology, Leiden University Medical Center, the Netherlands* ³*Department of Nephrology, Nijmegen Center for Molecular Life Sciences, Radboud University Nijmegen Medical Center, Nijmegen, the Netherlands* ⁴*Department of Physiology, Maastricht University Medical Center, Maastricht, the Netherlands*

Abstract

Glomerular endothelium is highly fenestrated and its contribution to glomerular barrier function is therefore subject of debate. In recent years a polysaccharide rich endothelial surface layer (ESL) has been postulated to act as filtration barrier for large molecules such as albumin. To test this hypothesis we disturbed the ESL in C57Bl/6 mice using chronic hyaluronidase infusion during 4 weeks, and monitored albumin passage using immunolabeling and correlative light-electron microscopy, that allows for complete and integral assessment of glomerular albumin passage. ESL ultrastructure was visualized by transmission electron microscopy using cupromeronic blue and by localization of ESL binding lectins using confocal microscopy. We demonstrate that glomerular fenestrae are filled with dense negatively charged polysaccharide structures which are largely removed in the presence of circulating hyaluronidase, leaving the polysaccharide surfaces of other glomerular cells intact. Both retention of cationic ferritin in the glomerular basement membrane and systemic blood pressure were unaltered. Enzyme treatment, however, induced albumin passage across the endothelium in 90% of glomeruli, while this could not be observed in controls. Yet, there was no net albuminuria due to binding and uptake of filtered albumin by the podocytes and parietal epithelium. ESL structure and function completely recovered within 4 weeks upon cessation of hyaluronidase infusion. Thus, the polyanionic ESL component hyaluronan is a key component of the glomerular endothelial protein permeability barrier.

Introduction

The glomerular endothelium is highly fenestrated and its pores are estimated to be around 60-80 nm in diameter. While fenestrae may facilitate the formation of high volumes of ultrafiltrate, it would also imply loss of macromolecules such as albumin, as suggested by intravital microscopy studies [1]. In vivo, endothelium is covered with a polysaccharide-protein gel-like structure, the glycocalyx, or endothelial surface layer (ESL). The composition and biological activity of this surface layer can widely differ in a tissue-specific manner. The main constituents of the ESL are protein cores, typically syndecans, with large heparan sulfate side chains (+/- 60 %) or chondroitin sulfate (+/- 15 %) [2]. In addition, plasma proteins such as albumin and orosomucoid bind to these negatively charged proteoglycans and glycosaminoglycans [3]. Hyaluronan integrates into this gel like a mesh, anchoring to CD44 on the cell membrane [4]. Hyaluronan consists of repeating disaccharides composed of N-acetylglucosamine (GlcNAc) and glucuronic acid (GlcA) and is the largest polysaccharide found in vertebrates. Together these polysaccharides form a very active biologically surface layer, which may stretch out up to 500 nm into the vascular lumen [2]. Many growth factors such as fibroblast growth factor (FGF), vascular endothelial growth factor (VEGF), and circulating complement inhibitors such as factor H, require prior engagement with this surface layer before they can interact with their functional ligands [5-7]. Heparan sulfate repeats can also activate antithrombin-III, and bind extracellular superoxide dismutases, while after activation of the endothelial cell they function as receptors for platelet and leukocyte adhesion [8-12]. The pivotal role of the ESL is illustrated by the fact that up to now no successful genetic mice models could be generated where structural polysaccharide components of the ESL are lacking. These properties have put the ESL in the center of interest as a modulator of endothelial cell function. The ESL has also been postulated to act as a barrier against albumin filtration. The combination of negatively charged heparan sulfates and the mesh like structure of the less charged hyaluronan may theoretically prevent albumin filtration through the fenestrae [13]. In fact, it could be demonstrated that the Frank Starling filtration equilibrium in non-renal microvasculature is generated by the inability of albumin to permeate the ESL and its resulting oncotic gradients over this layer [14]. Moreover, acute infusion of high dosages of enzymes that degrade the ESL results in increased fractional albumin clearance, extrapolating this concept also to the kidney [15,16].

In the current study we explore the effects of chronic disruption of the ESL on albumin filtration over the glomerular endothelium and the possible effects on glomerular morphology. To this end, we use a new electron microscopy technique that allows visualization of the ESL and albumin transport within the entire glomerular section at nanometer resolution [17]. To study the functional role of the ESL with respect to prevention of albumin filtration, it was perturbed by chronic low dose infusion of hyaluronidase, a hyaluronan degrading enzyme, which has been shown to increase the permeation of the ESL, for example in the cremaster muscle [13].



Material and methods

All materials are from Sigma-Aldrich (St. Louis, MO, USA) or stated otherwise.

Mice and experimental groups

Experiments were performed using C57Bl/6 mice (B6, Charles River, France) at 14 weeks of age. Mice were randomly divided into 2 groups and implanted with an osmotic minipump (Alzet, Cupertino, CA, USA) containing hyaluronidase (group 1, total n = 26) or inactivated hyaluronidase (group 2, total n = 22).

Anesthesia during surgical procedures was performed using i.p. injection of 0.2 ml of a cocktail of midazolam (1 mg/mL, Roche Nederland B.V., Woerden), dexmedetomidine (50 µg/mL, Orion corporation, Espoo, Finland) and fentanyl (10 µg/mL, Hameln pharmaceuticals gmbh, Hameln, Germany) in H₂O. After 4 weeks, 6 mice from each group were sacrificed, the pumps of 6 additional mice per group were removed and these animals were allowed to recover for an additional 4 weeks. In a subset of control B6 mice (n = 2) and B6 mice with an osmotic minipump containing hyaluronidase for 4 weeks (n = 3), the glomerular ESL was stained using cupromeronic blue. In addition, 14 weeks-old B6 mice received an osmotic minipump containing various concentrations of hyaluronidase for 2 weeks to determine the optimal concentration (n = 15) or an osmotic minipump containing either hyaluronidase (n = 8) or inactivated hyaluronidase (n = 5) for 2 weeks for blood pressure measurements. All animals had free access to food and tap water. The experimental protocol was approved by the local Animal Ethical Committee of Maastricht University (hyaluronidase concentration determination and blood pressure measurements) and Leiden University (others). All animal work was performed in compliance with the Dutch government guidelines.

Hyaluronidase solution

Bovine testicular hyaluronidase (100 U/µL in saline) was injected into an osmotic minipump, which releases its content at a rate of 0.25 µL/hr (25 U/hr), into the right jugular vein for 4 weeks. The effect of protease contamination of the hyaluronidase solution is negligible after infusion into the circulation (data not shown). In a subset of animals, concentrations of 40 U/µL (10 U/hr), 100 U/µL (25 U/hr) and 400 U/µL (100 U/hr) in saline were used and released into the right jugular vein for 2 weeks. In parallel, heat-inactivated hyaluronidase (boiled for 30 minutes at 90°C, resuspended by vortex) was used as control [18].

Systemic tracer dilution determination

At 16 weeks of age, distribution volume determinations of labeled erythrocytes and 40 kDa high molecular weight dextrans were performed to assess systemic vascular red blood cell- (V_{rbc}), plasma- (V_{plasma}), ESL- (V_{glx}) and total vascular volume (V_{total}) as previously described [21]. Short-term hyperglycemia increases ESL permeability and acutely decreases lineal density of capillaries with flowing red blood cells [22]. In brief, RBC were labeled with carboxyfluorescein diacetate, succinimidyl ester (CFSE, Invitrogen) and mixed with a

stock solution (10 mg/mL) of 40 kDa Texas Red labeled dextran. Following intravenous injection of 0.1 mL of this tracer mix, blood samples were drawn at 2, 5, 10, 15, 20 and 30 minutes. Capillaries were centrifuged, Ht was determined and plasma was stored at -20°C. Circulating labeled RBC fraction was determined using flow-cytometry (FACSCalibur; Becton Dickinson). Circulating V_{plasma} was calculated using the following formula: $([1 - \text{Ht}] \times V_{\text{rbc}})/\text{Ht}$ [23,24]. In each plasma sample, fluorescence was measured at 610 nm (D40-TR) using a spectrofluorophotometer (VICTOR; Perkin-Elmer, the Netherlands). Concentration-time curves of D40-TR were fitted with a mono-exponential function to determine initial tracer distribution volume.

Non-invasive tail blood pressure measurement

Blood pressure (BP) was measured in conscious animals using the tail-cuff method (CODA-2, Kent Scientific, Torrington, CT). Briefly, each session consisted of 5 acclimatization cycles followed by 15 BP measurements cycles. On the data collection day, 2 sessions of 15 BP measurements were obtained; a set was accepted if the computer identified >50% successful readings. The average from one session was used for systolic BP (SBP), diastolic BP (DBP), mean BP and heart rate in each individual mouse.

Urine collection and analysis

Mice were kept in metabolic cages for 24 hours two days before pump implantation and two days before the end of the experiment (week 0 and week 4 or 8). Mice from the recovery groups were kept additionally in metabolic cages two days before pump removal (week 4) and two weeks before perfusion fixation (week 6). Urine was centrifuged and subsequently stored at -20°C. Rocket immuno-electrophoresis was used to quantify albumin levels in urine (protocol modified from Tran et al.) [19]. Urine creatinin levels were determined by a kinetic colorimetric assay using a commercially available kit (Creatinin Jaffé method, Roche diagnostics) and a Cobas Integra 800 analyzer (Roche Mannheim, Germany). Protein levels were determined by the TPUC3 protocol using a Cobas C analyzer (Roche Diagnostics, Mannheim, Germany).

Tissue preparation

A subset of mice received, 15 minutes before the induction of anesthesia (see above), 200 μL of ferritin (equine spleen, 25 mg/ml) via the tail vein. In anesthetized mice the abdominal aorta was exposed and cannulated distal to the renal arteries. The right renal artery was ligated at the renal stalk and immediately fixated by injecting 2% paraformaldehyde (PFA) in PBS before removal of the kidney. The kidney capsule of the unperfused excised right kidney was removed and kidney was cut in half. One half was fixated overnight at 4°C in 2% PFA in PBS for detection of endogenous albumin and lectins), the other half was placed in 1.5% glutaraldehyde (GA) and 1% PFA in PBS overnight at 4°C for detection of ferritin (see below). From 6 additional mice, 3 were treated with active and 3 with inactive hyaluronidase for 4 weeks. Both kidneys, unperfused, were isolated directly and snap-frozen in liquid nitrogen for immunohistochemistry.



Detection of endothelial surface layer

For electron microscopic illustration of ESL in the glomerulus, the left kidney was perfused with 0.1% BSA and 5 U/ml heparin in HBSS at 2 mL/min to remove blood followed by 0.05% cupromeronic Blue (CB) in sodium acetate buffer (25 mM, pH 5.8) containing 1.5% GA, 1.0% PFA and 25 mM MgCl₂ for 5 minutes at 2 mL/min. After excision of the left kidney, the capsule was removed and the kidney was sliced in small tissue samples (\approx 2 mm³) and incubated overnight at 4°C in the fixation solution containing CB as above. These CB stained samples were washed twice in sodium acetate buffer (25 mM, pH 5.8) and incubated for 1 hour in 0.5% phospho-tungstic acid in 50% ethanol. Samples were further dehydrated and embedded in epon. Transmission electron microscopy (TEM) data were collected on a Tecnai 12 (BioTWIN) from 100 nm sections as above, using the same settings.

Correlative microscopy for detection of endogenous albumin

Kidney tissue was dissected at 100 μ m thickness with a vibratome (Leica Microsystems B.V., Rijswijk, the Netherlands). Part of the slices are blocked with 10% normal goat serum and 0.3% Triton 100 in PBS for 30 minutes on ice followed by incubation o/n at 4°C with horseradish peroxidase-conjugated goat anti-mouse albumin (Bethyl Labs, USA, diluted to 1/400) in 1% heat inactivated normal goat serum in PBS. After washing about 1mL of 3,3'-diaminobenzidine reaction solution (15 mL DAB solution + 10-15 μ L H₂O₂, 30%, (Dako, Denmark)) was added, incubated for 30 minutes at 4°C, washed again and incubated for 1 hour with 1.5% GA and 1% PFA in cacodylate, rinsed in cacodylate and postfixed in 1% osmium tetroxide + 1.5% potassium ferrocyanide. Samples were dehydrated and processed further into epon. Sequential 100 nm sections were mounted on a copper slot grid covered with Formvar support film and a 3 nm carbon coating for TEM, and on a water drop on a clean glass slide for reflection contrast microscopy (RCM).²⁰ The sample was mounted with immersion oil (Immersol 518F, Zeiss) on a RCM-adapted microscope (reflection contrast device RV; Leica, Wetzlar Germany). Images were recorded with a 100 \times , 1.25 NA objective. TEM sections were stained with an aqueous solution of lead citrate and uranyl acetate before visualization and data was collected at an acceleration voltage of 120 kV, on a Tecnai 12 (BioTWIN) transmission electron microscope, equipped with an Eagle CCD camera (FEI company, Eindhoven, the Netherlands).

Ultrastructural large scale virtual slides

To place the presented high power magnification images in their proper context, additional online ultrastructural large scale virtual slides are provided (CCDB database website URL) as described previously by Faas et al. [17]. The virtual slides for the samples were recorded using automated data acquisition and stitching software with 25,740 \times magnification at the detector plane, corresponding to 1.2 nm pixel size at the specimen level. This results in a slide with an overview of the glomerulus, in which you can zoom in into high detail. Using this correlative microscopy approach the DAB precipitate can be visualized both with RCM and TEM. While RCM allows for the screening of large numbers of glomeruli from kidneys from different mice, TEM enables to localize the DAB precipitation at high resolution [17].

Confocal Microscopy

Remaining kidney tissue slices (see albumin staining) were washed twice with HBSS (Gibco) containing 0.5% BSA, 5mM HEPES and 0.03 mM EDTA (HBSS-BSA). Slices were stained overnight with 10 µg/mL of various fluorescently labeled lectins, i.e. *Lycopersicon esculentum* (LEA-FITC), *Bandeiraea simplicifolia* (BSI-TRITC) or *Triticum vulgare* (WGA-TRITC) or 5 µg/ml monoclonal mouse anti-mouse CD31 antibody (Santa Cruz Biotechnology, Santa Cruz, CA, USA) in HBSS-BSA and after a brief wash, with Alexa Fluor 488 or Alexa 568 conjugated goat anti-mouse IgG (10 µg/mL, Molecular Probes, Grand Island, NY, USA). Slices in HBSS-BSA were fixed to the bottom of a petridish and were examined using a CLSM (710-NLO; Carl Zeiss, Göttingen, Germany) and a 40x objective lens (Plan Neo Fluor NA 1.3/oil DIC; Carl Zeiss). Confocal 12-bit gray-scale axial images (xy dimensions, 100×100µm) of the glomerulus were recorded using ZEN-2009 Image software (Carl Zeiss). The images were analyzed with the public domain National Institutes of Health IMAGE program (available at <http://rsb.info.nih.gov/nih-image>). For each image, amount and location of intensity profiles were quantified by calculating the distance from the peak of the CD31 signal to the half-width of the intra- or extra luminal lectin signal along a line of interest.

Detection of ferritin particles

Kidney samples fixated overnight at 4°C in 1.5% GA and 1% PFA in PBS were dissected at 100 µm thickness with a vibratome. Slices were washed with PBS and 0.1 M sodium cacodylate buffer, incubated for 1 hour with 1.5% GA and 1% PFA in sodium cacodylate buffer, rinsed in sodium cacodylate buffer and postfixed in 1% osmium tetroxide and 1.5% potassium ferrocyanide. Samples were dehydrated and processed further into epon. TEM data were collected at an acceleration voltage of 120kV on a Tecnai 12 (BioTWIN).

Immunohistochemistry

Frozen kidney sections (2 µm) were fixated in 2% PFA /0.3% Triton X-100 (TX-100) in PBS for 10 minutes, washed in PBS and blocked for 30 minutes at room temperature in 2% fetal calf serum (FCS; Bodinco, Alkmaar, The Netherlands), 2% bovine serum albumin (BSA) and 0.2% fish gelatin (Amersham Biosciences, Buckinghamshire, UK) in PBS. Sections were incubated for 45 minutes with primary antibodies (1-10 µg/ml) against mouse synaptopodin (Progen Biotechnik GmbH, Heidelberg, Germany), nephrin (R&D Systems Europe Ltd., Abingdon, United Kingdom) or desmin (Tebu-Bio, Heerhugowaard, The Netherlands) Subsequently, sections were rinsed, incubated for 45 minutes with the Alexa 488 or 594-conjugated secondary antibodies (5 µg/mL; Life Technologies Europe BV, Bleiswijk, The Netherlands). Finally, sections were rinsed with PBS, postfixed with 1% PFA in PBS and embedded in VectaShield mounting medium H-1000 (Brunschwig Chemie, Amsterdam, The Netherlands). The staining intensities of antibodies were scored in 50 glomeruli on a 0-10 scale (0 = no staining, 1 = 10% staining intensity of podocytes, 10 = 100% staining intensity). Differences between groups were determined by Mann-Whitney U testing using GraphPad Prism, version 5.0 software (GraphPad Software, Inc., San Diego, CA). P values < 0.05 were considered as significant.



Glomerular glycocalyx as barrier against albumin filtration

Statistical analysis

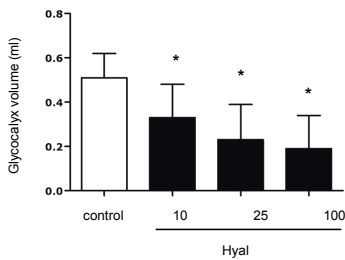
Results are all presented as mean \pm SD, morphometric data are given as mean \pm SEM. Differences between groups were determined by Mann-Whitney U testing using GraphPad Prism (GraphPad Software, Inc., San Diego, CA). A p-value of < 0.05 was considered statistically significant.

Results

Hyaluronidase infusion degrades the glomerular endothelial surface layer

Since complete removal of the ESL in vivo can result in massive thrombosis and instantaneous vessel occlusion, we aimed for a partial degradation to study the early effects of ESL loss on glomerular permeability properties. An osmotic minipump filled with bovine testicular hyaluronidase was implanted together with a catheter into the right jugular vein, to chronically degrade hyaluronan from the ESL within the murine blood circulation. While a concentration of 100U/hr resulted in massive vascular occlusions and poor prognosis within a week (data not shown), a concentration of 25U/hr resulted in about 50% reduction in systemic ESL volume after two weeks (**figure 1A**), as measured by the change in distribution volume of 40kDa dextrans, which can freely access the ESL, minus the distribution volume of labeled erythrocytes, which cannot access to the ESL. No behavioral changes, weight-loss or significant changes in blood pressure or heart rate were observed in relation to infusion of either active- or inactive hyaluronidase (**figure 1B**).

A



B

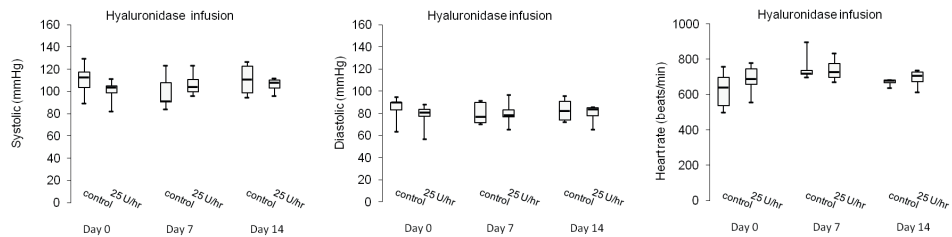


Figure 1: Effect of hyaluronidase on vasculature. A, Dose-response of ESL volume in mice after 2 weeks of treatment with 0, 10, 25 or 100 U of hyaluronidase released per hour. Change in ESL volume was assessed by means of non-parametric Mann-Whitney U test. * $P < 0.05$ vs. control. B, Systolic- and diastolic blood pressure (left, middle) and heart-rate (right) at the start, during- and at the end of the hyaluronidase treatment for two weeks. Change in blood pressure and heart-rate was assessed by means of non-parametric Mann-Whitney U test. $P =$ not significant.



Glomerular glycocalyx as barrier against albumin filtration

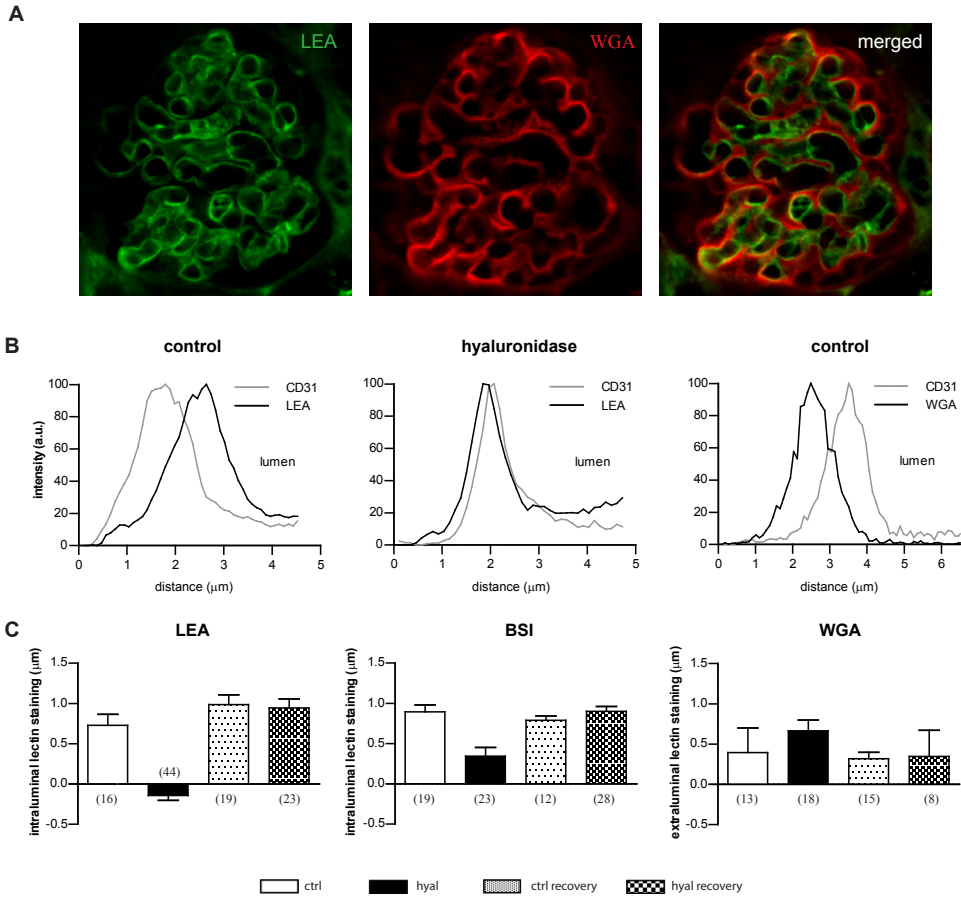


Figure 2: Fluorescent images of lectin stained glomeruli. A, Cross sectional average intensity projection of a murine glomerulus, stained with fluorescein-labeled lectins *Lycopersicon esculentum* (LEA-FITC) or *Triticum vulgare* (WGA-TRITC) and merged projection. B, Example of fluorescence intensity plots explaining localization and quantification of lectin staining according to the endothelial cell position (marked with anti-CD31 antibody). Intraluminal localization is calculated by the distance of the CD31 peak (endothelial cell) to the half width maximum intensity of the LEA peak (outer border ESL) (left and middle). WGA staining is present outside of the endothelial perimeter (right). C, Distribution of lectin intra- (LEA, BSI) or extra (WGA) luminal surface coverage after 4 weeks of active- (hyal) or inactive (ctrl) hyaluronidase treatment and after 4 weeks recovery upon osmotic-minipump removal. Values are means \pm SEM (20-40 independent measurements/glomerulus of 4 kidneys). Difference in lectin coverage between intra- and extra luminal compartment was assessed by means of non-parametric Mann-Whitney U test. * $P < 0.001$ vs. control.

The changes in ESL were visualized at 4 weeks of chronic infusion of active hyaluronidase, with inactive hyaluronidase as a control. Renal sections were stained with lectins that bind to b-(1,4)-linked N-acetyl-glucosamine residues (*Lycopersicon esculentum*, LEA), α -D-galactosyl and N-acetyl- α -D-galactosamine residues (*Bandeiraea simplicifolia*, BS-I) or N-acetylneuraminic acids and N-acetyl-b-D-glucosamine (*Triticum vulgare*, WGA) (**figure 2A**).

These lectins previously were shown to stain specific carbohydrate moieties in the ESL that correspond with intraluminal carbohydrates at the ultrastructure level [25]. To measure ESL thickness, the distance from the peak of the fluorescence signal of the endothelial cell membrane marker CD31, to the half max-intensity lectin-signal was determined (**figure 2B**). In comparison to chronic infusion of inactivated hyaluronidase, both LEA (-0.14 ± 0.06 vs. 0.73 ± 0.14 μm , $p < 0.001$) and BS-I (0.34 ± 0.11 vs. 0.90 ± 0.08 μm , $p < 0.001$), were significantly reduced upon 4 weeks of chronic hyaluronidase infusion. After removal of the osmotic-minipump and closure of the catheter, recovery of the glomerular ESL was monitored, and both lectins (LEA and BS-I) returned to control levels (**figure 2C**, left and middle panel). In contrast, WGA predominantly bound to structures outside the endothelial perimeter when compared to CD31, which appeared podocyte specific (**figure 2 A-C**). This extra-capillary carbohydrate staining was unaffected by hyaluronidase infusion (0.66 ± 0.13 vs. 0.40 ± 0.31 μm , $p = \text{ns}$) for 4 weeks and remained unchanged after 4 weeks of recovery (**figure 2C right**).



Ultra structural characterization of the glomerular endothelial surface layer

To identify changes in glomerular endothelial surface carbohydrate structures at the ultrastructure level, kidneys were perfused for a short period with the cationic dye cupromeronic blue and further processed for transmission electron microscopy (TEM). In this way polysaccharides are fixated in a charge dependent way. Throughout the glomerulus cupromeronic blue staining was observed at various layers within the permeability barrier (**figure 3A**). As may be appreciated from the high resolution TEM images, compositionally different layers on the endothelial surface and the filled fenestrae could be observed (**figure 3B and C** left panel).

The ESL staining showed dense plugs in the endothelial fenestrae and a dense layer covering the endothelial surface, which was coated by a more loosely attached layer (**figure 3B**, right panel and **3C**, left panel). In the same capillary loop the non-fenestrated endothelial part displayed a denser layer of stained material (**figure 3B** left panel), which resembled previous observations of ESL in other non-fenestrated vascular beds [26,27]. The most striking difference between hyaluronidase-treated kidneys and their controls was the local absence of the dense plugs from the endothelial fenestrae (**figure 3C** right panel).

Cupromeronic blue stained remaining structures covering the fenestrated endothelial surface, whereas the densely stained structures covering the podocytes and their foot processes were not affected by chronic hyaluronidase infusion. Therefore, in the mild dosage used, hyaluronidase infusion appeared to have predominantly removed the electron dense structures from the glomerular fenestrae.

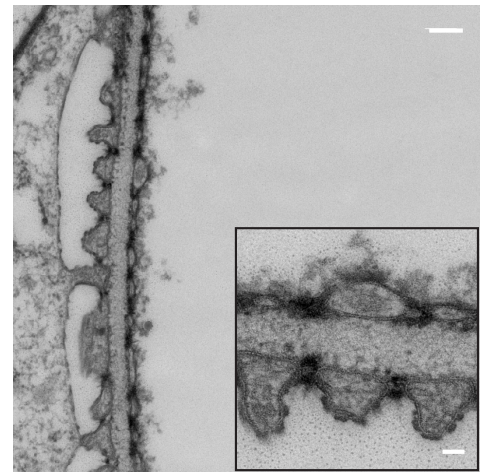
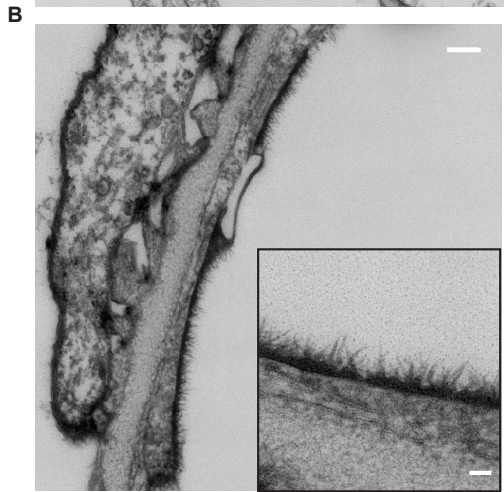
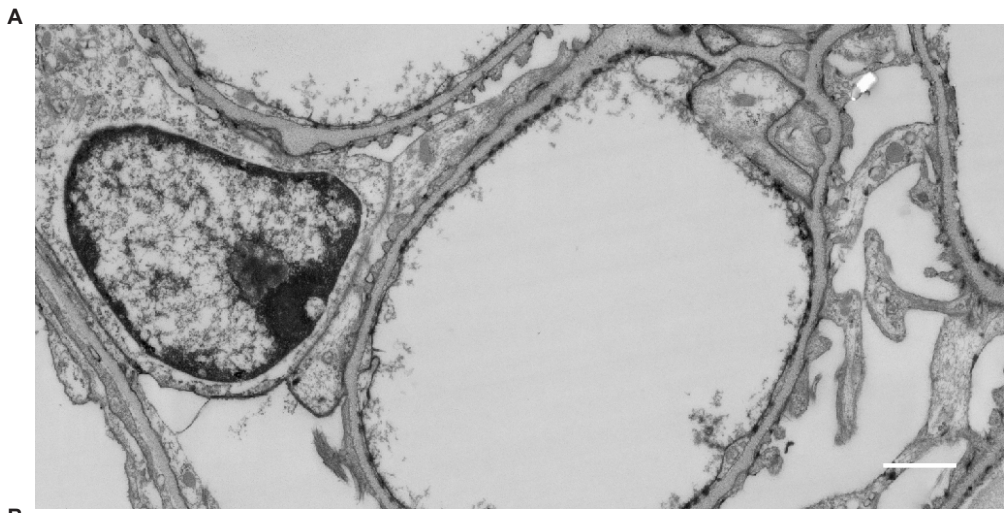
Hyaluronidase infusion does not change glomerular basement membrane permeability

To exclude an effect of hyaluronidase on the glomerular basement membrane (GBM) barrier characteristics, retention of neutral ferritin in the GBM was measured. Total ferritin (2.3 ± 0.9 vs. 2.9 ± 0.9 ferritin particles/10,000nm²) in the GBM and the subepithelial ferritin (4.5 ± 0.9 vs. 5.3 ± 1.2 subepithelial ferritin particles/ μ m of GBM length) both remained unchanged, indicating that the hyaluronidase did not alter the composition and permeability characteristics of the GBM (**figure 4**).

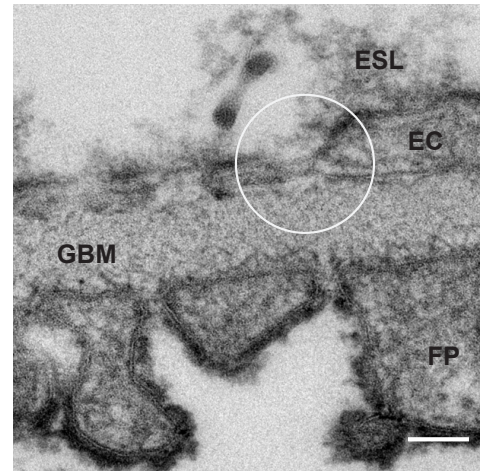
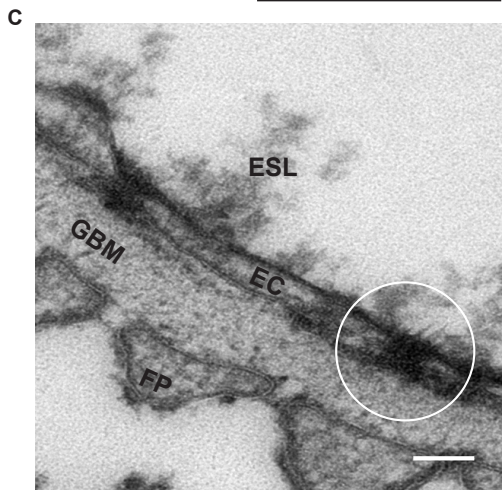
Perturbation of the glomerular endothelial surface layer results in albumin filtration

Figure 3. Transmission electron microscopic images of a cupromeronic blue stained glomerulus.

A, Overview. Bar = 1 μ m B, Capillary section with staining on top of fenestrated (right) and non-fenestrated (left) endothelium. Bar = 200 nm B, Electron microscopic detail of glomerular filtration barrier (inlay). Bar = 50 nm C, Detail of glomerular filtration barrier consisting of podocytic foot processes (FP), glomerular basement membrane (GBM), endothelium (EC) and endothelial surface layer (ESL) covering the cell membrane and filling up the fenestrae (in circle, left). Chronic hyaluronidase treatment for 4 weeks removed ESL from within the fenestrae (in circle, right). Bar = 100 nm



4



To determine the effect of the ESL perturbation by hyaluronidase on the filtration barrier for albumin, kidney slices were stained for endogenous albumin. The slices were stained with anti-albumin conjugated to HRP and incubated with diaminobenzidine (DAB) to be able to visualize albumin with reflection contrast microscopy (RCM) and TEM simultaneously. Because the kidneys were fixed with paraformaldehyde alone, only bound albumin could be visualized. All unbound luminal proteins including albumin were washed away during staining and processing for TEM. Sections stained for bound endogenous albumin were first visualized using RCM (**figure 5**).

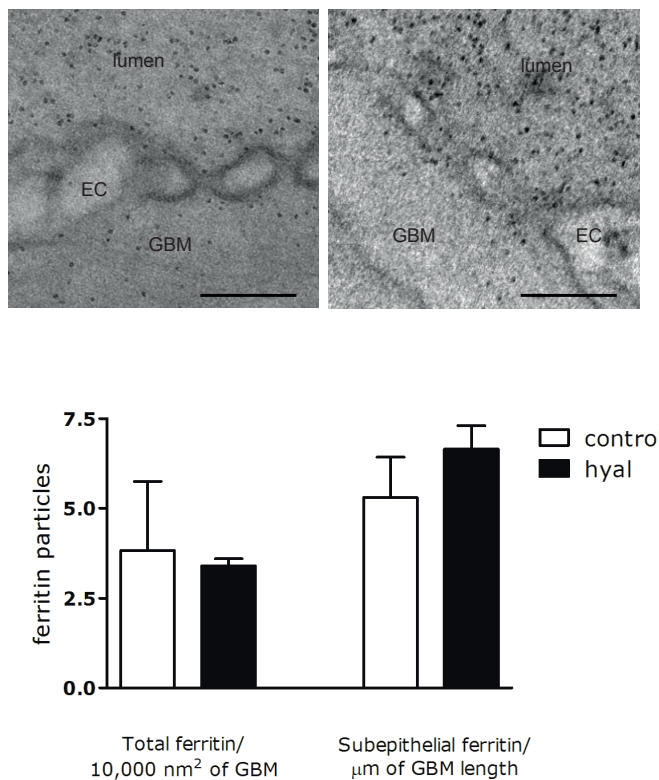


Figure 4: Ferritin particles in the glomerular basement membrane. A, Electron microscopic detail of ferritin particles (black dots) in the glomerular basement membrane (GBM) in control and hyaluronidase treated mice (1 hour after a single-intravenous injection). Bar = 100 nm. B, Ferritin particles were counted in the total surface area of the GBM (expressed as number of ferritin particles/10,000 nm²) or only at the subepithelial (podocyte) aspect (expressed as number of ferritin particles/μm of GBM length). Values are means ± SEM (n= 3-5 glomeruli). Difference in amount of ferritin particles was assessed by means of unpaired-sample t test (two-way). P = not significant

Reflection of DAB was scanned and glomeruli were counted positive when DAB reflection was visible at the glomerular filtration barrier. A striking 90% of the glomeruli were positive for albumin after hyaluronidase treatment (31 glomeruli/5 kidneys) as observed by disperse reddish reflections outside the capillary loops (**figure 5** and <https://electronmicroscopy.lumc.nl/index.html>: Data, Suppl. Mat., Dane.AmJPath). In contrast, no albumin staining was detected in the controls (22 glomeruli/3 kidneys) and after the recovery period (15 glomeruli/3 kidneys).

Using a newly developed technique to correlate the reflection found by RCM in high detail (at a 1.2 nm/pixel resolution), some matching glomeruli in consecutive virtual slides were imaged [17]. The virtual slide allows digital analysis at nanometer resolution of a whole glomerular cross-section in an unbiased approach, in this case for DAB stained albumin. The RCM images and the corresponding TEM virtual slides were correlated to determine the exact location of the bound endogenous albumin.

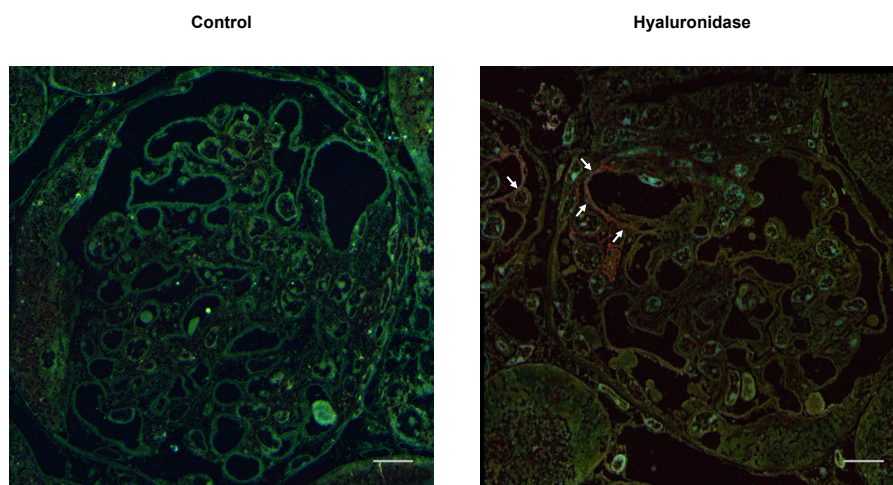


Figure 5: Reflection contrast microscopy of stained albumin in mouse glomeruli. Reflection Contrast Microscopy (RCM) overview of glomerular filtration barrier stained for endogenous bound albumin (arrows) using horse radish peroxidase (HRP) conjugated anti-mouse albumin antibody and diaminobenzidine (DAB) precipitation and stained with osmium tetroxide (1%) and potassium ferrocyanide (1.5%) after 4 weeks of inactive- (left) or active (right) hyaluronidase treatment. Upper panels = 10 μ m. These online slides can be found at (CCDB database website URL)



In the hyaluronidase-treated group albumin was mainly detected near the podocyte foot processes; especially in the subpodocytic spaces (**figure 6a** middle, both images and <https://electronmicroscopy.lumc.nl/index.html>: Data, Suppl. Mat., Dane.AmJPath). In contrast to the hyaluronidase-treated group, no albumin could be found past the endothelial layer and the glomerular basement membrane in control glomeruli (**figure 3a** left and <https://electronmicroscopy.lumc.nl/index.html>: Data, Suppl. Mat., Dane.AmJPath). Furthermore, after 4 weeks of recovery, the albumin that was found after the hyaluronidase treatment was no longer present (**figure 6a** right).

To determine whether the perturbed filtration barrier shown with TEM also resulted in proteinuria and albuminuria, 24-hours urine was collected. Samples were taken and measured before implanting the osmotic minipump (0 wks), after 4 weeks of hyaluronidase treatment (4 wks) and during the 4 weeks of recovery (6 and 8 wks). Although albumin clearly was shown to be able to pass the filtration barrier in the TEM images after hyaluronidase, no differences could be found in albumin/creatinin (**figure 6b**) or protein/creatinin (**figure 6c**) levels. Since albumin also binds to podocytes and parietal epithelial cells in the hyaluronidase-treated group, this may suggest that uptake and degradation of albumin have occurred as well (**figure 7**).

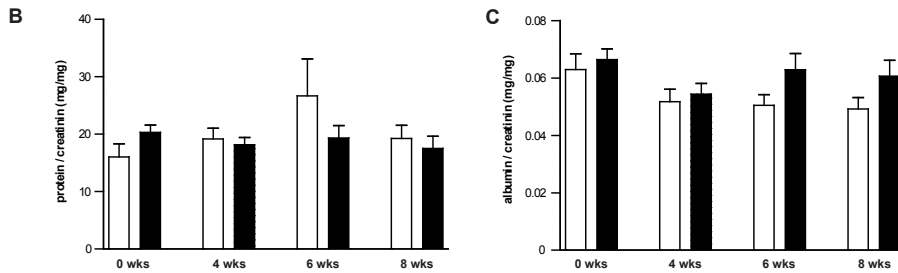
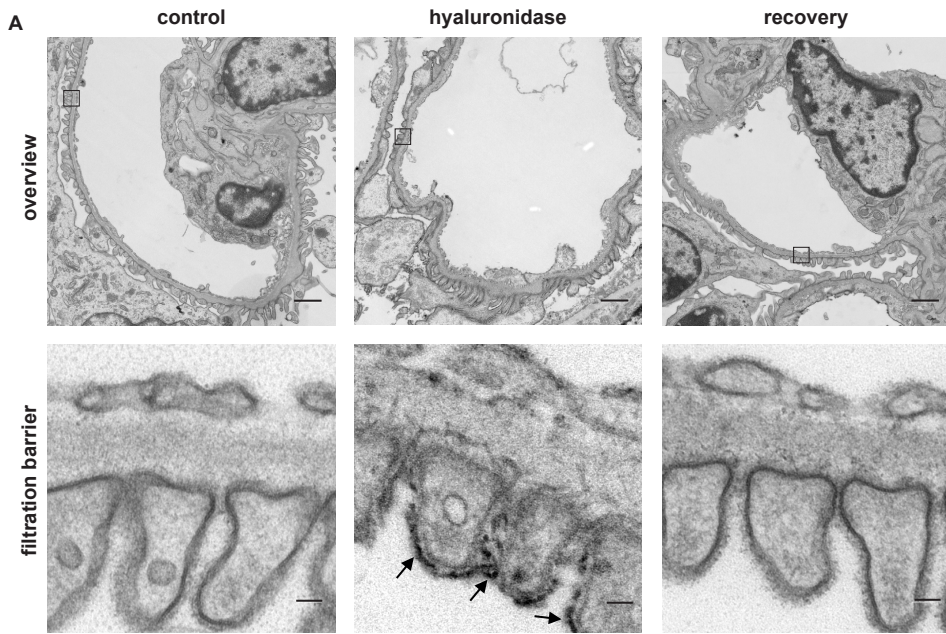


Figure 6: Electron microscopic images of glomerular filtration barrier. A, Electron microscopic overview (upper panel) and detail (lower panel) of glomerular filtration barrier stained for endogenous bound albumin (arrows) using horse radish peroxidase (HRP) conjugated anti-mouse albumin antibody and diaminobenzidine (DAB) precipitation and stained with osmium tetroxide (1%) and potassium ferrocyanide (1.5%) after 4 weeks of inactive- (left) or active (middle) hyaluronidase treatment or after additional 4 weeks recovery upon osmotic-minipump removal (right). Upper panels: bar = 1 μ m, lower panels: bar = 50 nm. The online slides can be found at CCDB database website URL. B-C Urine measurements at start, during 4 weeks of hyaluronidase treatment and after 4 weeks of recovery in inactive- (white bars) and active (black bars) hyaluronidase treated mice. Measurements were done before implanting the osmotic minipump (0 wks), after 4 weeks of hyaluronidase treatment (4 wks) and during the 4 weeks of recovery (6 and 8 wks). Values are means \pm SD ($n = 6$ samples per group). B, protein-creatinine ratio (mg/mg in 24-hrs urine). C, Urinary albumin-creatinin ratio (mg/mg in 24-hrs urine). Change in albumin-creatinin ratio was assessed by means of non-parametric Mann-Whitney U test. $P =$ not significant.

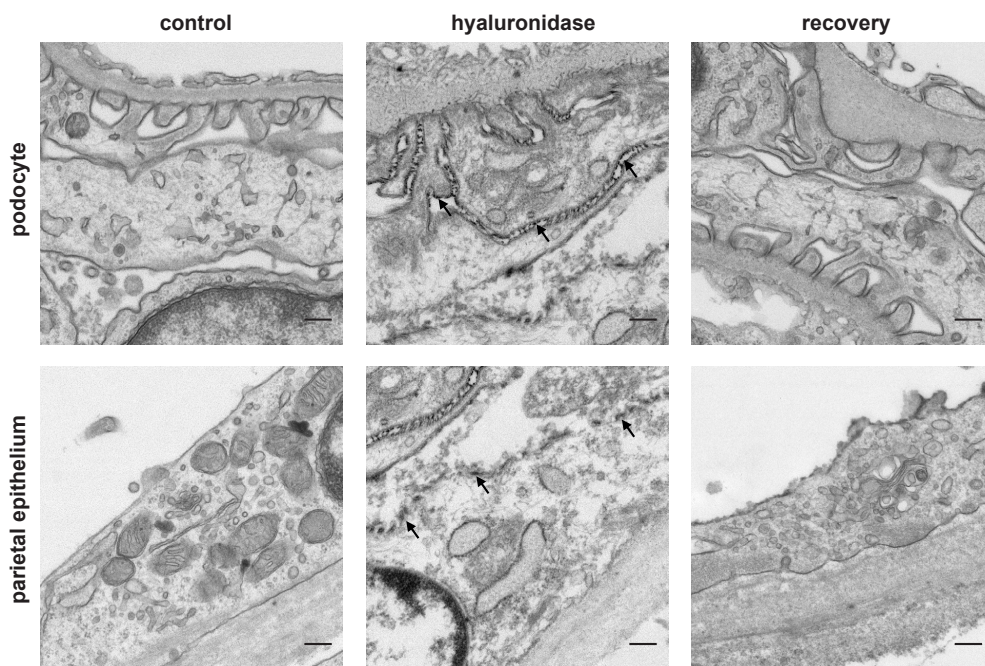


Figure 7: Electron microscopic images of podocytes and parietal epithelium. Electron microscopic detail of glomerular podocyte body (upper panels) and parietal epithelial cell (middle panels) stained for endogenous bound albumin (arrows) using horse radish peroxidase (HRP) conjugated anti-mouse albumin antibody and diaminobenzidine (DAB) precipitation and stained with osmium tetroxide (1%) and potassium ferrocyanide (1.5%) after 4 weeks of inactive- (top) or active (middle) hyaluronidase treatment or after 4 weeks recovery upon osmotic-minipump removal (bottom). Bar = 200 nm.

To investigate whether albumin binding would also induce podocyte phenotype changes in response to injury, nephrin, synaptopodin and desmin protein expression was studied (figure 8). While there was a tendency towards a proliferating and migrating phenotype such as can be observed during podocyte effacement (low nephrin, low synaptopodin, high desmin) during hyaluronidase treatment, the model used was probably too mild to demonstrate this phenomenon clearly.

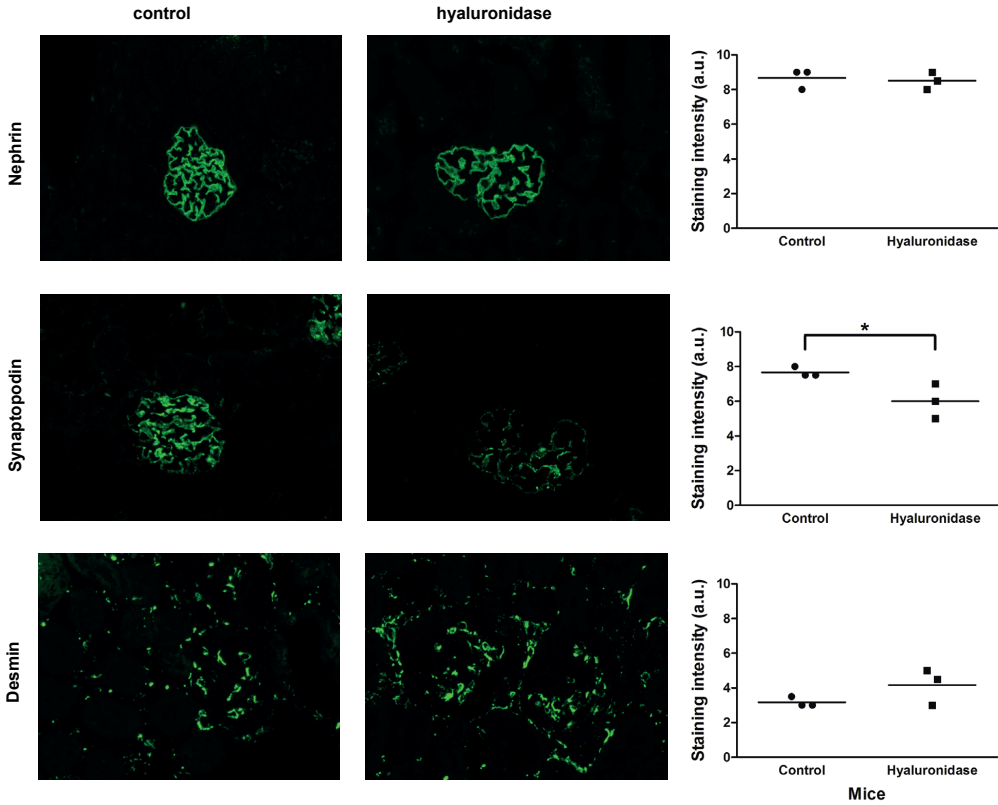


Figure 8: Immunofluorescent staining of podocyte damage markers. Immunofluorescent localization of nephrin (top panels), synaptopodin (middle panels) and desmin (bottom panels) in kidneys of control or hyaluronidase treated mice for 4 weeks. Quantification (right row) of fluorescent intensity values are means of (n=50 glomeruli per n = 3 kidneys). Change in staining intensity was assessed by means of a Mann-Whitney U test. *P < 0.05 vs. control.



Discussion

Our data show that glomerular fenestrae are filled with dense negatively charged polysaccharide structures. Upon infusion of hyaluronidase, in a dosage that leaves the polysaccharide surfaces of other glomerular cells intact, but predominantly removes the polysaccharides in the endothelial fenestrae, albumin passage across the endothelium can be observed in almost all the glomeruli. Such albumin passage was not observed for the control animals. Treatment with low dose hyaluronidase is relatively selective in removing the ESL in the fenestrae while the looser glomerular surface layer appears structurally unaltered. Rostgaard and Qvortrup, have previously suggested the presence of sulfated carbohydrates in the glomerular fenestrae [28]. Our current data indicate that the glomerular fenestrae are relatively enriched with, easy accessible, hyaluronan. The fact that hyaluronan is less charged than the heparan sulfates in ESL may explain the ability to produce a dense mesh in the fenestrae. Interestingly, hyaluronan meshes previously have been shown to slow down the diffusion of macromolecules through the surface layer [29,30].

While hyaluronidase treatment theoretically also could affect the polysaccharide coating on other glomerular cells, the large scale ultra structural mapping, as well as the lectin staining demonstrated no structural changes between the different treatment groups. Chronic removal of the ESL also did not affect the glomerular ultrastructure and basement membrane function, while the changes in ESL and albumin filtration were completely reversible upon cessation of the hyaluronidase infusion. These observations lend further support to the notion that the glomerular ESL is dynamically regulated and that its changes reflect changes in endothelial function.

Strikingly, the trans-endothelial passage of albumin was not accompanied by albuminuria or proteinuria. This is in contrast to our earlier experiments in apolipoprotein E (apoE) deficient mice on a high fat-, high cholesterol diet, which were infused with hyaluronidase [18]. A possible explanation for this discrepancy is that the apoE deficient mice reflect a double hit, where loss of ESL was superimposed on preexisting vascular and renal injury. This is supported by the fact that proteinuria in that model could only be provoked by co-administration of the high fat-, high cholesterol diet. A recent study using multi-photon fluorescence imaging in spontaneous Munich-Wistar-Fromter (MWF) rats, also could relate wide spread ESL loss to the occurrence of albuminuria [31]. In the current study we sought to determine the role of the ESL in physiological glomerular filtration and aimed at a selective reversible ESL alteration where in fact only the hyaluronan mesh in the ESL was disrupted. This setting allows a clear conclusion on the potential of the glomerular ESL to prevent albumin filtration, however, the model may be less suitable to study the relationship between endothelial dysfunction and its association with albuminuria.

While we did not observe an increased protein excretion in the urine, we did observe albumin bound to podocytes and parietal epithelium. Podocytes are known to express

the megalin and cubulin transporters [32,22]. They also express scavenger receptors such as CXCL16 and the receptor for advanced glycation endproducts (RAGE). This raises the possibility that albumin was taken up by podocytes, as has also been demonstrated for tubular epithelium. Such uptake could initiate inflammatory signaling and contribute to podocyte transformation and effacement, as was postulated by Morigi et al. [34]. In our model, the albumin passage towards the podocyte space was associated with a trend towards loss of synaptopodin and increased desmin expression, but the model was probably too short and/or too mild to observe morphological changes in the podocytes. Additionally, one cannot entirely exclude that hyaluronidase treatment has caused minor changes of polysaccharide surface structures on the epithelial cells in such a way that albumin could more easily stick to these cells. However, both our cupromeronic blue and lectin analysis of the epithelial surface layer did not reveal any morphological changes after hyaluronidase treatment. At the tubular epithelium level this bound albumin was not found. Tubular uptake can, however, not be excluded as –in contrast to the glomeruli- we could not survey the whole tubular compartment.

A limitation of our study was the fact that we did not selectively disrupt the glomerular ESL but also affected the surface layer in other vascular endothelial beds. With respect to albumin filtration it is therefore of note that the enzyme treatment did not result in changes in blood pressure. At first sight, endothelial specific inducible knock down of the hyaluronidase synthesizing enzyme perhaps might be a more specific approach to test the functional role of the glomerular ESL. However, our experimental work in progress so far would indicate that, in vivo, only minor modifications of the ESL are tolerated. Complete removal of ESL immediately results in severe thrombotic microangiopathy as can also be observed with our experiments using high doses of hyaluronidase. In addition, enzymatic degradation of the podocytic surface layer has been shown to instantly result in podocyte detachment together with massive amounts of ferritin in the urinary space [35]. In this study, these morphological differences are not present yet. However, we do already see a perturbation of the glomerular filtration barrier. This suggests that the degradation of the endothelial surface layer presented in this study, most likely reflects an early time-point in the development of glomerular damage and albuminuria.

In conclusion, the glomerular endothelial surface layer functions as a selective protein permeability barrier, a reduction of the key component hyaluronan within this layer facilitates albumin passage across the endothelial layer and the GBM towards the epithelial compartment.

This work was supported by the Dutch Kidney Foundation (grants C08.2265 & C09.03).

We appreciate the biotechnical support on the blood pressure measurements and all the support for the use of the electron and reflection contrast microscopy given by Daniel Potter and Hanneke Cobelens (dept. of Physiology, MUMC, Maastricht) and Frans Prins (dept. of Pathology, LUMC, Leiden), respectively.



References

1. Russo LM, Sandoval RM, Campos SB, Molitoris BA, Comper WD, Brown D: Impaired tubular uptake explains albuminuria in early diabetic nephropathy, *J Am Soc Nephrol* 2009, 20:489-494
2. Reitsma S, Slaaf DW, Vink H, van Zandvoort MA, oude Egbrink MG: The endothelial glycocalyx: composition, functions, and visualization, *Pflugers Arch* 2007, 454:345-359
3. Friden V, Oveland E, Tenstad O, Ebefors K, Nystrom J, Nilsson UA, Haraldsson B: The glomerular endothelial cell coat is essential for glomerular filtration, *Kidney Int* 2011, 79:1322-1330
4. Weinbaum S, Tarbell JM, Damiano ER: The structure and function of the endothelial glycocalyx layer, *Annu Rev Biomed Eng* 2007, 9:121-167
5. Allen BL, Filla MS, Rapraeger AC: Role of heparan sulfate as a tissue-specific regulator of FGF-4 and FGF receptor recognition, *J Cell Biol* 2001, 155:845-858
6. Fromm JR, Hileman RE, Weiler JM, Linhardt RJ: Interaction of fibroblast growth factor-1 and related peptides with heparan sulfate and its oligosaccharides, *Arch Biochem Biophys* 1997, 346:252-262
7. Lehtinen MJ, Rops AL, Isenman DE, van der Vlag J, Jokiranta TS: Mutations of factor H impair regulation of surface-bound C3b by three mechanisms in atypical hemolytic uremic syndrome, *J Biol Chem* 2009, 284:15650-15658
8. Chappell D, Dorfler N, Jacob M, Rehm M, Welsch U, Conzen P, Becker BF: Glycocalyx protection reduces leukocyte adhesion after ischemia/reperfusion, *Shock* 2010, 34:133-139
9. Mulivor AW, Lipowsky HH: Role of glycocalyx in leukocyte-endothelial cell adhesion, *Am J Physiol Heart Circ Physiol* 2002, 283:H1282-1291
10. Vink H, Constantinescu AA, Spaan JA: Oxidized lipoproteins degrade the endothelial surface layer : implications for platelet-endothelial cell adhesion, *Circulation* 2000, 101:1500-1502
11. Rops AL, Jacobs CW, Linssen PC, Boezeman JB, Lensen JF, Wijnhoven TJ, van den Heuvel LP, van Kuppevelt TH, van der Vlag J, Berden JH: Heparan sulfate on activated glomerular endothelial cells and exogenous heparinoids influence the rolling and adhesion of leucocytes, *Nephrol Dial Transplant* 2007, 22:1070-1077
12. Rops AL, van den Hoven MJ, Baselmans MM, Lensen JF, Wijnhoven TJ, van den Heuvel LP, van Kuppevelt TH, Berden JH, van der Vlag J: Heparan sulfate domains on cultured activated glomerular endothelial cells mediate leukocyte trafficking, *Kidney Int* 2008, 73:52-62
13. Henry CB, Duling BR: Permeation of the luminal capillary glycocalyx is determined by hyaluronan, *Am J Physiol* 1999, 277:H508-514
14. Levick JR, Michel CC: Microvascular fluid exchange and the revised Starling principle, *Cardiovasc Res* 2010, 87:198-210
15. Jeansson M, Haraldsson B: Glomerular size and charge selectivity in the mouse after exposure to glucosaminoglycan-degrading enzymes, *J Am Soc Nephrol* 2003, 14:1756-1765

16. Jeansson M, Haraldsson B: Morphological and functional evidence for an important role of the endothelial cell glycocalyx in the glomerular barrier, *Am J Physiol Renal Physiol* 2006, 290:F111-116
17. Faas FG, Avramut MC, B MvdB, Mommaas AM, Koster AJ, Ravelli RB: Virtual nanoscopy: Generation of ultra-large high resolution electron microscopy maps, *J Cell Biol* 2012, 198:457-469
18. Meuwese MC, Broekhuizen LN, Kuikhoven M, Heeneman S, Lutgens E, Gijbels MJ, Nieuwdorp M, Peutz CJ, Stroes ES, Vink H, van den Berg BM: Endothelial surface layer degradation by chronic hyaluronidase infusion induces proteinuria in apolipoprotein E-deficient mice, *PLoS One* 2010, 5:e14262
19. Tran TN, Eubanks SK, Schaffer KJ, Zhou CY, Linder MC: Secretion of ferritin by rat hepatoma cells and its regulation by inflammatory cytokines and iron, *Blood* 1997, 90:4979-4986
20. Prins FA, Velde IC, de Heer E: Reflection contrast microscopy: The bridge between light and electron microscopy, *Methods Mol Biol* 2006, 319:363-401
21. Zuurbier CJ, Demirci C, Koeman A, Vink H, Ince C: Short-term hyperglycemia increases endothelial glycocalyx permeability and acutely decreases lineal density of capillaries with flowing red blood cells, *J Appl Physiol* 2005, 99:1471-1476
22. VanTeeffelen JW, Brands J, Jansen C, Spaan JA, Vink H: Heparin impairs glycocalyx barrier properties and attenuates shear dependent vasodilation in mice: Hypertension 2007, 50:261-267
23. Nieuwdorp M, Meuwese MC, Vink H, Hoekstra JB, Kastelein JJ, Stroes ES: The endothelial glycocalyx: a potential barrier between health and vascular disease: *Curr Opin Lipidol* 2005, 16:507-511
24. Nieuwdorp M, van Haften TW, Gouverneur MC, Mooij HL, van Lieshout MH, Levi M, Meijers JC, Holleman F, Hoekstra JB, Vink H, Kastelein JJ, Stroes ES: Loss of endothelial glycocalyx during acute hyperglycemia coincides with endothelial dysfunction and coagulation activation in vivo. *Diabetes* 2006, 55:480-6
25. Mulivor AW, Lipowsky HH: Inflammation- and ischemia-induced shedding of venular glycocalyx, *Am J Physiol Heart Circ Physiol* 2004, 286:H1672-1680
26. van den Berg BM, Spaan JA, Rolf TM, Vink H: Atherogenic region and diet diminish glycocalyx dimension and increase intima-to-media ratios at murine carotid artery bifurcation, *Am J Physiol Heart Circ Physiol* 2006, 290:H915-920
27. van den Berg BM, Vink H, Spaan JA: The endothelial glycocalyx protects against myocardial edema, *Circ Res* 2003, 92:592-594
28. Rostgaard J, Qvortrup K: Sieve plugs in fenestrae of glomerular capillaries--site of the filtration barrier?, *Cells Tissues Organs* 2002, 170:132-138
29. Laurent TC, Fraser JR: Hyaluronan, *FASEB J* 1992, 6:2397-2404
30. Laurent TC, Laurent UB, Fraser JR: The structure and function of hyaluronan: An overview, *Immunol Cell Biol* 1996, 74:A1-7
31. Salmon AH, Ferguson JK, Burford JL, Gevorgyan H, Nakano D, Harper SJ, Bates DO, Peti-Peterdi J: Loss of the endothelial glycocalyx links albuminuria and vascular dysfunction, *J Am Soc Nephrol* 2012, 23:1339-1350



Glomerular glycocalyx as barrier against albumin filtration

32. Prabakaran T, Christensen EI, Nielsen R, Verroust PJ: Cubilin is expressed in rat and human glomerular podocytes, *Nephrol Dial Transplant* 2012,
33. Prabakaran T, Nielsen R, Larsen JV, Sorensen SS, Feldt-Rasmussen U, Saleem MA, Petersen CM, Verroust PJ, Christensen EI: Receptor-mediated endocytosis of alpha-galactosidase A in human podocytes in Fabry disease, *PLoS One* 2011, 6:e25065
34. Morigi M, Buelli S, Angioletti S, Zanchi C, Longaretti L, Zoja C, Galbusera M, Gastoldi S, Mundel P, Remuzzi G, Benigni A: In response to protein load podocytes reorganize cytoskeleton and modulate endothelin-1 gene: implication for permselective dysfunction of chronic nephropathies, *Am J Pathol* 2005, 166:1309-1320
35. Kanwar YS, Rosenzweig LJ: Altered glomerular permeability as a result of focal detachment of the visceral epithelium, *Kidney Int* 1982, 21:565-74



4

5

Association of kidney function with changes in the endothelial surface layer

CJASN 9: 698-704, 2014

Martijn J.C. Dane^{1,3}, Meriem Khairoun¹, Dae Hyun Lee¹, Bernard M. van den Berg¹,
Bart J.M. Eskens², Margien G.S. Boels¹, Jurgen W.G.E. van Teeffelen², Angelique
L.W.M.M. Rops³, Johan van der Vlag³, Anton Jan van Zonneveld¹, Marlies E.J.
Reinders¹, Hans Vink², Ton J. Rabelink¹

¹*Department of Nephrology, Eindhoven laboratory for Vascular Medicine,
Leiden University Medical Center, the Netherlands* ²*Department of Physiology, Maastricht
University Medical Center, Maastricht, the Netherlands* ³*Department of Nephrology, Nijmegen
Center for Molecular Life Sciences, Radboud University Nijmegen Medical Center, Nijmegen,
the Netherlands*

Abstract

End-stage renal disease (ESRD) is accompanied by endothelial dysfunction. Since the endothelial glycocalyx (endothelial surface layer, ESL) governs interactions between flowing blood and the vessel wall, perturbation could influence disease progression. In this study we used a novel non-invasive sidestream-darkfield (SDF) imaging method, which measures the accessibility of red blood cells to the ESL in the microcirculation (perfused boundary region, PBR), to investigate whether renal function is associated with ESL dimensions. PBR was measured in control participants (n=10), in patients with ESRD (n=23), in participants that have normal kidney function after successful living donor kidney transplantation (n=12) and in patients who developed interstitial fibrosis / tubular atrophy after kidney transplantation (n=10). In addition, the endothelial activation marker Angiopoietin-2 (Ang2) and shed ESL components syndecan-1 and soluble thrombomodulin (sTM) were measured using ELISA. Compared to healthy controls (1.82±0.16 µm), ESRD patients had a larger PBR (+0.23, [95%CI, 0.459 to 0.003], P<0.05), which signifies loss of ESL dimensions. This large PBR was accompanied by higher circulating levels of syndecan-1 (+57.71 [CI95%, 17.38 to 98.04] p<0.01) and sTM (+12.88 [95%CI, 0.29 to 25.46], p<0.001). After successful transplantation, the PBR was indistinguishable from healthy controls, without elevated levels of sTM or syndecan-1. In contrast however, patients who developed IFTA showed a large PBR (+0.36 [95%CI, 0.09 to 0.63]; p<0.01) and higher levels of endothelial activation markers. In addition, a significant correlation between PBR, Ang2 and eGFR was observed (PBR vs. GFR: spearman's rho 0.31 p<0.05 and PBR vs. Ang2: spearman's rho -0.33 p<0.05). In this study we have shown that reduced renal function is strongly associated with low ESL dimensions. After successful kidney transplantation the ESL is indistinguishable from control.. Our new SDF-based method allows rapid and unbiased assessment of these ESL dimensions in clinical medicine.

Introduction

Patients with end stage renal disease (ESRD) have a dysfunctional endothelium and increased morbidity and mortality, mainly due to their increased risk for cardiovascular disease [1,2]. The mechanisms responsible for activation of the endothelium in chronic renal failure are multifactorial and include the presence of uremic toxins (in particular asymmetric dimethyl arginine), low grade inflammation, and hypertension [3]. One of the earliest changes upon this endothelial activation has been postulated to be compositional- and dimensional alterations of the endothelial surface layer (ESL) [4].

The ESL is a carbohydrate gel-like layer composed of proteoglycans, glycoproteins and loosely bound plasma molecules [5-7]. It has been postulated to govern the interaction between blood and the vessel wall. Heparan sulfates, the main constituent of the ESL, have been shown to activate antithrombin III and to prevent leucocyte interaction with the endothelium [8-11]. In addition, the ESL regulates endothelial permeability and acts as shear stress sensor in the control of vasomotor function [12,13]. It is therefore very likely that alterations in, or loss of, ESL function can predispose for the development of vascular disease [14,15]. Under inflammatory conditions the ESL induces changes in surface heparan sulfate composition that facilitate the recruitment of inflammatory cells [14]. With sustained inflammation, the production of heparanase is induced in the glomerulus, which may partially degrade the ESL. Prevention of this ESL loss in diabetic heparanase knock-out mice also prevented the development of proteinuria and kidney injury [16]. Thus, ESL function and dimensions are also an important determinant of progression of kidney disease.

Because the ESL is being produced and shed continuously and its dimensions are, among others, based on blood pressure and plasma proteins, it is very challenging to analyze [5-7]. Most methods that aim to detect changes in ESL are based on the measurement of shed ESL components like proteoglycans, hyaluronan or heparan sulfates in the plasma. The only direct measurements for ESL properties are currently done in animals only, using perfusion-staining or intra-vital techniques [13,17,18]. Until recently, ESL changes were measured using an invasive and time consuming method, by using the distribution of labeled red blood cells (RBC) and low molecular weight dextrans [19]. Recently, a non-invasive tool for analyzing the ESL was developed using sidestream-darkfield (SDF) imaging. ESL dimensions were calculated as the difference in RBC column width before (functionally perfused capillary diameter) and after (anatomical capillary diameter) leukocyte passage. This technology correlates well with the invasive techniques based on tracer dilution to assess the volume of the ESL, which is very labor intensive and subject to investigator bias [20]. We use a new approach in which spatiotemporal changes in the ability of RBCs to penetrate the ESL can be detected [21]. This method is fully automated and blinded to the investigator. In contrast to previous methods, in which the ESL quantity was measured in volume or thickness, this method analyses ESL quality: a larger PBR, or increased accessibility to RBCs, reflects a disturbance of the ESL structure.



Kidney function correlates with endothelial glycocalyx stability

In the present study we utilized this method to investigate the hypothesis that renal failure is associated with perturbation of the endothelial ESL, i.e. larger PBR, and its relation to the presence of shed ESL components syndecan-1 and thrombomodulin (sTM) and the endothelial activation marker angiotensin-2 (Ang2). In addition we measured the ESL in patients who received kidney transplantation.

Material and methods

Study population

In a previous study, endothelial function has been shown to be estrogen-dependent and thus varies during the menstrual cycle [22]. Furthermore, in a currently on-going study we could demonstrate a small but significant difference in baseline PBR between man and woman (unpublished data). As the exact reason of these differences is still unclear, we only studied male participants in the current study to exclude gender as a possible confounding factor. A total of 53 male patients and 10 age-matched male controls were enrolled in a cross-sectional study in which PBR was measured (table 1). 31 Patients were included after being diagnosed with ESRD (eGFR<15 mL/min/1.73 m²), 12 with stable renal function after kidney transplantation (eGFR=30mL/min/1.73 m² or higher or more, stable group) and 10 with interstitial fibrosis and tubular atrophy (IFTA) developed after kidney transplantation, (eGFR<30mL/min/1.73 m² or less and histopathologic proof, IFTA group). This latter group was included to investigate whether loss of function of the transplanted kidney would result in perturbation of the ESL. All procedures were approved by the Leiden University Medical Center (LUMC) institution's Medical Ethical Committee and complied with the declaration of Helsinki's guidelines. Informed consent was obtained from all patients.

Transplantation

All patients received kidney transplantation at the LUMC between 1984 and 2012. Transplantations were performed as described previously [23]. Patients were treated with prednisone (tapered to a dose of 10 mg by 6 weeks and a dose of 5-7.5 mg by 3 months), cyclosporine (area under the curve (AUC) 5400 ng.h/mL first 6 weeks then 3250 ng.h/mL) or tacrolimus (AUC 210 ng.h/mL first 6 weeks, then 125 ng.h/mL) and mycophenolate mofetil (MMF) (AUC 30-60 ng.h/mL). From the year 2000 on, these patients received induction treatment with basiliximab (40 mg at day 0 and 4) or daclizumab (100 mg/day on the day of transplantation and 10 days after transplantation). Patients were treated routinely with oral val-ganciclovir prophylaxis for 3 months, except for a CMV negative donor recipient status. The clinical and research activities being reported are consistent with the Principles of the Declaration of Istanbul as outlined in the 'Declaration of Istanbul on Organ Trafficking and Transplant Tourism.

Imaging of the sublingual microvasculature

Imaging of microcirculation: To detect the dynamic lateral RBC movement into the glycocalyx of the microcirculation (expressed as PBR), sidestream dark field (SDF) intravital microscopy (MicroVision Medical Inc., Wallingford, PA) [24] was performed to visualize the sublingual microvasculature. The method of calculation is based on the method published before and is fully automated to ensure unbiased analysis of the ESL [21]. The SDF camera uses green light emitting diodes (540nm) to detect the haemoglobin of passing RBC. The images were captured using a 5x objective with a 0.2 NA (numerical aperture), providing a 325- fold magnification in 720 x 576 pixels at 23 frames per second.



The image acquisition is automatically mediated through the Glycocheck software (Glycocheck BV, Maastricht, the Netherlands). With this method it is possible to detect increased penetration of RBCs into the glycocalyx (increased PBR) when the glycocalyx is perturbed or degraded.

Calculating the PBR: The software automatically identifies all available measurable microvessels, in focus and without movement of the imaging unit and defines vascular segments every 10µm along the length of these vessels (**figure 1A,B**). Subsequently, a sequence of 40 frames is recorded in time, containing on average 300 vascular segments. Then the observer moves the SDF imaging unit to a different location for another recording session of 40 frames, until a total of minimal 3,000 vascular segments are recorded. After these measurements, 21 line markers are placed at an interval of 0.5µm around all vascular segments (**figure 1C,D**).

From these line markers in the recorded movies, the PBR is calculated. First, the width of the red blood cell column is measured by determining both inflection points of the intensity plot profiles of all line markers (**figure 1E**). This results in 840 red blood cell column widths per vascular segment (21 line markers * 40 frames). Second, for every vascular segment, the measurements of all these RBC column widths are combined into a graph as shown in **figure 1F**. The number of observed RBC positions (as a percentage of the total) is plotted against the measured column width. From this graph the median column width is derived, being the 50th percentile of the curve. By linear regression analysis, the slope of the line between the 25th and the 75th percentile is measured. The point where this line intersects with the x-axis is a reliable marker (based on all 840 measurements) of the most outward location of the RBC, the perfused diameter (PD).

The PBR is defined as the distance between RBC column width and PD. Because the PBR is present on both sides of the RBC column, it is calculated using the equation: $[PD - \text{median RBC column width}] / 2$. The calculated PBR values, classified according to their corresponding RBC column width between 5 – 25 µm, are averaged to provide a single PBR value for each participant. Finally, the PBR is schematically shown in **figure 1G**.

Quality checks: To ensure a reliable and reproducible measurement quality checks are performed during the whole analysis procedure. First, the software only selects the vascular segments of which at least 11 of the 21 line markers have a positive signal for the presence of an RBC (>50% of the vascular segment is filled with RBCs) to use for the subsequent analyses from the first frame of the different recordings. By selecting only the vascular segments that are filled for more than 50%, the influence of hematocrit on the PBR measurements is minimized.

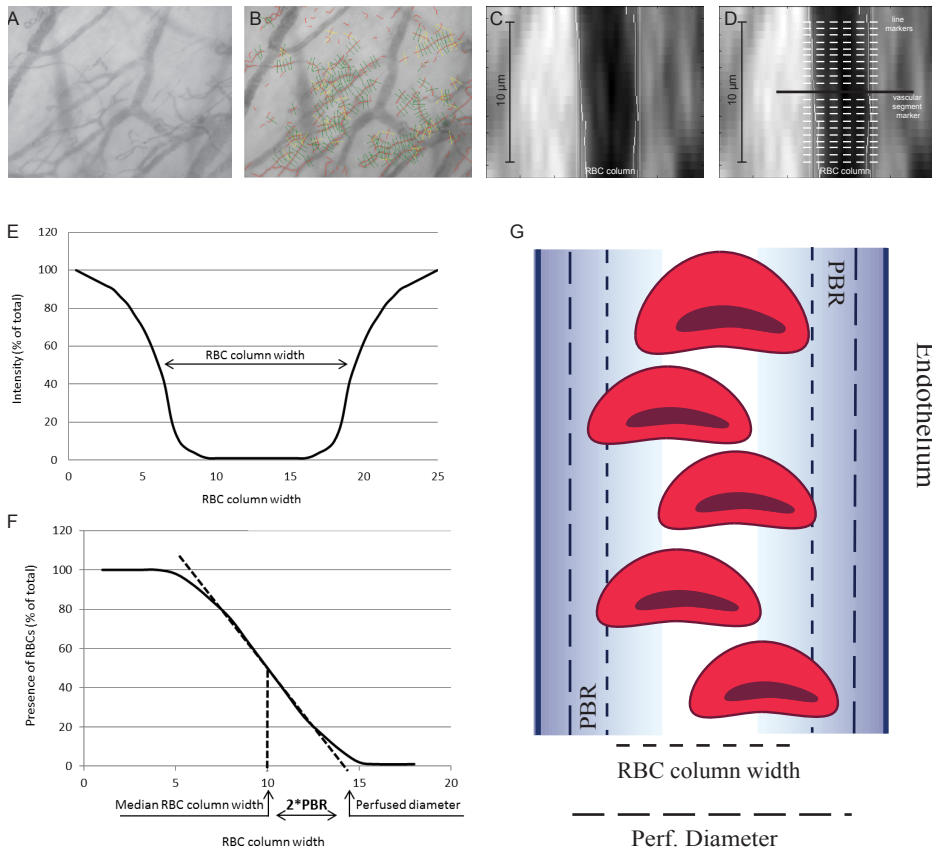


Figure 1: Image acquisition and logarithm to calculate PBR in sublingual microvasculature.
 A: Example of one frame made using the SDF camera. The camera detects the haemoglobin of passing RBCs by green light emitting diodes (540nm) and the software automatically identifies all available measurable micro-vessels in focus. B: Example of the same frame of the acquired image after vascular segments have been defined every 10µm along the length of these vessels, until at least 3000 vascular segments are recorded. C: Zoomed in example of one vascular segment of the RBC column. D: Schematic example with the vascular segment marker and the 21 line markers on and around the vascular segment marker. E: Example of a plot profile of the RBC column width measured at one line marker. F: Graph of all RBC column widths measured at one vascular segment. From this plot the median RBC column width can be calculated. The perfused diameter can be determined by using linear regression on the area of the curve from the 25th to the 75th percentile. Next the PBR can be calculated from these two parameters. G: Schematic image of cross section of a blood vessel with the RBC column width, perfused diameter and PBR explained.

The second quality check is performed during the measurement of all RBC column widths (figure S1E). In the second quality check all measured segments are tested on minimal RBC width-, position of the column (centred or not) and the signal to noise ratio. In the third quality check the curve fit for calculating the median RBC column width and PD is tested (R^2 of 25th to 75th percentile > 0.75) (figure S1F). Measurement points that do not fulfil the criteria of these quality checks are not used for the calculation of the PBR.

Validation of the SDF method

To validate the measurements, a direct test to determine whether loss of glycocalyx dimension is reflected by outward radial displacement of circulating RBCs has been performed using intravital microscopy. For this experiment, B6.Cg-Tg(TIE2GFP)287Sato/1J mice were used (Jackson Laboratories, Bar Harbor, ME). In these mice endothelial cells (EC) can be imaged by the specific expression of GFP in ECs. These GFP-EC mice were prepared for intravital microscopic observation of the cremasteric microcirculation as described before.[25] The preparation was transferred to the stage of an intravital microscope (Leitz, Wetzlar, Germany), coupled to a cooled CCD video camera (C9100; Hamamatsu, Hamamatsu City, Japan). Microvessels were alternately observed using bright-field microscopy with a 435 nm band pass interference filter (blue light) in the light path for depiction of the RBC column and epi-illumination for examination of the GFP signal using the appropriate filters for fluorescein. A salt water immersion objective lens (x50, n.a. 1.0) was used. From these two images from the same microvessel segment (figure S2), the anatomic vessel width was determined using the endothelial position by the GFP intensity peak while the perfused diameter was determined by the width of the RBC profile at half height intensity. The RBC-EC gap, or the space between endothelial cell and RBC column, is calculated from the difference between vessel diameter and corresponding perfused diameter, divided by two (as the gap is present on both sides of the RBC column). To determine the effect of glycocalyx degradation on the outward displacement of the RBC column, paired measurements in a total 16 vessels in 7 mice have been performed before and 30 minutes after hyaluronidase treatment (35 U, jugular vein infusion).

Laboratory and urinary assessments

All persons enrolled in this study underwent blood sampling before the morning intake of immunosuppression. Creatinine, hematocrit and hemoglobin were measured. For all patients the eGFR was calculated from the plasma creatinine concentration using the Modification of Diet in Renal Disease (MDRD) formula. Simultaneously, blood was collected for analysis of Ang2 and sTM in serum and syndecan-1 in plasma. Ang2 (ELISA; R&D Systems, Minneapolis, MN, USA), sTM and syndecan-1 (ELISA; Diaclone Research, Besancon, France) concentrations were measured by their respective enzyme-linked immunosorbent assay according to the protocol supplied by the manufacturer.

Statistical analyses

Continuous normally distributed data are presented as mean \pm SD, unless stated otherwise. Differences between the groups were tested by analysis of variance (ANOVA) and shown

as (difference compared to control [95% confidence interval], p-value). When criteria for parametric testing were not met, median and interquartile range (IQR) are presented and tested with the Mann-Whitney test. Correlations between interval variables were calculated using the Spearman rank correlation coefficient. Differences were considered statistically significant if $p < 0.05$. Data analysis was performed using SPSS version 20.0 (SPSS Inc, Chicago, IL) and GraphPad Prism, version 5.0 (GraphPad Prism Software Inc, San Diego, CA).



Results

Method validation in mice

To validate the PBR measurements, the gap between endothelial cells and RBC column (RBC-EC gap) was measured in mice before and 30 minutes after i.v. administration of the glycocalyx degrading enzyme hyaluronidase (supplemental methods). RBC-EC gaps ranged from 0.3 – 2.6 microns (vessel diameters 5 – 35 microns). Hyaluronidase treatment reduced the RBC-EC gap from 1.30 to 0.52 microns (average vessel diameter 16.0 microns) (**figure 2**). To exclude that changes in the RBC-EC gap originate from changes in the vessel diameter, the vessel diameter was measured before and after hyaluronidase treatment (**figure 2**). Because no changes could be observed in these paired measurements ($p=0.91$) the influence of vessel diameter can be excluded, thereby confirming that the observed changes originate from the changes in RBC column size as a result of the degradation of the ESL.

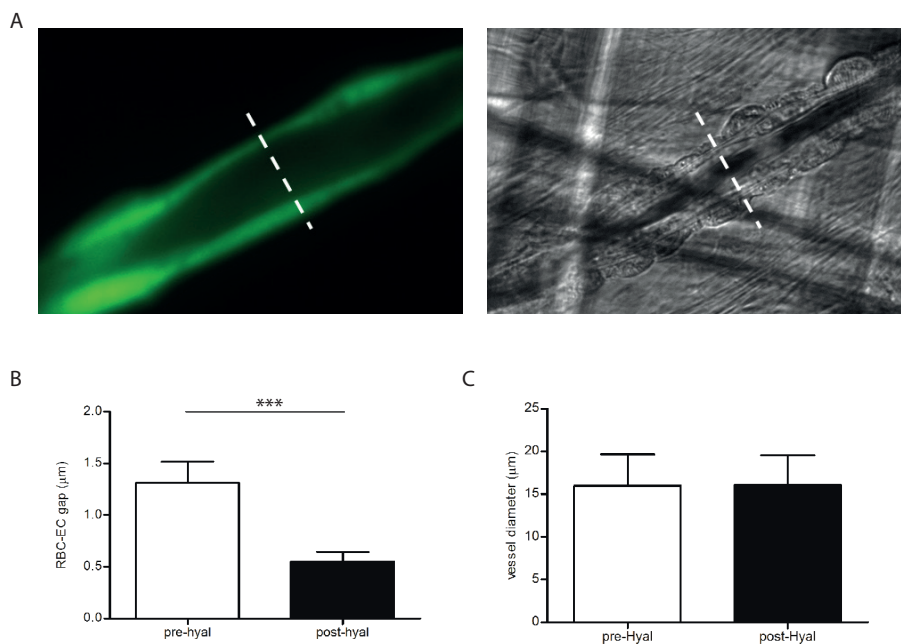


Figure 2: Validating the method in hyaluronidase treated mice. A: Example of the epifluorescence- (GFP, green) and trans-illumination (RBC, black) images made for measurement of both the vessel width using the endothelial cell GFP signal and the perfused diameter using the RBC column width. B: Paired measurements of changes in EC-RBC gap before and after hyaluronidase treatment. (***) $P<0,001$ C: Paired measurements of changes in vessel diameter before and after hyaluronidase treatment show no differences.

Patient Characteristics

Clinical characteristics of all patients included in this study are described in table 1. No differences were observed in age, blood pressure or BMI. The eGFR, was significantly lower in all patient groups compared to controls ($p < 0.05$). Hemoglobin and mean corpuscular volume (MCV) levels were significantly lower in patients with ESRD and IFTA compared to controls (**table 1**) ($P < 0.05$).

Comparison of ESL among patient groups

Changes in ESL related to endothelial activation are hypothesized to be one of the first changes in the development of cardiovascular disease [4,14]. Therefore; we measured the distance in which the RBCs can penetrate the ESL of which the calculated PBR reflects the ESL barrier properties. In this study, the PBR in controls was comparable to the PBR measured in controls in an earlier published study with lacunar stroke patients [21]. Compared to healthy controls ($1.82 \pm 0.16 \mu\text{m}$), the PBR in patients with ESRD was significantly different ($+0.23$, [95%CI, 0.459 to 0.003], $P < 0.05$). Patients who developed IFTA also showed a different PBR ($+0.36$ [95%CI, 0.09 to 0.63]; $p < 0.01$). Interestingly, the PBR in stable transplanted participants was larger, but statistically indistinguishable from healthy controls ($1.85 \pm 0.20 \mu\text{m}$, $p = 1$) (**Figure 3**). To determine the influence of dialysis on the PBR, we compared patients who received dialysis ($n = 9$) with patients without dialysis ($n = 14$) within the ESRD group. No difference was observed between these patient groups (2.02 ± 0.21 vs. $2.07 \pm 0.29 \mu\text{m}$ respectively, $p = 0.62$), which suggest that dialysis does not contribute to the observed differences in PBR (**Figure 4**).



Kidney function correlates with endothelial glycocalyx stability

Characteristic	control (n=10)	ESRD (n=23)	Stable (n=12)	IFTA (n=10)
Age (yrs)	44.8 (±10.3)	50.6 (±12.4)	54.1 (±13.9)	56.0 (±9.4)
Smoking, N (%)	0	1	2 (17%)	2 (20%)
Time since Tx (median years) (IQR)	-	-	5.0 (1.0-7.5)	8.0 (3.0-14.5)
BMI (kg/m ²)	25.6 (±3.7)	25.92 (±4.1)	26.2 (±3.4)	23.8 (±3.0)
eGFR (ml/min/1,73 m ²)	86.8 (± 17.2)	8.2 (± 2.7)*	61.2 (±16.8)*	22.3 (±9.03)*
Systolic BP (mmHg)	132.8 (±11.6)	139.5 (±12.9)	132.4 (±9.1)	141.9 (±20.5)
Diastolic BP (mmHg)	80.6 (±7.1)	83.0 (±12.54)	78.1 (±6.2)	81.5 (±6.9)
Hemoglobin (mmol/L)	9.25 (±0.45)	7.71 (±1.00)*	8.96 (±1.24)	7.17 (±1.18)*
Hematocrit (L/L)	0.43 (±0.03)	0.38 (± 0.05)	0.44 (±0.05)	0.37 (±0.05)*
MCV (fL)	88.8 (±2.6)	92.9 (±4.1)	89.7 (±3.4)	95.4 (± 5.5)*
Median proteinuria (g/24hr) (I.Q.R)	-	2.04 (±1.81)	0.23 (±0.10)	2.27 (±2.38)
Anti-coagulation, N (%)	-	5 (22%)	0 (0%)	6 (60%)
Anti-hypertensives, N (%)	-	23 (100%)	8 (67%)	10 (100%)
Statins, N (%)	-	12 (52%)	2 (17%)	6 (60%)
Immunosuppressives, N (%)	-	4 (17%)	12 (100%)	10 (100%)

Comparing endothelial dysfunction and shed proteoglycans

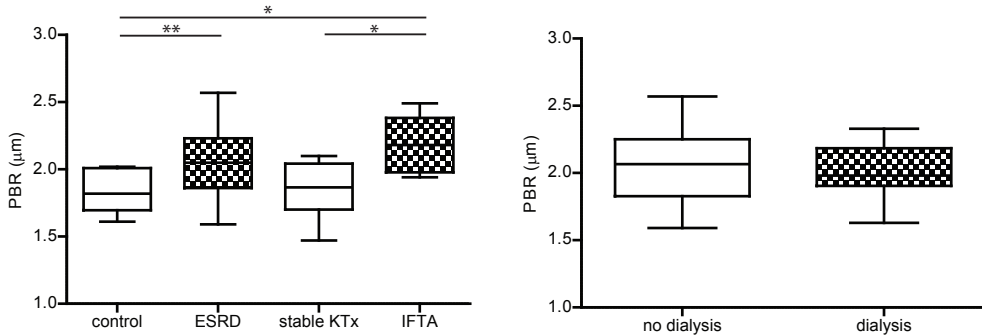


Figure 3: Measurements of the perfused boundary region in participants with and without loss of renal function. PBR in healthy control participants (control, n=10), and in patients diagnosed with end stage renal disease (ESRD, n=23), stable kidney transplantation (stable KTx, n=12) and interstitial fibrosis and tubular atrophy (IFTA, n=10). Box-plot whiskers indicate 1st and 99th percentile. *P<0.05, **P<0.01

Figure 4: Measurements of the perfused boundary region in ESRD patients with and without dialysis. PBR in patient who did receive dialysis (n=9), and in patients who did not receive dialysis (n=14), within the ESRD group. Box-plot whiskers indicate 1st and 99th percentile.



The endothelial activation state was determined by measuring serum Ang2 levels. In agreement with increasing PBR, the Ang2 level was higher, although not significant, compared to control levels (4.21 ± 3.23 and 2.09 ± 1.16 ng/mL, $p=0.19$) in ESRD serum samples (**figure 5a**). There was no difference in Ang2 levels in the successfully transplanted or the IFTA group (1.68 ± 0.85 and 3.59 ± 2.34 ng/mL, both $p=1$). Next, markers of shed ESL compounds were measured. Serum sTM levels between control participants (7.06 ± 1.17 ng/mL) and ESRD patients were significantly different ($+12.88$ [95%CI, 0.29 to 25.46], $p<0.001$). Patients diagnosed with IFTA had even higher serum sTM levels ($+34.86$ [95%CI 19.87 to 49.86], $p<0.001$). In participants with a stable KTx, sTM levels were indistinguishable from control (12.98 ± 3.01 ng/mL, $p=1$) (**figure 5b**). In accordance, shed syndecan-1 levels were high compared to control (49.8 ± 17.4 ng/mL) in ESRD patients ($+57.71$ [CI95%, 17.38 to 98.04] $p<0.01$). However, shed syndecan-1 levels were not significantly different from controls in both IFTA and stable KTx samples (54.8 ± 32.7 and 64.0 ± 15.2 ng/mL, respectively) (**figure 5c**).

Association between renal function and the endothelial surface layer

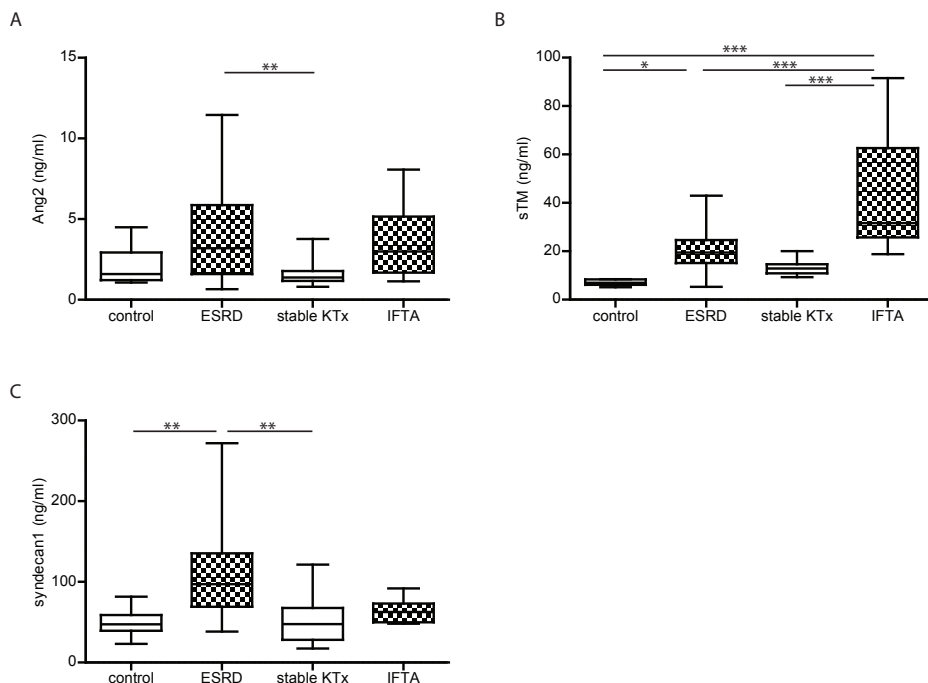


Figure 5: Measurements of circulatory endothelial and ESL damage markers in participants with- and without loss of renal function. Markers were measured in healthy control participants (control, n=10), and in patients diagnosed with end stage renal disease (ESRD, n=23), stable kidney transplantation (stable KTx, n=12) and interstitial fibrosis and tubular atrophy (IFTA, n=10). A: serum Angiopoietin2 B: serum sTM and C: plasma shed syndecan-1. Box-plot whiskers indicate 1st and 99th percentile. *P<0.05, **P<0.01 ***P<0.001

To examine any relation between renal failure, health status of the microcirculation and ESL composition, the following correlations were achieved (**table 2**). Firstly, the endothelial cell activation marker Ang2 inversely correlated with renal function, as assessed by the eGFR (Spearman's rho=-0.40, p<0.01), suggesting a relation between endothelial dysfunction and renal failure. Similarly, PBR was inversely correlated with the eGFR (Spearman's rho = -0.33, p<0.05) and positively correlated with serum Ang2 levels (Spearman's rho = 0.31, p<0.05). A comparable inverse correlation of sTM and syndecan-1 with eGFR (Spearman's rho = -0.53 and -0.67, respectively; both p<0.001) supports the indication that endothelial activation and a perturbed ESL are associated with global renal function.

Association between PBR and shed endothelial surface layer markers

Since both PBR and shed ESL markers associated with the observed differences in renal function, we tested the possible relation between the endothelial surface markers (**table 2**). Although we were able to find a positive correlation between PBR and sTM (Spearman's rho=0.33, p<0.05) and between sTM and shed syndecan-1 (Spearman's rho=0.45, p<0.001), no significant correlation between PBR and shed syndecan-1 was found (spearman's rho=0.13 p=0.35).

		eGFR (ml/min/1,73 m ²)	PBR (μm)
PBR	Spearman's rho	-0.33	-
		P<0.05	-
Ang2	Spearman's rho	-0.40	0.31
		P<0.01	P<0.05
sTM	Spearman's rho	-0.57	0.33
		P<0.001	P<0.05
Syndecan-1	Spearman's rho	-0.67	0.13
		P<0.001	P=0.35



Discussion

We show that patients with impaired kidney function have a larger PBR, i.e. loss of endothelial surface layer. Interestingly, ESL dimensions in patients with a stable kidney transplant were indistinguishable from healthy controls, while loss of renal function in patients developing IFTA resulted again in perturbation of the ESL. These changes in PBR are reflected by the presence of circulating ESL components, sTM and syndecan-1.

In the current study we used a new non-invasive, automated, and easy to apply approach to measure the ability of RBC to penetrate the ESL, quantitatively defined as the perfused boundary region. The automated software analysis results in an average PBR of 1.82 μ m in healthy control participants, which is lower than the previously published PBR of 3.3 μ m [26], but far more reliable because this new method uses over 3000 measurement sites and stringently removes artifacts and background signal. Moreover, it ensures unbiased data analysis.

Ang2 is released by endothelial cells upon their activation [27,28]. The paracrine release of Ang2 interferes with Ang1 signaling from perivascular cells towards the endothelium, resulting in capillary destabilization and angiogenic responses [29,30]. The correlation we show between Ang2, eGFR and PBR indicates that the endothelial activation during renal failure is associated with a loss of ESL dimensions.

TM, is an anticoagulant cell surface proteoglycan which is shed from the endothelial cell surface layer after inflammatory stimulation, resulting in the soluble TM we measured in serum [31]. Although it is also expressed in low amounts by dendritic cells and monocytes, it is mainly expressed by endothelial cells, thereby making it a reasonable marker for shedding of proteoglycans from the ESL. In this study we show a negative correlation between serum sTM and renal function (eGFR), which has also been shown in type 1 diabetic patients after simultaneous pancreas-kidney transplantation [23]. Although shedding from the ESL most likely explains higher sTM, reduced clearance by the kidneys needs to be considered as well. A study in diabetic patients, however, showed that urinary sTM was not influenced by GFR [32]. Also the size of sTM would preclude filtration by the kidney. Together, these data indicate that the high levels of sTM are a direct result of increased TM shedding from the ESL.

In addition to TM, syndecan-1 is also shown to be expressed at the luminal endothelial surface [33,34]. Its shedding from the ESL under inflammatory conditions is thought to contribute to plasma levels of soluble syndecan-1 [35]. In agreement, syndecan-1 shedding has been shown previously to be associated with ischemia-reperfusion injury, septic shock and post cardiac arrest syndrome [33,36,37]. In addition, patients with early diabetic nephropathy have higher shed syndecan-1 levels compared to healthy controls [38]. Alternatively, reduced renal clearance of syndecan-1 could as well be involved in elevated plasma levels in patients with renal failure. While little is known about the exact

clearance mechanism of syndecan-1, its large molecular weight excludes a direct straight forward relationship with GFR. Although the large PBR and sTM levels coincided with high syndecan-1 levels in ESRD patients, transplant recipients with IFTA and reduced renal function still showed low levels of syndecan-1.

Interestingly, in patients who were stable after kidney transplantation, sTM and PBR was not similar, but also not significantly different from the measured PBR in ESRD patients or the healthy controls. This position in between healthy controls and ESRD patients might be explained by the fact that kidney function is still not optimal compared to healthy controls. The higher level of sTM in IFTA patients compared to ESRD patients is absent for syndecan-1, which suggests that the various pathologies that underlie renal failure in these patients affect the shedding of ESL components differently.

All together, the plasma and serum biomarkers and PBR measurements corroborate the observation that loss of renal function is associated with endothelial activation and ensuing loss of ESL thickness. A question is whether mucosal ESL thickness is representative for systemic changes. However, as with other endothelial function measurements, systemic factors will induce representative functional endothelial changes throughout the circulation. Using dextran distribution we previously validated in patients with diabetes that such mucosal changes in ESL thickness are indeed accompanied by changes in systemic ESL thickness [39]. In addition, ESL changes have also been shown to coincide in both the retinal and the sublingual microcirculation in patients with type 2 diabetes [40].

In this study we cannot completely exclude the effect of immunosuppression in the transplant patients on the mechanical properties of the ESL. Nonetheless, a clear change in PBR was observed between the kidney recipients with stable function versus the IFTA group, while both groups were treated with immunosuppressive medication, suggesting that renal function per se is a more important determinant of PBR. Another question is whether changes in RBC deformability may have contributed to the observed PBR measurements. A study by Martinez et al did not observe any alteration in erythrocyte deformability between control participants and patients with CKD with or without dialysis, which makes a contribution of RBC deformability to the observed differences in PBR less likely for these patients [41].

Changes in the ESL have been postulated to precede vascular (and renal) damage [4]. Because measuring PBR in the microcirculation is a non-invasive and fast method to assess changes in the ESL in patients, this is a promising new method for clinical monitoring of the systemic microvasculature to predict the risk for cardiovascular disease and to follow the vascular effect of interventions, such as kidney transplantation.

Acknowledgements

The study was supported by the Dutch Kidney Foundation (grant number C08.2265 and the Glycoren consortium grant CP09.03)



References

1. Santoro D, Bellingeri G, Conti G, Pazzano D, Satta E, et al. (2010) Endothelial dysfunction in chronic renal failure. *J Ren Nutr* 20: S103-108.
2. Schiffrin EL, Lipman ML, Mann JF (2007) Chronic kidney disease: effects on the cardiovascular system. *Circulation* 116: 85-97.
3. Moody WE, Edwards NC, Madhani M, Chue CD, Steeds RP, et al. (2012) Endothelial dysfunction and cardiovascular disease in early-stage chronic kidney disease: cause or association? *Atherosclerosis* 223: 86-94.
4. Rabelink TJ, de Boer HC, van Zonneveld AJ (2010) Endothelial activation and circulating markers of endothelial activation in kidney disease. *Nat Rev Nephrol* 6: 404-414.
5. Reitsma S, Slaaf DW, Vink H, van Zandvoort MA, oude Egbrink MG (2007) The endothelial glycocalyx: composition, functions, and visualization. *Pflugers Arch* 454: 345-359.
6. Weinbaum S, Tarbell JM, Damiano ER (2007) The structure and function of the endothelial glycocalyx layer. *Annu Rev Biomed Eng* 9: 121-167.
7. Pries AR, Secomb TW, Gaehtgens P (2000) The endothelial surface layer. *Pflugers Arch* 440:653-666.
8. Boels MG, Lee DH, van den Berg BM, Dane MJ, van der Vlag J, et al. (2013) The endothelial glycocalyx as a potential modifier of the hemolytic uremic syndrome. *Eur J Intern Med*.
9. Mertens G, Cassiman JJ, Van den Berghe H, Vermylen J, David G (1992) Cell surface heparan sulfate proteoglycans from human vascular endothelial cells. Core protein characterization and antithrombin III binding properties. *J Biol Chem* 267: 20435-20443.
10. Rops AL, van den Hoven MJ, Baselmans MM, Lensen JF, Wijnhoven TJ, et al. (2008) Heparan sulfate domains on cultured activated glomerular endothelial cells mediate leukocyte trafficking. *Kidney Int* 73: 52-62.
11. Constantinescu AA, Vink H, Spaan JA (2003) Endothelial cell glycocalyx modulates immobilization of leukocytes at the endothelial surface. *Arterioscler Thromb Vasc Biol* 23:1541-1547.
12. Weinbaum S, Zhang X, Han Y, Vink H, Cowin SC (2003) Mechanotransduction and flow across the endothelial glycocalyx. *Proc Natl Acad Sci U S A* 100: 7988-7995.
13. Dane MJ, van den Berg BM, Avramut MC, Faas FG, van der Vlag J, et al. (2013) Glomerular Endothelial Surface Layer Acts as a Barrier against Albumin Filtration. *Am J Pathol* 182: 1532-1540.
14. Becker BF, Chappell D, Bruegger D, Annecke T, Jacob M (2010) Therapeutic strategies targeting the endothelial glycocalyx: acute deficits, but great potential. *Cardiovasc Res* 87:300-310.
15. Broekhuizen LN, Mooij HL, Kastelein JJ, Stroes ES, Vink H, et al. (2009) Endothelial glycocalyx as potential diagnostic and therapeutic target in cardiovascular disease. *Curr Opin Lipidol* 20: 57-62.
16. Gil N, Goldberg R, Neuman T, Garsen M, Zcharia E, et al. (2012) Heparanase is essential

- for the development of diabetic nephropathy in mice. *Diabetes* 61: 208-216.
17. Salmon AH, Ferguson JK, Burford JL, Gevorgyan H, Nakano D, et al. (2012) Loss of the endothelial glycocalyx links albuminuria and vascular dysfunction. *J Am Soc Nephrol* 23:1339-1350.
 18. Smith ML, Long DS, Damiano ER, Ley K (2003) Near-wall micro-PIV reveals a hydrodynamically relevant endothelial surface layer in venules in vivo. *Biophys J* 85: 637-645.
 19. Nieuwdorp M, van Haften TW, Gouverneur MC, Mooij HL, van Lieshout MH, et al. (2006) Loss of endothelial glycocalyx during acute hyperglycemia coincides with endothelial dysfunction and coagulation activation in vivo. *Diabetes* 55: 480-486.
 20. Nieuwdorp M, Meuwese MC, Mooij HL, Ince C, Broekhuizen LN, et al. (2008) Measuring endothelial glycocalyx dimensions in humans: a potential novel tool to monitor vascular vulnerability. *J Appl Physiol* 104: 845-852.
 21. Martens RJ, Vink H, van Oostenbrugge RJ, Staals J (2013) Sublingual Microvascular Glycocalyx Dimensions in Lacunar Stroke Patients. *Cerebrovasc Dis* 35: 451-454.
 22. Lambert J, Stehouwer CD (1996) Modulation of endothelium-dependent, flow-mediated dilatation of the brachial artery by sex and menstrual cycle. *Circulation* 94: 2319-2320.
 23. Khairoun M, de Koning EJ, van den Berg BM, Lievers E, de Boer HC, et al. (2013) Microvascular damage in type 1 diabetic patients is reversed in the first year after simultaneous pancreas-kidney transplantation. *Am J Transplant* 13: 1272-1281.
 24. Goedhart PT, Khalilzade M, Bezemer R, Merza J, Ince C (2007) Sidestream Dark Field (SDF) imaging: a novel stroboscopic LED ring-based imaging modality for clinical assessment of the microcirculation. *Opt Express* 15: 15101-15114.
 25. Constantinescu A, Spaan JA, Arkenbout EK, Vink H, Vanteffelen JW (2011) Degradation of the endothelial glycocalyx is associated with chylomicron leakage in mouse cremaster muscle microcirculation. *Thromb Haemost* 105: 790-801.
 26. Vlahu CA, Lemkes BA, Struijk DG, Koopman MG, Krediet RT, et al. (2012) Damage of the Endothelial Glycocalyx in Dialysis Patients. *Journal of the American Society of Nephrology*.
 27. Fiedler U, Reiss Y, Scharpfenecker M, Grunow V, Koidl S, et al. (2006) Angiotensin-2 sensitizes endothelial cells to TNF- α and has a crucial role in the induction of inflammation. *Nat Med* 12: 235-239.
 28. David S, Kumpers P, Hellpap J, Horn R, Leitolf H, et al. (2009) Angiotensin 2 and cardiovascular disease in dialysis and kidney transplantation. *Am J Kidney Dis* 53: 770-778.
 29. Khairoun M, van der Pol P, de Vries DK, Lievers E, Schlagwein N, et al. (2013) Renal ischemia/reperfusion induces a dysbalance of angiotensins, accompanied by proliferation of pericytes and fibrosis. *Am J Physiol Renal Physiol*.
 30. de Vries DK, Khairoun M, Lindeman JH, Bajema IM, de Heer E, et al. (2013) Renal Ischemia-Reperfusion Induces Release of Angiotensin-2 From Human Grafts of Living and Deceased Donors. *Transplantation*.
 31. Boehme MW, Deng Y, Raeth U, Bierhaus A, Ziegler R, et al. (1996) Release of thrombomodulin from endothelial cells by concerted action of TNF- α and



- neutrophils: in vivo and in vitro studies. *Immunology* 87: 134-140.
32. Aso Y, Inukai T, Takemura Y (1998) Mechanisms of elevation of serum and urinary concentrations of soluble thrombomodulin in diabetic patients: possible application as a marker for vascular endothelial injury. *Metabolism* 47: 362-365.
 33. Rehm M, Bruegger D, Christ F, Conzen P, Thiel M, et al. (2007) Shedding of the endothelial glycocalyx in patients undergoing major vascular surgery with global and regional ischemia. *Circulation* 116: 1896-1906.
 34. Chappell D, Jacob M, Paul O, Rehm M, Welsch U, et al. (2009) The glycocalyx of the human umbilical vein endothelial cell: an impressive structure ex vivo but not in culture. *Circ Res* 104: 1313-1317.
 35. Bartlett AH, Hayashida K, Park PW (2007) Molecular and cellular mechanisms of syndecans in tissue injury and inflammation. *Mol Cells* 24: 153-166.
 36. Grundmann S, Fink K, Rabadzhieva L, Bourgeois N, Schwab T, et al. (2012) Perturbation of the endothelial glycocalyx in post cardiac arrest syndrome. *Resuscitation* 83: 715-720.
 37. Sallisalmi M, Tenhunen J, Yang R, Oksala N, Pettila V (2012) Vascular adhesion protein-1 and syndecan-1 in septic shock. *Acta Anaesthesiol Scand* 56: 316-322.
 38. Svennevig K, Kolset SO, Bangstad HJ (2006) Increased syndecan-1 in serum is related to early nephropathy in type 1 diabetes mellitus patients. *Diabetologia* 49: 2214-2216.
 39. Nieuwdorp M, Mooij HL, Kroon J, Atasever B, Spaan JA, et al. (2006) Endothelial glycocalyx damage coincides with microalbuminuria in type 1 diabetes. *Diabetes* 55: 1127-1132.
 40. Broekhuizen LN, Lemkes BA, Mooij HL, Meuwese MC, Verberne H, et al. (2010) Effect of sulodexide on endothelial glycocalyx and vascular permeability in patients with type 2 diabetes mellitus. *Diabetologia* 53: 2646-2655.
 41. Martinez M, Vaya A, Alvarino J, Barbera JL, Ramos D, et al. (1999) Hemorheological alterations in patients with chronic renal failure. Effect of hemodialysis. *Clin Hemorheol Microcirc* 21: 1-6.



6

Deeper penetration of erythrocytes into the endothelial glycocalyx is associated with impaired microvascular perfusion

PLoS One 9: e96477, 2014.

Dae Hyun Lee¹; Martijn J.C. Dane¹; Bernard M. van den Berg¹; Margien G.S. Boels¹; Jurgen W. van Teeffelen³; Renée de Mutsert²; Martin den Heijer²; Frits R. Rosendaal²; Johan van der Vlag⁴; Anton Jan van Zonneveld¹; Hans Vink³; Ton J. Rabelink¹; for the NEO study group.

¹*Department of Nephrology and Einthoven laboratory for Vascular Medicine, Leiden University Medical Center, the Netherlands.* ²*Department of Clinical Epidemiology, Leiden University Medical Center, the Netherlands.* ³*Department of Physiology and Glycocheck, Maastricht University Medical Center, the Netherlands.* ⁴*Department of Nephrology, Nijmegen Centre for Molecular Life Sciences, Radboud University Nijmegen Medical Centre, Nijmegen, the Netherlands.*

Abstract

Changes in endothelial glycocalyx are one of the earliest changes in development of cardiovascular disease. The endothelial glycocalyx is both an important biological modifier of interactions between flowing blood and the vessel wall, and a determinant of organ perfusion. We hypothesize that deeper penetration of erythrocytes into the glycocalyx is associated with reduced microvascular perfusion. The population-based prospective cohort study (the Netherlands Epidemiology of Obesity [NEO] study) includes 6,673 middle-aged individuals (oversampling of overweight and obese individuals). Within this cohort, we have imaged the sublingual microvasculature of 915 participants using sidestream darkfield (SDF) imaging together with a recently developed automated acquisition and analysis approach. Presence of RBC (as a marker of microvascular perfusion) and perfused boundary region (PBR), a marker for endothelial glycocalyx barrier properties for RBC accessibility, were assessed in vessels between 5 and 25 μ m RBC column width. A wide range of variability in PBR measurements, with a mean PBR of 2.14 μ m (range: 1.43- 2.86 μ m), was observed. Linear regression analysis showed a marked association between PBR and microvascular perfusion, reflected by RBC filling percentage (regression coefficient β : -0.034; 95% confidence interval: -0.037 to -0.031). We conclude that microvascular beds with a thick (“healthy”) glycocalyx (low PBR), reflects efficient perfusion of the microvascular bed. In contrast, a thin (“risk”) glycocalyx (high PBR) is associated with a less efficient and defective microvascular perfusion.

Introduction

Cardiovascular disease is the leading cause of death in developed countries and one of the earliest changes in the pathogenesis of cardiovascular disease is microvascular dysfunction [1]. Within the inner vessel wall, a luminal endothelial glycocalyx is strategically located to continuously interact with the flowing blood. This endothelial glycocalyx is a thick gel-like meshwork of proteoglycans, glycosaminoglycans and plasma proteins; it functions as an important biological modifier in the interaction between the blood and the vessel wall [2,3]. Degradation and modification of the endothelial glycocalyx is, therefore, thought to be one of the earliest changes occurring in the pathogenesis of vascular disease [4,5]. For example, the endothelial glycocalyx exerts an anti-inflammatory and anti-thrombotic role by covering various glycoprotein adhesion receptors for leukocytes [6] and platelets [7]. Also, the endothelial glycocalyx has a protective role against protein leakage, as shown by our group previously, when selective degradation of endothelial glycocalyx with hyaluronidase led to glomerular albumin leakage [4].

Another function of the endothelial glycocalyx has been proposed to be the regulation of microvascular perfusion. The concept that the glycocalyx contributes to the regulation of microvascular perfusion was originally hypothesized by the group of Duling in 1990 when they showed that the adenosine-induced increase in capillary tube hematocrit in hamster cremaster muscle vessels was diminished after enzymatic glycocalyx degradation [8]. Further evidence for the role of the glycocalyx in regulation of functional microvascular perfusion has subsequently been gathered [9-13]. Changes in glycocalyx composition have been demonstrated to result in a decrease of shear-dependent nitric oxide (NO)-mediated arteriolar vasodilation [14], to decrease functional capillary density [15] and to induce platelet- and leukocyte adhesion in microvessels [6,7,16]; all effects that potentially affect microvascular perfusion. Loss of microvascular perfusion is a principal process in chronic organ failure, including heart, kidney and vascular dementia. The central concept is that endothelial (EC) activation turns pericytes into myofibroblasts, resulting in loss of capillaries, tissue hypoxia and subsequent organ fibrosis. However, there is currently no data on the relation between health of the endothelial glycocalyx and microvascular perfusion regulation in man.

Of the several methods to measure glycocalyx health *in vivo*, we have utilized the property of the endothelial glycocalyx to function as a barrier to maintain a certain distance between red blood cells (RBC) and the endothelial cell membrane [17-19]. To determine the spatio-temporal variation in radial displacement of individual RBCs into the endothelial glycocalyx in microvessels we used sidestream darkfield (SDF) imaging. SDF imaging is a non-invasive technique which visualizes hemoglobin within the RBC by reflected light emitting diode (LED) light from the microvasculature [20]. With this technique, it has been shown that the RBCs (diameter of 7 to 8 μ m) maintain a certain distance from the endothelium of capillaries (diameter of 5 μ m), which was postulated to be due to the barrier function of the glycocalyx against the RBC [19]. Using SDF imaging,



we imaged the longitudinal and radial distribution of RBC in sublingual microvessels to obtain information about the in vivo endothelial glycocalyx barrier properties in humans [21]. This concept has recently been tested in various patient groups with cardiovascular disease or risk factors, such as end-stage renal disease [17,21], stroke [18], premature coronary artery disease [22] and critically ill patients (septic and non-septic)[23], in which it was indicated that a perturbed glycocalyx allowed the erythrocytes to penetrate deeper towards the endothelium, resulting in an increase in the perfused boundary region (PBR). In addition to the lateral RBC movements, the longitudinal presence of RBCs (along known as vascular segments per surface area) is measured, allowing a simultaneous examination of the glycocalyx exclusion properties and the microvascular spatio-temporal RBC perfusion. We hypothesized that impaired glycocalyx barrier properties in the sublingual microcirculation is associated with changes in microvascular perfusion capacity in the general population.

Methods

Study Design and study population

We performed a cross-sectional analysis among participants recruited for the Netherlands Epidemiology of Obesity (NEO) study [24] to examine the association between endothelial glycocalyx integrity and microvascular perfusion. The NEO study is a population-based, prospective cohort study of 6,673 individuals aged between 45 and 65 years, with oversampling of overweight and obese individuals, to study pathways that lead to obesity-related diseases for a better understanding of the mechanisms underlying development of disease in obesity. Detailed information about the study design and data collection has been described previously [24]. Men and women aged between 45 and 65 years with a self-reported BMI of 27 kg/m² or higher and living in the greater area of Leiden (in the west of the Netherlands) were eligible to participate in the NEO study. In addition, all inhabitants aged between 45 and 65 years from one municipality (Leiderdorp, the Netherlands) were invited, irrespective of their BMI, allowing for a reference BMI distribution. SDF imaging was performed in a random subgroup of 937 participants from the 1394 participants who were included from January 2012 to October 2012. The study was carried out in accordance with the Declaration of Helsinki. Approval was obtained from the Committee of Medical Ethics of Leiden University Medical Center and all participants gave written informed consent.

General Measurements

Prior to the NEO study visit, participants completed a questionnaire about demography, lifestyle and medical history and fasted for at least 10 hours. Participants came to the research site in the morning to undergo several baseline measurements including anthropometric measurements, and blood sampling. Hemoglobin (Hb) was measured by the SLS hemoglobin detection method and hematocrit (Hct) by the RBC cumulative pulse height detection method with a Sysmex XE-2100 system (Sysmex, UK). Extensive physical examination was conducted, including anthropometry and blood pressure measurements. Blood pressure was measured three times in a seated position on the right arm with a 5 minutes resting interval using a validated automatic oscillometric device (OMRON, Model M10-IT, Omron Health Care Inc., IL, USA). Prehypertension and hypertension were diagnosed according to JNC 7 criteria [25].

Imaging of microcirculation

Intravital microscopy was performed at bedside with a SDF camera (MicroVision Medical Inc., Wallingford, PA) to visualize the sublingual microvasculature. The SDF camera uses green light emitting diodes (540nm) to detect the hemoglobin of passing RBC. The images were captured using a 5x objective with a 0.2 NA (numerical aperture), providing a 325- fold magnification in 720 x 576 pixels (tissue dimension: 950 X 700µm; tissue area: 0.665mm²) at 23 frames per second.



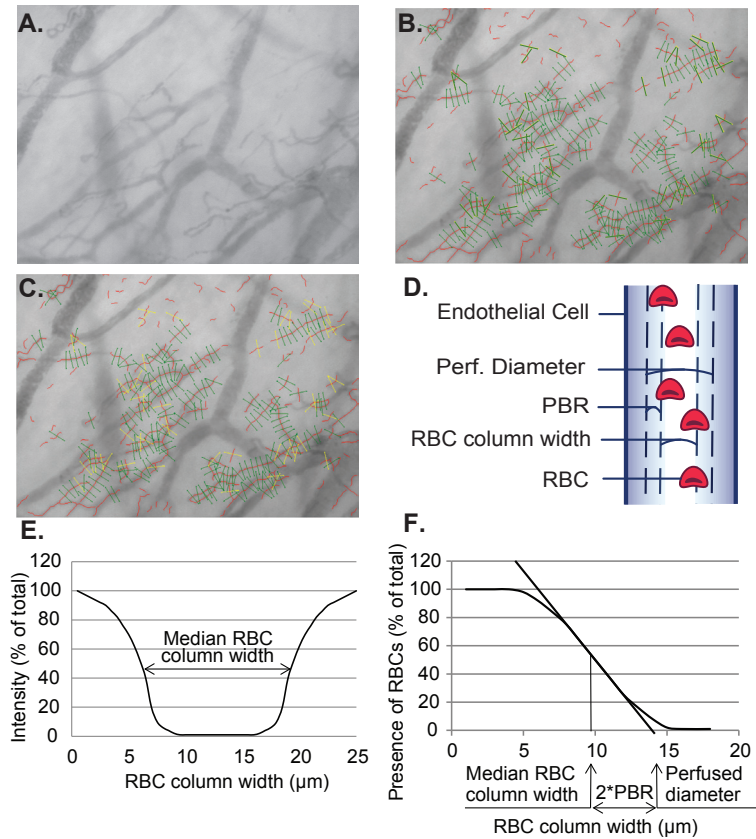


Figure 1: Glycocheck algorithm on endothelial PBR determination and microvascular perfusion properties. A) Red blood cells (RBC) are detected through reflection of light emitting diodes by hemoglobin. Images captured by the sidestream darkfield camera are sent to the computer for quality checks and assessment. The black contrast is the perfused lumen of the vessels. B) In each recording, the software automatically places the vascular segments (green), every $10\mu\text{m}$ along the vascular segments (black contrast). C) After the acquisition, for the analysis, the software undergoes several quality check in the first frame of each recording (see text), to select vascular segments with sufficient quality for further analysis. Invalid vascular segments (yellow) are distinguished from the valid vascular segments (green). During the whole recording session of 40 frames, the percentage of time in which a particular valid vascular segment has RBCs present is used to calculate RBC filling percentage. D) Depiction of the concept of glycocalyx thickness by lateral RBC movement is shown here. E) For each vascular segment, the intensity profile is calculated to derive median RBC column width. F) Then, the distribution of RBC column width is used to calculate the perfused diameter, median RBC column width, and subsequently the perfused boundary region (PBR).

The system makes up to 840 measurements of the width of the RBC column at a specific site. These individual width measurements are obtained after 8-fold pixel size interpolations of the corresponding radial intensity profiles, allowing detection of small changes in width between individual width measurements as small as $0.1\mu\text{m}$, which translates in accuracy of estimates of boundary layer of approximately $0.05\mu\text{m}$. The image acquisition is automatically mediated through the Glycocheck software (Glycocheck BV, Maastricht, the Netherlands) (**Figure 1**. for illustration of software algorithm). It detects the dynamic lateral RBC movement into the glycocalyx, which is expressed as the perfused boundary region (PBR, in μm). Therefore, a perturbed or degraded glycocalyx would allow more RBCs to penetrate deeper towards the endothelial surface, which is reflected by an increase in PBR (**figure 1d**). The method of calculating the PBR has been used and validated in various publications [17,18,21-23].

In short, the software automatically identifies all available measurable micro-vessels (below $30\mu\text{m}$ thickness) during the acquisition by contrast between the RBC and the background, in focus and without movement of the imaging unit (raw data in **figure 1a**). With this, it places vascular segments every $10\mu\text{m}$ along the length of these vessels. Subsequently, a sequence of 40 frames is recorded containing, on average, 300 major vascular segments (depicted as green lines in **figure 1b**). Next, the observer moves the camera to a different location to record another 40 frames, until a minimum total of 3,000 vascular segments are placed. After acquisition, the software undergoes a series of quality checks to only measure vascular segments that are of good quality. First, on the first frame of each recording session, ten line markers are placed every $0.5\mu\text{m}$ along each side of the vascular segments (total of 21 line markers). Only those that have sufficient contrast on more than 60% of the 21 line markers of each vascular segment are considered a valid vascular segment (green lines in **figure 1c**), in contrast to the invalid vascular segment (yellow lines in **figure 1c**). Since all vascular segments are placed every $10\mu\text{m}$, the length of perfused microvascular length can be expressed by multiplying $10\mu\text{m}$ and the number of valid vascular segments per area of tissue visualized (valid microvascular density). For the second quality check, during the measurement of RBC column widths for all 40 frames of recording session, the software screens for minimal RBC width, position of RBC column and the signal-to-noise ratio. At this step, the software calculates the percentage of vascular segments with RBC present during all 40 frames of the recording session, to determine the RBC filling percentage. Both the valid microvascular density and the RBC filling percentage were used as an estimate for the microvascular perfusion. For the last quality check, the curve fit for calculating the median RBC column widths is tested also for irregularities (**figure 1e**). Thus, after all these quality checks, those that fulfill these criteria are subject to analysis for the radial distribution of RBC, as a measurement of glycocalyx function.

For each vascular segment, the dynamic lateral position of RBCs (per RBC column width) is determined. The intensity profiles of the distribution of RBC column widths are used to calculate a cumulative distribution. From this distribution, the median RBC column



width is obtained while a linear regression analysis of the RBC column width is performed to derive the perfused diameter (the X-axis intercept of the extrapolated regression line) is calculated (**figure 1f**). Then, the PBR is defined as the distance between RBC column width and perfused diameter and is calculated using the equation, $([\text{Perfused diameter} - \text{median RBC column width}] / 2)$. Next, the calculated PBR values, classified according to their corresponding RBC column width between 5 – 25 μm , are averaged to provide a single PBR value for each participant.

Statistical Analysis

In the NEO study there is an oversampling of persons with a BMI of 27 kg/m² or higher. For the present study, to correctly represent associations in the general population,[26] adjustments for the oversampling of individuals with a BMI ≥ 27 kg/m² were made. This was done by weighting individuals towards the BMI distribution of participants from the Leiderdorp municipality, whose BMI distribution was similar to the BMI distribution of the general Dutch population [26]. All results were based on weighted analyses. Consequently, results apply to a population-based study without an oversampling of BMI ≥ 27 kg/m². Participants with unsuccessful measurements through SDF imaging (including participants with incomplete recording sessions (less than 10; n=16) and abnormal video images, such as consistent presence of air bubbles (n=6), all PBR outlier values), preventing correct analysis were excluded (n=22). In the end, 915 participants were included in the analysis of data. Baseline characteristics of the population were expressed as mean (\pm standard deviation [SD]), median (interquartile range), or as percentage. We performed linear regression analysis to investigate the associations of perfused boundary region with RBC filling percentage and valid microvascular density, while adjusting for age and sex. All statistical analyses were performed using SPSS version 20.0 (Chicago, IL), STATA Statistical Software (Statacorp, College Station, Texas) and GraphPad version 5.0 (GraphPad Prism Software Inc., San Diego, CA). A p-value <0.05 was defined as statistically significant.

Results

General clinical characteristics

The clinical characteristics of individuals with measured SDF are shown in **Table 1**. All participants were between 45 to 65 year old. Of all participants, 42% were lean, 42% were overweight, and 16.0% were obese. The mean systolic blood pressure was 131mmHg (S.D.: 16mmHg) and diastolic blood pressure was 83mmHg (S.D.: 10mmHg), with 36% with hypertension.

Table 1. General Clinical Characteristics

	Total (n=915)
Gender (% of male/ female)	46/ 54
Age (year)	56.1± 6.0
BMI (kg/m ²)	26.4±4.2
Hb (mmol/L)	8.71 ± 1.1
Hct	0.41 ± 0.12
Hypertension (%)	33.5%
Systolic BP (mmHg)	131.0±16.2
Diastolic BP (mmHg)	83.2±9.7

Hb, hemoglobin; Hct, hematocrit; BP, blood pressure. Data is presented as mean ± standard deviation.

Determination of microcirculatory properties

From the RBC column width and perfused diameter, perfused boundary region was calculated to derive the glycocalyx barrier function (**Table 2**, #1 to #3). Overall, the mean PBR was 2.14µm with a wide range of variability (range: 1.43- 2.86µm) (**table 2**). Despite the wide distribution of PBR in our cohort, there was a difference in PBR between men and women (mean: 2.09µm and 2.18µm, respectively). In addition to the glycocalyx barrier function by means of PBR, microvascular perfusion outcomes were calculated, resulting in a mean valid microvascular density of 3213µm/mm² (**table 2**, #5) and a mean RBC filling percentage of 73.2% (**table 2**, #6). In other words, there is 3246µm of perfused microvessels per mm² of tissue area which was in 73.2% positive for the presence of RBCs at a given time point during the 40 frames of video recording.



Table 2. Sidestream darkfield imaging derived variables characteristics.

#	Parameter	Total	Men	Women
1	RBC Column width (µm)	10.56 ± 1.12	10.74 ± 1.10	10.41 ± 1.11
2	Perfused diameter (µm)	14.84 ± 1.18	14.92 ± 1.19	14.77 ± 1.17
3	Perfused boundary region (µm)	2.14 ± 0.25	2.09 ± 0.24	2.18 ± 0.25
4	Total microvascular density (µm/mm ²)	4314±882	4223±821	4391±924
5	Valid microvascular density (µm/mm ²)	3213±691	3144±627	3272±736
6	RBC filling (%)	73.2 ± 5.0	74.0 ± 4.8	72.4 ± 5.0

Data is presented as mean ± standard deviation.

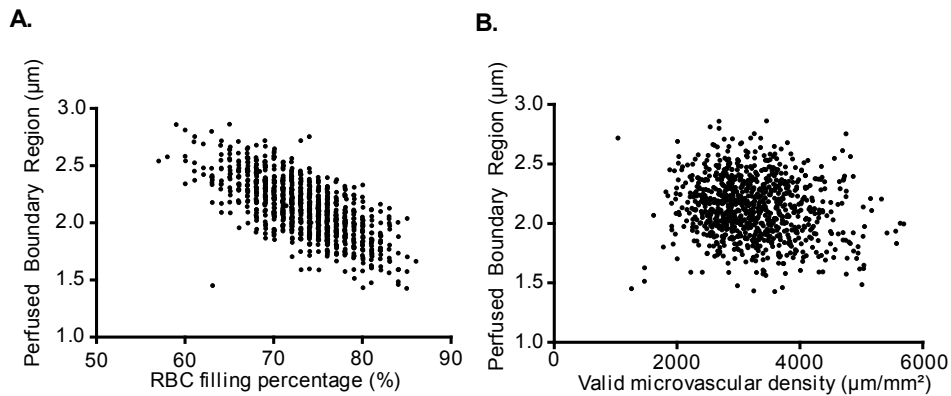


Figure 2. Scatterplot between PBR and outcomes of microvascular perfusion. The perfused boundary region (PBR), a measurement for glycocalyx accessibility to red blood cells (RBC), is associated significantly with spatio-temporal aspects of microvascular perfusion variables: A) RBC filling percentage (percentage of time in which a particular vascular segment is perfused) B) Valid microvascular density. In particular, lower PBR (less accessible glycocalyx, thus a better and thicker glycocalyx) is associated with higher RBC filling percentage (temporal perfusion).

Association of the glycocalyx barrier properties with microcirculatory perfusion

To test the hypothesis whether impaired glycocalyx barrier properties are associated with impaired microvascular perfusion, we examined the association between PBR and the two used estimates for microvascular perfusion (**table 3 and figure 2**). Of the two microvascular perfusion outcomes, RBC filling percentage was associated with PBR (regression coefficient β : -0.034; 95% CI: -0.037 to -0.031) and explained 47% of variability of perfused boundary region (R^2 : 0.475, $p < 0.001$). The valid microvascular density was also associated with PBR but explained the variability of PBR to a lesser extent (R^2 : 0.030), although still significant. Examples of video-clips obtained from participants with different PBR values and corresponding changes in microvascular perfusion are shown in Supplemental Video 1 and 2 (high and low PBR, respectively).

Table 3. Linear regression analysis show association between perfused boundary region and microvascular perfusion parameters.

Independent variable *	Regression coefficient β	r-Square	95% CI for coefficient β^{\dagger}	
			Lower Bound	Upper Bound
RBC filling percentage	-0.034	0.475	-0.037	-0.031
+Age, sex, BMI ‡	-0.034	0.482	-0.036	-0.031
Valid micro-vascular density §	-0.054	0.02	-0.083	-0.025
+Age, sex, BMI ‡	-0.059	0.06	-0.087	-0.030

* Dependent variable: Perfused boundary region (PBR)

† 95% confidence interval for regression coefficient β

‡ Linear regression analysis adjusted for age, sex and BMI

§ Valid microvascular density expressed as millimeter of microvessel length per mm^2 of area of tissue (mm/mm^2) for linear regression analysis due to difference in scale from PBR.



Discussion

We have measured the RBC accessibility into the endothelial glycocalyx, i.e. perfused boundary region (PBR) together with RBC filling percentage and valid microvascular density in the sublingual microvasculature of over 900 participants recruited for the NEO study.

In this study we observed a strong association between changes in endothelial glycocalyx properties (PBR) and estimates of microvascular perfusion in the sublingual microcirculation (**Figure 2 and Table 3**). The strongest association existed between PBR and RBC filling percentage, which represents the microvascular perfusion changes over time.

The mechanically stable gel-like layer on the endothelial surface limits the area in which RBCs and large plasma proteins are distributed (RBC exclusion properties of glycocalyx), which is reflected by a low PBR (**figure 3a**). An earlier observation of individual RBC in capillaries showed that compression of the RBCs by intact glycocalyx result in more elongated RBCs (7-8 μ m length and 3-4 μ m width), and therefore a more efficient and faster passage of these RBCs [19]. Also, this would lead to increased RBC longitudinal passage, allowing more oxygen exchange capacity.

The relation between PBR and vascular perfusion has been studied, however, in a variety of different physiological stimulants, such as by exercise, nitroglycerine, adenosine or insulin [9,10,22]. For instance, nitroglycerine challenge in a healthy population led to an increase in PBR and a recruitment of reserve capacity, further arguing that in a healthy state of acute physiological need, the glycocalyx has the potential to become more porous to facilitate the increased metabolic demand [10]. With such transient stimuli, both PBR and perfusion increases, leading to a temporary local increase in oxygen/ nutrient exchange. Therefore the observed variation in PBR and its correlation with perfusion could theoretically be explained by this dynamic regulation. Nonetheless, we have performed our measurements in a strictly controlled environment (e.g. overnight fasting, resting for more than 15 minutes, exclusion of caffeine and smoking). Thus, the observed variation in PBR and clear negative correlation (**figure 2b**) with the microvascular perfusion would argue for differences in vascular health in our population.

Therefore, in an unhealthy vascular state, PBR increase (reflecting increased outward penetration of RBC) together with decreased RBC filling percentage and functional microvascular density, reflects poor perfusion (**figure3b**). When the glycocalyx is degraded for a prolonged time, protein extravasation increases with subsequent edema formation [4,27], and a reduction in nitric oxide bioavailability [14], all together leading to endothelial dysfunction and perfusion defects [10,15].

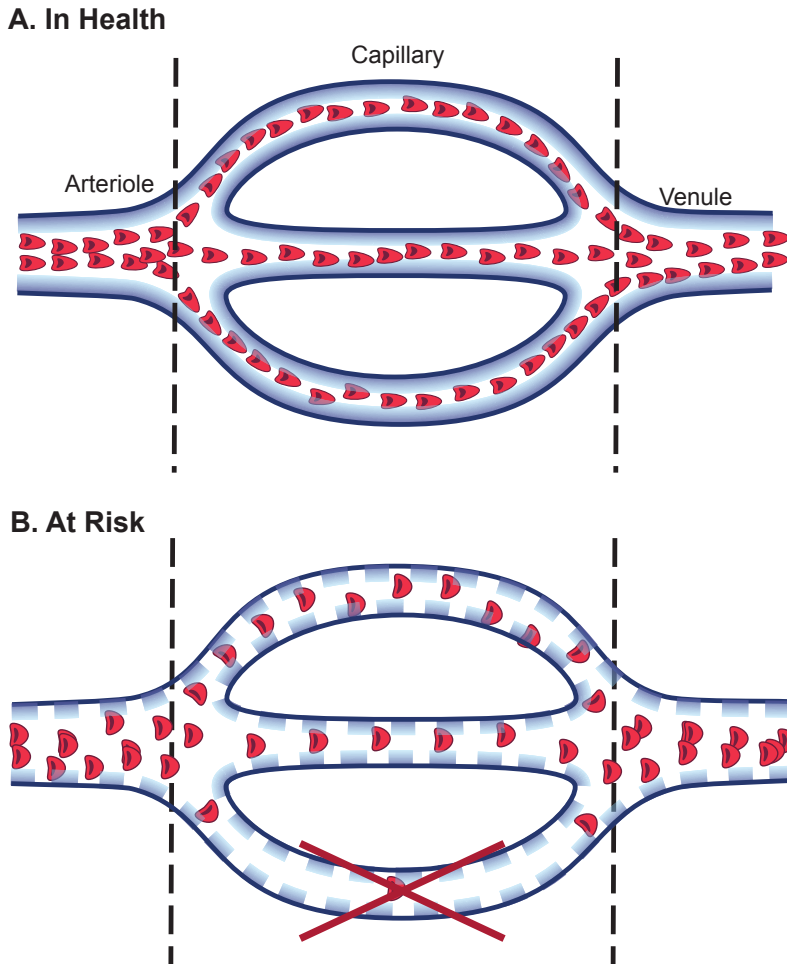


Figure 3. Schematic illustration on relation between glycocalyx accessibility and microvascular perfusion. A) Healthy state: Intact glycocalyx prevents red blood cells (RBC, red dots) from penetrating into its domain, reflected by a low perfused boundary region (PBR), and nicely aligned elongated RBC. The vessels are well perfused (higher tube hematocrit of microvessel and elongated shape of erythrocyte) resulting in a higher percentage of vessel segments with RBC present at any particular time point (high RBC filling percentage). B) Risk State: Altered composition of glycocalyx (lined dots) allows RBCs to penetrate deeper into the glycocalyx, closer to the anatomical border of lumen (endothelium), reflected by the high PBR. Due to the widening of RBC distribution width and volume, there is more space in between each RBC, as shown by decreased RBC filling percentage (less positive contrast per vascular segment per time point). Also, prolonged state of glycocalyx degradation leads to edematous and non-functioning vessels, leading to shorter vessel density per area of tissue (reduced valid microvascular density in risk PBR), depicted by the loss of bottom vessel.



For instance, in patients with diabetes, there is increased hyaluronidase activity [28], which probably decreases glycocalyx volume and functional capillary density [15,28,29]. The increase in distance between RBCs (reflected by low RBC filling percentage) might be due to both RBC changes into a wider shape [19] and more intravascular volume in which RBC could distribute. Ultimately, these changes lead to slow, diffuse and inefficient perfusion [30], as schematically depicted in **figure 3**.

Variability in the width of the RBC column, and thus PBR could theoretically also decrease to lower values when the glycocalyx layer becomes very thin. However, it is empirically and consistently found in all available and known (clinical) data, that PBR progressively increases with the severity of disease and glycocalyx damage. The most striking increases in PBR are found in critically diseased patients with severe septic shock in the ICU (unpublished data), who are supposed to have shed off the glycocalyx [6,23]. In these subjects the level of PBR increase correlates directly with mortality and cardiovascular organ complications. It therefore appears that relatively infrequent deeper penetration of RBCs into the layer during degradation / damage of glycocalyx precedes the radial outside movement of the majority of the RBCs in the RBC column, resulting in increases in PBR on top of potential increases in median width of the RBC column. Moreover, in the present study, we performed the measurements in a large group of relative healthy participants, making the loss of glycocalyx in the microvasculature also a relative unlikely event.

A question obviously is, whether glycocalyx assessment of the sublingual microcirculation is representative for glycocalyx dimensions in other tissues. Glycocalyx thickness and functional properties may indeed differ substantially from one organ to another [31]. However, as with other measurements of endothelial function, systemic factors will affect representative functional endothelial changes throughout the circulation. For example, using the SDF technique we and others have shown that sublingual vascular changes correlate with changes in the microvasculature of gastric, renal and nervous system organs [17,18,21,32-38]. In addition, we have shown in diabetic subjects that glycocalyx dimensions correlated with systemic glycocalyx volume changes [28]. Also, changes in the sublingual PBR in patients with coronary artery disease or stroke imply that local microvascular abnormalities indeed reflect changes in the systemic microvasculature [18,22].

During the past few years, there have been several methodological advances introduced in estimating glycocalyx dimensions. In the past, SDF glycocalyx dimensions were calculated as the difference in RBC column width before (functionally perfused capillary diameter) and after (anatomical capillary diameter) leukocyte passage [28,39]. Thereby, it measures the transient change in thickness due to leukocyte- induced compression of the glycocalyx. These previous measurements have shown reduced glycocalyx dimensions in various cardiovascular diseases such as diabetes [28,29], obesity [39], and hypercholesterolemia [40].

Manually capturing leukocyte passages for a longer time period and analyzing the results is, however, a labor intensive process. In addition, it is subject to investigator bias. The current method of SDF imaging we have used, which detects the dynamic changes in the erythrocyte movements, acquires and analyses the recordings in an unbiased, fully automated fashion.

While this technique estimates the glycocalyx thickness and microvascular perfusion non-invasively and automatically, it does have its limitations. First, the SDF camera only detects RBCs. Therefore, the perfused diameter and PBR is not the anatomical diameter of the vessel or the thickness of the anatomical glycocalyx, respectively. Nonetheless, by measuring the distribution of RBCs in a dense spatio-temporal manner, the software measures the location of the RBCs and can thereby statistically calculate the perfused diameter and PBR. In addition, we have recently validated that the measurement for PBR reflects actual anatomical glycocalyx damage, as shown by reduced distance between endothelial cell and RBC after hyaluronidase treatment using intravital microscopy [21]. Second, by visualizing the spatio-temporal location of the RBCs, the software estimates the microvascular perfusion by how often a certain vascular segment has a passing RBC. However, conventional outcome of perfusion variables includes RBC velocity or the anatomical microvascular density in a tissue [32]. Also, during the acquisition of approximately 2 seconds, the software cannot detect the vessel if there are no RBCs passing through. Therefore, it cannot visualize all vessels.

In conclusion, SDF imaging of the mucosal microvasculature in an adjusted subgroup of participants recruited for the NEO study, to represent associations in a general population, showed a wide range of variability in RBC accessibility to the glycocalyx, which was negatively associated with microvascular perfusion. This means that with a thick (“healthy”) glycocalyx (reflected by a low PBR) there is efficient perfusion of the microvascular bed. In contrast, a thin (“risk”) glycocalyx (reflected by a high PBR) is associated with less efficient and perturbed perfusion. The strong, and until now unknown, correlations of PBR with microvascular perfusion in man, indicate that values of PBR might allow us to report on relations between these parameters during follow up of these subjects, and relate it to future cardiovascular risk. This is clinically very relevant as microvascular rarefaction is a principal process in development of chronic organ failure.



Acknowledgements

We express our gratitude to all individuals who participate in the Netherlands Epidemiology in Obesity (NEO) study. We are grateful to all participating general practitioners for inviting eligible participants. The authors would like to thank Christa Broekhuizen, Vera van der Slot and Kimberly de Koning (Department of Epidemiology, Leiden University Medical Center) for data collection; Ingeborg de Jonge (Department of Epidemiology, Leiden University Medical Center) for helpful database management; all research nurses for collecting the data; Dr. Marku Mallat (Department of Nephrology, Leiden University Medical Center) for helpful statistical advice. The NEO study group: Frits R. Rosendaal, Renée de Mutsert, Saskia Middeldorp, Ton J. Rabelink, Johannes W.A. Smit, Johannes A. Romijn, Klaus F. Rabe, J. Wouter Jukema, Albert de Roos, Saskia le Cessie, Pieter S. Hiemstra, Margreet Kloppenburg, Ton W.J. Huizinga, Hanno Pijl, Jouke T. Tamsma, Eelco J.P. de Koning, Pim J.J. Assendelft, Pieter H. Reitsma, Ko Willems van Dijk, Aiko P.J. de Vries, Hildo J. Lamb, Ingrid M. Jazet, Olaf M. Dekkers, Nienke R. Biermasz, Christa M. Cobbaert (Leiden University and Medical Center, Leiden, the Netherlands), Martin den Heijer, Jacqueline M. Dekker and Brenda W. Penninx (VU Medical Center, Amsterdam, The Netherlands).

Reference

1. Deanfield JE, Halcox JP, Rabelink TJ (2007) Endothelial function and dysfunction: testing and clinical relevance. *Circulation* 115: 1285-1295.
2. Reitsma S, Slaaf DW, Vink H, van Zandvoort MA, oude Egbrink MG (2007) The endothelial glycocalyx: composition, functions, and visualization. *Pflugers Arch* 454: 345-359.
3. Weinbaum S, Tarbell JM, Damiano ER (2007) The structure and function of the endothelial glycocalyx layer. *Annu Rev Biomed Eng* 9: 121-167.
4. Dane MJC, van den Berg BM, Avramut MC, Faas FGA, van der Vlag J, et al. (2013) Glomerular Endothelial Surface Layer Acts as a Barrier against Albumin Filtration. *American Journal of Pathology* 182: 1532-1540.
5. Rabelink TJ, de Boer HC, van Zonneveld AJ (2010) Endothelial activation and circulating markers of endothelial activation in kidney disease. *Nat Rev Nephrol* 6: 404-414.
6. Schmidt EP, Yang Y, Janssen WJ, Gandjeva A, Perez MJ, et al. (2012) The pulmonary endothelial glycocalyx regulates neutrophil adhesion and lung injury during experimental sepsis. *Nat Med* 18:1217.
7. Reitsma S, Oude Egbrink MG, Heijnen VV, Megens RT, Engels W, et al. (2011) Endothelial glycocalyx thickness and platelet-vessel wall interactions during atherogenesis. *Thromb Haemost* 106: 939-946.
8. Desjardins C, Duling BR (1990) Heparinase treatment suggests a role for the endothelial cell glycocalyx in regulation of capillary hematocrit. *Am J Physiol* 258: H647-654.
9. Eskens BJM, Mooij HL, Cleutjens JPM, Roos JMA, Cobelens JE, et al. (2013) Rapid Insulin-Mediated Increase in Microvascular Glycocalyx Accessibility in Skeletal Muscle May Contribute to Insulin-Mediated Glucose Disposal in Rats. *Plos One* 8: e55399.
10. VanTeeffelen JW, Brands J, Vink H (2010) Agonist-induced impairment of glycocalyx exclusion properties: contribution to coronary effects of adenosine. *Cardiovasc Res* 87: 311-319.
11. Brands J, Spaan JA, Van den Berg BM, Vink H, VanTeeffelen JW (2010) Acute attenuation of glycocalyx barrier properties increases coronary blood volume independently of coronary flow reserve. *Am J Physiol Heart Circ Physiol* 298: H515-523.
12. Vink H, Duling BR (2000) Capillary endothelial surface layer selectively reduces plasma solute distribution volume. *Am J Physiol Heart Circ Physiol* 278: H285-289.
13. VanTeeffelen JW, Dekker S, Fokkema DS, Siebes M, Vink H, et al. (2005) Hyaluronidase treatment of coronary glycocalyx increases reactive hyperemia but not adenosine hyperemia in dog hearts. *Am J Physiol Heart Circ Physiol* 289: H2508-2513.
14. Mochizuki S, Vink H, Hiramatsu O, Kajita T, Shigeto E, et al. (2003) Role of hyaluronic acid glycosaminoglycans in shear-induced endothelium-derived nitric oxide release. *Am J Physiol Heart Circ Physiol* 285: H722-726.
15. Cabrales P, Vazquez BY, Tsai AG, Intaglietta M (2007) Microvascular and capillary perfusion following glycocalyx degradation. *J Appl Physiol* 102: 2251-2259.
16. Constantinescu AA, Vink H, Spaan JA (2003) Endothelial cell glycocalyx modulates



- immobilization of leukocytes at the endothelial surface. *Arterioscler Thromb Vasc Biol* 23:1541-1547.
17. Vlahu CA, Lemkes BA, Struijk DG, Koopman MG, Krediet RT, et al. (2012) Damage of the endothelial glycocalyx in dialysis patients. *J Am Soc Nephrol* 23: 1900-1908.
 18. Martens RJ, Vink H, van Oostenbrugge RJ, Staals J (2013) Sublingual microvascular glycocalyx dimensions in lacunar stroke patients. *Cerebrovasc Dis* 35: 451-454.
 19. Vink H, Duling BR (1996) Identification of distinct luminal domains for macromolecules, erythrocytes, and leukocytes within mammalian capillaries. *Circulation Research* 79: 581-589.
 20. Goedhart PT, Khalilzada M, Bezemer R, Merza J, Ince C (2007) Sidestream Dark Field (SDF) imaging: a novel stroboscopic LED ring-based imaging modality for clinical assessment of the microcirculation. *Opt Express* 15: 15101-15114.
 21. Dane MJ, Khairoun M, Lee DH, van den Berg BM, Eskens BJ, et al. (2014) Association of Kidney Function with Changes in the Endothelial Surface Layer. *Clin J Am Soc Nephrol*. doi: 10.2215/CJN.08160813
 22. Mulders TA, Nieuwdorp M, Stroes ES, Vink H, Pinto-Sietsma SJ (2013) Non-invasive assessment of microvascular dysfunction in families with premature coronary artery disease. *Int J Cardiol* 168: 5026-5028.
 23. Donati A, Damiani E, Domizi R, Romano R, Adrario E, et al. (2013) Alteration of the sublingual microvascular glycocalyx in critically ill patients. *Microvasc Res* 90: 86-89.
 24. de Mutsert R, den Heijer M, Rabelink TJ, Smit JW, Romijn JA, et al. (2013) The Netherlands Epidemiology of Obesity (NEO) study: study design and data collection. *Eur J Epidemiol* 28: 513-523.
 25. Chobanian AV, Bakris GL, Black HR, Cushman WC, Green LA, et al. (2003) Seventh report of the Joint National Committee on Prevention, Detection, Evaluation, and Treatment of High Blood Pressure. *Hypertension* 42: 1206-1252.
 26. Korn EL, Graubard BI (1991) Epidemiologic studies utilizing surveys: accounting for the sampling design. *Am J Public Health* 81: 1166-1173.
 27. van den Berg BM, Vink H, Spaan JA (2003) The endothelial glycocalyx protects against myocardial edema. *Circ Res* 92: 592-594.
 28. Nieuwdorp M, Mooij HL, Kroon J, Atasever B, Spaan JA, et al. (2006) Endothelial glycocalyx damage coincides with microalbuminuria in type 1 diabetes. *Diabetes* 55: 1127-1132.
 29. Broekhuizen LN, Lemkes BA, Mooij HL, Meuwese MC, Verberne H, et al. (2010) Effect of sulodexide on endothelial glycocalyx and vascular permeability in patients with type 2 diabetes mellitus. *Diabetologia* 53: 2646-2655.
 30. Edul VS, Enrico C, Laviolle B, Vazquez AR, Ince C, et al. (2012) Quantitative assessment of the microcirculation in healthy volunteers and in patients with septic shock. *Crit Care Med* 40: 1443-1448.
 31. Boels MG, Lee DH, van den Berg BM, Dane MJ, van der Vlag J, et al. (2013) The endothelial glycocalyx as a potential modifier of the hemolytic uremic syndrome. *Eur J Intern Med*.
 32. De Backer D, Hollenberg S, Boerma C, Goedhart P, Buchele G, et al. (2007) How to

- evaluate the microcirculation: report of a round table conference. *Crit Care* 11: R101.
33. Piagnerelli M, Ince C, Dubin A (2012) Microcirculation. *Crit Care Res Pract* 2012: 867176.
 34. Sallisalimi M, Oksala N, Pettila V, Tenhunen J (2012) Evaluation of sublingual microcirculatory blood flow in the critically ill. *Acta Anaesthesiol Scand* 56: 298-306.
 35. Pranskunas A, Pilvinis V, Dambrauskas Z, Rasimaviciute R, Planciuniene R, et al. (2012) Early course of microcirculatory perfusion in eye and digestive tract during hypodynamic sepsis. *Crit Care* 16: R83.
 36. Klijn E, Den Uil CA, Bakker J, Ince C (2008) The heterogeneity of the microcirculation in critical illness. *Clin Chest Med* 29: 643-654, viii.
 37. Verdant CL, De Backer D, Bruhn A, Clausi CM, Su F, et al. (2009) Evaluation of sublingual and gut mucosal microcirculation in sepsis: a quantitative analysis. *Crit Care Med* 37: 2875-2881.
 38. Creteur J, De Backer D, Sakr Y, Koch M, Vincent JL (2006) Sublingual capnometry tracks microcirculatory changes in septic patients. *Intensive Care Med* 32: 516-523.
 39. Nieuwdorp M, Meuwese MC, Mooij HL, Ince C, Broekhuizen LN, et al. (2008) Measuring endothelial glycocalyx dimensions in humans: a potential novel tool to monitor vascular vulnerability. *J Appl Physiol* 104: 845-852.
 40. Meuwese MC, Mooij HL, Nieuwdorp M, van Lith B, Marck R, et al. (2009) Partial recovery of the endothelial glycocalyx upon rosuvastatin therapy in patients with heterozygous familial hypercholesterolemia. *J Lipid Res* 50: 148-153.



7

Summary and general discussion

Function and assessment of the endothelial glycocalyx

The endothelial glycocalyx (EG) covers the endothelium throughout the whole vasculature. Its strategic location, between the circulating blood and the endothelium with its underlying tissue, points towards a potentially important functional role for the glycocalyx. The layer is involved in almost all functions of the endothelium; it contributes to the permeability barrier, it protects against coagulation and inflammation and is involved in NO regulation, shear sensing and cell-cell signaling. Perturbation of this gel-like layer is associated with inflammation and various vasculature-related pathologies. Moreover, since the endothelial glycocalyx is in direct contact with pathogenic factors (e.g. elevated glucose, increased lipids and disturbed shear stresses) it has been proposed to be one of the first casualties during endothelial activation [1]. Consequently, alterations within the EG are proposed to be an early risk marker for vascular dysfunction. Monitoring changes is therefore proposed to identify early risk for cardiovascular disease. However, since it is difficult to keep the structure in its original *in vivo* state, visualization of this EG remains challenging.

In this thesis we studied the endothelial glycocalyx using a variety of visualization techniques. We showed an overview of the current techniques to visualize the endothelial glycocalyx in Chapter 2. By stimulating endothelial cells with prolonged shear stress, we aimed to mimic an *in vivo* situation and thereby stimulate EG production. With lectins and GAG-specific antibodies, we visualized compositional and dimensional changes within the endothelial glycocalyx after prolonged flow culture.

In chapter 4 we used thick freshly isolated kidney slices, to diminish the influence of processing techniques on EG structure. After staining with lectins and endothelial markers, we quantified the luminal endothelial glycocalyx thickness and density. In addition, we used electronic microscopy in combination with cupromeronic blue, a compound that stabilizes and stains the EG. This enables visualization of the exact location of the endothelial glycocalyx in high detail and revealed the presence of dense endothelial glycocalyx plugs within the endothelial fenestrae. Moreover, it revealed a structurally heterogeneous glycocalyx on top of the endothelial layer, depending most likely both on endothelial phenotype and location.

In chapter 5 and 6 we used a relatively new technique to noninvasively detect changes in the red blood cell exclusion properties of the endothelial glycocalyx, reflected by the perfused boundary region (PBR). By monitoring the sublingual vasculature with SDF imaging in human participants, this technique can be used to evaluate microvascular health and perhaps even predict cardiovascular risk. With the current technique, changes in EG in severely diseased patients have been detected noninvasively [2-4].

Structure and composition of the endothelial glycocalyx

In vitro, the endothelial glycocalyx lacks much of its barrier function when compared to the in vivo situation [5,6]. Furthermore, endothelial glycocalyx dimension is reduced in vitro [7]. Endothelial cells in culture normally lack exposure to continuous blood flow and in vivo studies revealed that a disturbed blood flow is associated with glycocalyx perturbation [8-10], while continuous laminar shear stress has been proposed to be involved in endothelial glycocalyx production [11-14]. We set out to determine the effect of prolonged shear stress on the endothelial surface glycocalyx in culture in Chapter 3. Particularly, we have focused on the role of prolonged shear stress on the compositional and functional changes in the luminal endothelial glycocalyx. We therefore reconstructed the endothelial layer to a 3-dimensional image and specifically quantified the luminal endothelial glycocalyx staining.

To determine overall changes in the endothelial glycocalyx, we used the lectin wheat germ agglutinin (WGA). We observed an increase in WGA intensity and thickness and found a more homogenous distribution of the WGA staining on top of the endothelial layer. Previously, WGA staining on endothelial cells was decreased in a model of spontaneous kidney failure in aged rats [15]. Consequently, the observed increase of WGA staining upon prolonged exposure to flow most likely reflects an improved glycocalyx structure.

Within the endothelial glycocalyx, heparan sulfates (HS) play a crucial role in signal transduction from the vasculature to the endothelium and its underlying tissues. In particular, variation in HS disaccharide sequence and sulfation patterns determines binding properties for circulating proteins [16,17]. Consequently, HS are involved in many cellular processes such as attachment, migration, differentiation, blood coagulation, lipid metabolism, and inflammation [16]. Therefore we also investigated HS compositional changes in the glycocalyx. For this, we used the HS-antibodies 10E4 and JM403. 10E4 has been shown to need mixed HS domains, containing both N-acetylated and N-sulfated disaccharide units, for binding [18]. In contrast, JM403 binding to HS depends on the presence of N-unsubstituted glucosamine [19]. In our study we found a marked increase of JM403 staining after 1 days of culture under flow. This coincided with an increase of IL-8 gene expression. After 7 days of flow culture, the JM403 staining was hardly present. Since its presence is relatively rare it has been proposed that the N-unsubstituted glucosamine residues contribute to selective protein binding and therefore in biological and pathological cell processes [20]. This is supported by the finding that these N-unsubstituted HS domains have been demonstrated to be involved in L-selectin binding [21]. The observed decrease in JM403 binding therefore indicates a reduction in pro-inflammatory HS epitopes within the endothelial glycocalyx.

The decreased adhesion of monocytes after blocking the epitope for JM403 binding not only supports this hypothesis, but also suggests a direct involvement of this HS epitope in binding of inflammatory cells. This study shows that prolonged shear stress induces



an anti-inflammatory glycocalyx/HS phenotype. Moreover, it shows that endothelial glycocalyx composition is changed upon a shift in environment, which adds an extra layer of regulation to cell-cell communication by changing the binding capacity for specific signalling- or adhesion proteins. Consequently, modification of the endothelial glycocalyx is a highly interesting target to fine-tune receptor-ligand interactions on the endothelium. This definitely underlines the necessity for studying HS modifications in endothelial function.

The endothelial glycocalyx as a barrier in glomerular filtration

Within the glomerulus, the glomerular filtration barrier (GFB) is the main site for filtration in the kidney. The GFB consists of endothelium with its glycocalyx, a glomerular basement membrane (GBM) and podocytes. Although it is well established that every single layer contributes to the glomerular filtration barrier (GFB), the exact function of the separate layers is still unknown. As early as 1976, Ryan and Karnovsky demonstrated that plasma albumin does not pass the highly fenestrated endothelial layer of the glomerular capillary wall [22]. The observation that the endothelial fenestrae, which are big enough to allow protein passage, were filled with endothelial glycocalyx indicates that this glycocalyx functions as a first barrier within the GFB [23,24].

In chapter 4 we demonstrated a role for the endothelial glycocalyx and more specifically the subcomponent hyaluronan in the glomerular filtration barrier. We show that glomerular fenestrae are filled with dense negatively charged polysaccharide structures. Upon infusion of hyaluronidase, albumin passage across the endothelium can be observed in almost all the glomeruli. Such albumin passage was not observed for the control animals. In conclusion, in this study we have shown that the glomerular EG functions as a selective protein permeability barrier. In support of this, endothelial glycocalyx disruption by displacing non-covalently bound proteins has been demonstrated to result in an acute increase of albuminuria [25]. Moreover, glycosaminoglycan-degrading enzymes such as chondroitinase and heparinase have also been shown to alter the charge selectivity of the glomerular filter [26,27]. In addition, in aged Munich-Wistar-Fromter rats, albuminuria associates with endothelial glycocalyx loss.

Although we used a model to specifically determine the role of hyaluronan in the glomerular filtration barrier, it is tempting to speculate about the implications of glycocalyx damage in the development of renal failure. Based on the presented data we suggest that damage of the endothelial glycocalyx results in very early damage in the glomerular filtration barrier. Consequently, during diseases in which glomerular failure is observed, glycocalyx damage might be one of the first changes upon exposure to risk factors. In diabetes, for example, an increase in heparanase and hyaluronidase has been demonstrated, most likely as a consequence of increased levels of risk factors such as hyperglycemia, and hyperlipidemia [28-31]. Moreover, both hyperglycemia and diabetes

have been associated with a reduction in endothelial glycocalyx volume [32,33]. As shown in our model, the perturbation of the ESL within the glomerular filtration barrier leads to protein leakage and binding (/uptake) by podocytes. This could initiate inflammatory signalling and contribute to podocyte transformation and effacement, as was postulated by Morigi et al. [34], and matches early activation of podocytes observed in our model. When prolonging the time of damage it seems to be reasonable to expect accumulation of damage leading to changes in podocyte morphology. Eventually loss of podocyte morphology leads to a severely damaged glomerular filtration barrier. Based on this model, we propose that the endothelial glycocalyx is the first casualty during prolonged risk factor exposure. Both the subsequent activation of endothelial cells, as the passage of proteins over the filtration barrier, leads to a disturbed cell-cell signalling within the GFB which can result in activation of endothelial cells, podocytes and mesangium (**figure 1**). However, although albumin passes the filtration barrier during this stage, we hypothesize that albuminuria only develops when chronic activation results in structural damage, such as podocyte flattening, mesangial expansion and loss of endothelial fenestrae [35].

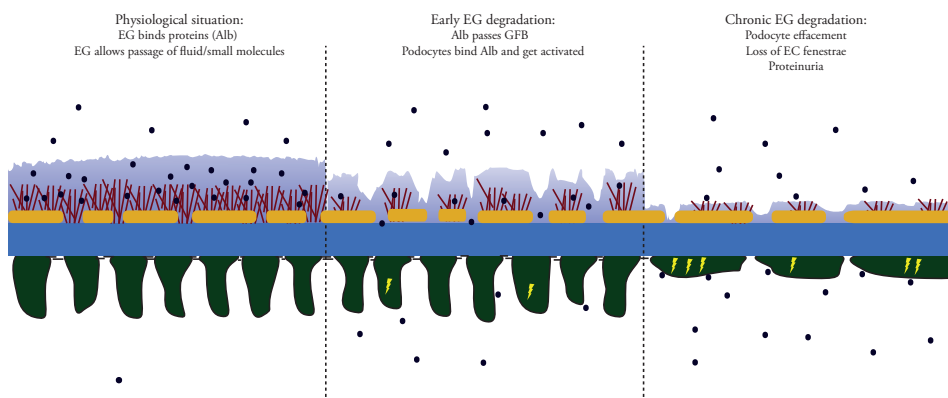


Figure 1: Schematic overview of the hypothesized mechanism of glomerular barrier failure. During a healthy situation the glycocalyx covers the glomerular endothelium and fills the fenestrae. Proteins, such as albumin, are adsorbed by the endothelial glycocalyx. In this way they form a barrier for circulating plasma proteins, which are consequently unable to cross the filtration barrier. In contrast, the gel-like glycocalyx allows passage of smaller molecules and fluids, thus facilitating glomerular filtration (left). During early endothelial glycocalyx modification and degradation, less protein can be bound and proteins can pass the filtration barrier. Here, proteins can bind to podocytes, parietal epithelial cells and tubular epithelial cells. These cells get activated as a result of binding and uptake of proteins (middle). Upon chronic EG degradation, proteins continuously pass the filtration barrier. As a result, podocytes are chronically activated and effacement will occur. Loss of the glomerular barrier structure will eventually result in large quantities of proteins passing the glomerular filtration barrier which leads to glomerular and kidney failure (right).



Summary and General Discussion

The observation that albuminuria in aged Munich Wistar Fromter rats associates with glycocalyx loss, suggests that widespread loss of the endothelial glycocalyx might link albuminuric kidney disease with systemic vascular dysfunction. Based on our data and these earlier studies, we propose that endothelial glycocalyx dysfunction is a central mediator in the development of both renal and cardiovascular failure [15,36]. This is supported by the Steno hypothesis, proposed by Deckert et al in 1989 [37]. In the Steno hypothesis, perturbation of the extracellular matrix, more specifically of the HS within this matrix, was proposed to be a key factor in the development of both renal failure and cardiovascular disease. We propose a revised hypothesis: Perturbation of the luminal extracellular matrix, thus endothelial glycocalyx, is the central mediator for the development of both renal and cardiovascular failure. More detailed studies, for example in a model in which one could follow both the development of glycocalyx damage as the effects on macrovascular- and renal pathologies in time, are of utmost importance to study this hypothesis. When this hypothesis can be supported by future studies, the endothelial glycocalyx might become a crucial target for therapeutics to prevent vascular damage and the subsequent risk for, among others, CVD and renal disease.

Estimating endothelial glycocalyx changes in patients using SDF imaging

As discussed in chapter 2, it is difficult to measure glycocalyx dimensions in patients. Until recently, shed syndecan-1 has been used, since glycocalyx shedding (e.g. in inflammatory conditions) is thought to contribute to plasma levels of soluble syndecan-1 [38]. However, the exact underlying mechanisms and dynamics of proteoglycan shedding and its link with various vascular pathologies are largely unknown, making it difficult to interpret this parameter. Moreover, the absence of shedding of one specific proteoglycan might not per definition mean that endothelial glycocalyx properties are unaltered. In chapter 5 we used and validated a newly developed technique to estimate endothelial glycocalyx changes in a fast and non-invasive manner. We used this automated, and easy to apply approach to measure the ability of RBC to penetrate the ESL, quantitatively defined as the perfused boundary region (PBR) [3,39]. Overall, measuring PBR shows to be an easier and less invasive method than measuring shed markers like syndecan and thrombomodulin. However, more studies are necessary to study the selectivity and sensitivity of the PBR as a marker for early vascular damage.

In chapter 5 we have shown that patients with an impaired kidney function have a larger PBR, which reflects a loss of endothelial surface layer dimensions. Also, ESL dimensions in patients with a stable kidney transplant were indistinguishable from healthy controls, while patients developing IFTA (Interstitial Fibrosis and Tubular Atrophy) revealed a larger PBR, i.e. ESL loss. These changes in PBR are reflected by the presence of the shed ESL components sTM and syndecan-1.

Previously, renal failure was shown to correlate with increased concentrations of shed hyaluronan [3], and release of the endothelium specific proteoglycan thrombomodulin coincides with diabetes and diabetic nephropathy [40,41]. Here, we showed that patients with renal failure have increased circulating levels of syndecan-1, which could be reversed by kidney transplantation. In addition a correlation between PBR, the glycocalyx shedding markers sTM and syndecan-1 and the endothelial activation marker Ang2 was observed. This also validates both glycocalyx measurements within this study.[42]

Plasma and serum biomarkers and PBR measurements corroborate the observation that loss of renal function is associated with endothelial activation and loss of ESL thickness. Furthermore, we show that we are able to discriminate between a group of participants with and without renal failure, thereby validating the PBR measurements. Although the causality still needs further study, the association of glycocalyx damage, renal failure and endothelial activation shown in this study further supports the earlier proposed role for endothelial glycocalyx perturbation as a central mediator in the development of both renal failure and CVD.

In Chapter 6, we set up a study to try to answer the question whether endothelial glycocalyx damage is predictive for the development of vasculature related pathologies. The NEO



study, described in this chapter, is a prospective cohort study of 6,673 individuals aged between 45 and 65 years, to study the mechanisms underlying the development of disease in obesity. Among others, we have estimated the ESL thickness in these participants as baseline measurement for future studies. Although in general this population is yet only at risk for cardiovascular disease, due to oversampling of BMI > 25, a high variation in PBR was observed. Nonetheless, no correlations with other known risk markers were observed, which might be explained by the observed high inter-individual variation. Future follow-up of this study cohort, allowing events to occur, should address whether PBR associates with the development of cardiovascular disease.

Within the baseline measurements of the NEO study we did observe an association between changes in endothelial glycocalyx properties (PBR) and estimates of microvascular perfusion in the sublingual microcirculation. The strongest association was observed between PBR and RBC filling percentage, which represents the microvascular perfusion changes over time. Although this population is only at risk for cardiovascular disease, the high variation in PBR and negative correlation of PBR with perfusion estimates might indicate the onset of the development of vascular dysfunction in a subset of these participants.

In conclusion, changes in the ESL have been postulated to associate with, and maybe even precede, vascular and renal damage [1]. In this thesis we confirm a correlation between glycocalyx dimensions, perfusion, renal failure and vascular activation. Because measuring PBR in the microcirculation is a non-invasive and fast method to assess changes in the ESL in patients, this is a promising new method for clinical monitoring of the systemic microvasculature. Furthermore, follow-up of the NEO study cohort should address whether PBR associates with, or might even predict the development of cardiovascular disease.

Conclusion and future perspectives

The endothelial glycocalyx is a highly interactive matrix that facilitates protein-protein and protein-receptor interactions and thereby serves as a key modifier of endothelial function. Both structural dimension as well as biochemical composition determines its properties as a bioactive scaffold.

The structure and modifications of carbohydrates are highly complex and exceed the complexity of proteins and genes. Studying glycocalyx composition has proven very challenging due to the structural fragility and the complex sugar biochemistry involved. However, modern imaging technology, as discussed in this thesis, opens up opportunities to take the glycocalyx into account when studying vascular and renal physiology. While it is still technically impossible to unequivocally chemically characterize HS and HA variability, most of our knowledge on disaccharide modification - function relationships needs to be derived from experiments where enzymes that edit the chemical composition of the glycocalyx are conditionally knocked out. The development of new methods to study the exact structure and composition of this luminal endothelial glycocalyx is therefore of key importance to obtain more insight in the endothelial glycocalyx function.

Together with earlier published data [43], our data in chapter 4 and 5 points towards a central role for endothelial glycocalyx perturbations in the development of both cardiovascular disease and renal failure. Consequently, the role of endothelial glycocalyx damage in development of vascular related pathologies needs to be further studied. The development of the SDF camera might enable us to study glycocalyx perturbations in large cohorts. For now, structural dimensions of the glycocalyx have been measured using SDF imaging in severely diseased patients [3,44,45]. However, to be able to detect early glycocalyx damage and thus predict the development of cardiovascular disease, further development and optimization of this technique is required.

Altogether, development of further insight in structure-function relationships of the glycocalyx will create new perspectives in our understanding of physiology and provide opportunities to innovate medicine. Development of technological innovations that enable the further interrogation and the modulation of glycocalyx function will prove to be a critical success factor.



References

1. Rabelink TJ, de Boer HC, van Zonneveld AJ (2010) Endothelial activation and circulating markers of endothelial activation in kidney disease. *Nat Rev Nephrol* 6: 404-414.
2. Donati A, Damiani E, Domizi R, Romano R, Adrario E, et al. (2013) Alteration of the sublingual microvascular glycocalyx in critically ill patients. *Microvasc Res*.
3. Vlahu CA, Lemkes BA, Struijk DG, Koopman MG, Krediet RT, et al. (2012) Damage of the endothelial glycocalyx in dialysis patients. *J Am Soc Nephrol* 23: 1900-1908.
4. Mulders TA, Nieuwdorp M, Stroes ES, Vink H, Pinto-Sietsma SJ (2013) Non-invasive assessment of microvascular dysfunction in families with premature coronary artery disease. *Int J Cardiol* 168: 5026-5028.
5. Potter DR, Damiano ER (2008) The hydrodynamically relevant endothelial cell glycocalyx observed in vivo is absent in vitro. *Circ Res* 102: 770-776.
6. Smith ML, Long DS, Damiano ER, Ley K (2003) Near-wall micro-PIV reveals a hydrodynamically relevant endothelial surface layer in venules in vivo. *Biophys J* 85: 637-645.
7. Chappell D, Jacob M, Paul O, Rehm M, Welsch U, et al. (2009) The glycocalyx of the human umbilical vein endothelial cell: an impressive structure ex vivo but not in culture. *Circ Res* 104: 1313-1317.
8. van Thienen JV, Fledderus JO, Dekker RJ, Rohlena J, van Ijzendoorn GA, et al. (2006) Shear stress sustains atheroprotective endothelial KLF2 expression more potently than statins through mRNA stabilization. *Cardiovasc Res* 72: 231-240.
9. Dekker RJ, van Thienen JV, Rohlena J, de Jager SC, Elderkamp YW, et al. (2005) Endothelial KLF2 links local arterial shear stress levels to the expression of vascular tone-regulating genes. *Am J Pathol* 167: 609-618.
10. Dekker RJ, van Soest S, Fontijn RD, Salamanca S, de Groot PG, et al. (2002) Prolonged fluid shear stress induces a distinct set of endothelial cell genes, most specifically lung Kruppel-like factor (KLF2). *Blood* 100: 1689-1698.
11. Ebong EE, Lopez-Quintero SV, Rizzo V, Spray DC, Tarbell JM (2014) Shear-induced endothelial NOS activation and remodeling via heparan sulfate, glypican-1, and syndecan-1. *Integr Biol (Camb)* 6: 338-347.
12. Koo A, Dewey CF, Jr., Garcia-Cardena G (2013) Hemodynamic shear stress characteristic of atherosclerosis-resistant regions promotes glycocalyx formation in cultured endothelial cells. *Am J Physiol Cell Physiol* 304: C137-146.
13. Gouverneur M, Spaan JA, Pannekoek H, Fontijn RD, Vink H (2006) Fluid shear stress stimulates incorporation of hyaluronan into endothelial cell glycocalyx. *Am J Physiol Heart Circ Physiol* 290: H458-452.
14. Bai K, Wang W (2013) Shear stress-induced redistribution of the glycocalyx on endothelial cells in vitro. *Biomech Model Mechanobiol*.
15. Salmon AH, Ferguson JK, Burford JL, Gevorgyan H, Nakano D, et al. (2012) Loss of the endothelial glycocalyx links albuminuria and vascular dysfunction. *J Am Soc Nephrol* 23:1339-1350.
16. Esko JD, Selleck SB (2002) Order out of chaos: assembly of ligand binding sites in heparan sulfate. *Annu Rev Biochem* 71: 435-471.
17. Rops AL, Jacobs CW, Linssen PC, Boezeman JB, Lensen JF, et al. (2007) Heparan sulfate

- on activated glomerular endothelial cells and exogenous heparinoids influence the rolling and adhesion of leucocytes. *Nephrol Dial Transplant* 22: 1070-1077.
18. van den Born J, Salmivirta K, Henttinen T, Ostman N, Ishimaru T, et al. (2005) Novel heparan sulfate structures revealed by monoclonal antibodies. *J Biol Chem* 280: 20516-20523.
 19. van den Born J, Gunnarsson K, Bakker MA, Kjellen L, Kusche-Gullberg M, et al. (1995) Presence of N-unsubstituted glucosamine units in native heparan sulfate revealed by a monoclonal antibody. *J Biol Chem* 270: 31303-31309.
 20. Wei Z, Deakin JA, Blaum BS, Uhrin D, Gallagher JT, et al. (2011) Preparation of heparin/ heparan sulfate oligosaccharides with internal N-unsubstituted glucosamine residues for functional studies. *Glycoconj J* 28: 525-535.
 21. Norgard-Sumnicht K, Varki A (1995) Endothelial heparan sulfate proteoglycans that bind to L-selectin have glucosamine residues with unsubstituted amino groups. *J Biol Chem* 270:12012-12024.
 22. Ryan GB, Karnovsky MJ (1976) Distribution of endogenous albumin in the rat glomerulus: role of hemodynamic factors in glomerular barrier function. *Kidney Int* 9: 36-45.
 23. Rostgaard J, Qvortrup K (2002) Sieve plugs in fenestrae of glomerular capillaries--site of the filtration barrier? *Cells Tissues Organs* 170: 132-138.
 24. Rostgaard J, Qvortrup K (1997) Electron microscopic demonstrations of filamentous molecular sieve plugs in capillary fenestrae. *Microvasc Res* 53: 1-13.
 25. Friden V, Oveland E, Tenstad O, Ebefors K, Nystrom J, et al. (2011) The glomerular endothelial cell coat is essential for glomerular filtration. *Kidney Int* 79: 1322-1330.
 26. Jeansson M, Haraldsson B (2003) Glomerular size and charge selectivity in the mouse after exposure to glucosaminoglycan-degrading enzymes. *J Am Soc Nephrol* 14: 1756-1765.
 27. Jeansson M, Haraldsson B (2006) Morphological and functional evidence for an important role of the endothelial cell glycocalyx in the glomerular barrier. *Am J Physiol Renal Physiol* 290: F111-116.
 28. Ikegami-Kawai M, Suzuki A, Karita I, Takahashi T (2003) Increased hyaluronidase activity in the kidney of streptozotocin-induced diabetic rats. *J Biochem* 134: 875-880.
 29. Gil N, Goldberg R, Neuman T, Garsen M, Zcharia E, et al. (2012) Heparanase is essential for the development of diabetic nephropathy in mice. *Diabetes* 61: 208-216.
 30. Wijnhoven TJ, van den Hoven MJ, Ding H, van Kuppevelt TH, van der Vlag J, et al. (2008) Heparanase induces a differential loss of heparan sulphate domains in overt diabetic nephropathy. *Diabetologia* 51: 372-382.
 31. Garsen M, Rops AL, Rabelink TJ, Berden JH, van der Vlag J (2014) The role of heparanase and the endothelial glycocalyx in the development of proteinuria. *Nephrol Dial Transplant* 29: 49-55.
 32. Nieuwdorp M, van Haefen TW, Gouverneur MC, Mooij HL, van Lieshout MH, et al. (2006) Loss of endothelial glycocalyx during acute hyperglycemia coincides with endothelial dysfunction and coagulation activation in vivo. *Diabetes* 55: 480-486.
 33. Nieuwdorp M, Mooij HL, Kroon J, Atasever B, Spaan JA, et al. (2006) Endothelial glycocalyx damage coincides with microalbuminuria in type 1 diabetes. *Diabetes* 55: 1127-1132.
 34. Morigi M, Buelli S, Angioletti S, Zanchi C, Longaretti L, et al. (2005) In response



- to protein load podocytes reorganize cytoskeleton and modulate endothelin-1 gene: implication for permselective dysfunction of chronic nephropathies. *Am J Pathol* 166: 1309-1320.
35. Pavenstadt H, Kriz W, Kretzler M (2003) Cell biology of the glomerular podocyte. *Physiol Rev* 83: 253-307.
 36. Salmon AH, Satchell SC (2012) Endothelial glycocalyx dysfunction in disease: albuminuria and increased microvascular permeability. *J Pathol* 226: 562-574.
 37. Deckert T, Feldt-Rasmussen B, Borch-Johnsen K, Jensen T, Kofoed-Enevoldsen A (1989) Albuminuria reflects widespread vascular damage. The Steno hypothesis. *Diabetologia* 32:219-226.
 38. Bartlett AH, Hayashida K, Park PW (2007) Molecular and cellular mechanisms of syndecan in tissue injury and inflammation. *Mol Cells* 24: 153-166.
 39. Martens RJ, Vink H, van Oostenbrugge RJ, Staals J (2013) Sublingual microvascular glycocalyx dimensions in lacunar stroke patients. *Cerebrovasc Dis* 35: 451-454.
 40. Iwashima Y, Sato T, Watanabe K, Ooshima E, Hiraishi S, et al. (1990) Elevation of plasma thrombomodulin level in diabetic patients with early diabetic nephropathy. *Diabetes* 39:983-988.
 41. Oida K, Takai H, Maeda H, Takahashi S, Tamai T, et al. (1990) Plasma thrombomodulin concentration in diabetes mellitus. *Diabetes Res Clin Pract* 10: 193-196.
 42. Dane MJ, Khairoun M, Lee DH, van den Berg BM, Eskens BJ, et al. (2014) Association of kidney function with changes in the endothelial surface layer. *Clin J Am Soc Nephrol* 9: 698-704.
 43. Nagy N, Freudenberger T, Melchior-Becker A, Rock K, Ter Braak M, et al. (2010) Inhibition of hyaluronan synthesis accelerates murine atherosclerosis: novel insights into the role of hyaluronan synthesis. *Circulation* 122: 2313-2322.
 44. Dane MJC, van den Berg BM, Avramut MC, Faas FGA, van der Vlag J, et al. (2013) Glomerular Endothelial Surface Layer Acts as a Barrier against Albumin Filtration. *American Journal of Pathology* 182: 1532-1540.
 45. Lee DH, Dane MJ, van den Berg BM, Boels MG, van Teeffelen JW, et al. (2014) Deeper penetration of erythrocytes into the endothelial glycocalyx is associated with impaired microvascular perfusion. *PLoS One* 9: e96477.



8

Nederlandse samenvatting

Curriculum Vitae

List of publications

Dankwoord

Nederlandse samenvatting

In dit proefschrift staat de endotheliale glycocalyx centraal. Hoofdstuk 1 is een algemene introductie, waarin de compositie en functie van de glycocalyx algemeen in zowel alle vaten, als meer specifiek in de glomerulus van de nier beschreven wordt. De glycocalyx is een vaat-beschermende gel-achtige laag tussen het stromende bloed en de vaatwand. Deze laag bevat eiwitten met vele suikerketens, vandaar de naam glycocalyx, (glykys = zoet, kalyx = schil). Deze suikerketens kunnen eiwitten binden en deze zo efficiënter bij de specifieke receptor op de doelcel brengen, of juist ver van deze receptor houden. Wanneer de endotheelcel geactiveerd raakt, bijvoorbeeld tijdens ontstekingen, veranderen deze bindingsplaatsen zo dat andere eiwitten uit het bloed (bijvoorbeeld eiwitten die ontsteking bevorderen) hier kunnen binden en hun effect kunnen uitoefenen op de cel. Aangezien de endotheelcel continu in direct contact staat met het bloed, is de glycocalyx betrokken bij bijna alle functies van het endotheel. In eerdere studies is aangetoond dat de glycocalyx beschermt tegen ontsteking, stolling en de ontwikkeling van eiwitlekage. Een beschadigde glycocalyx kan daarom leiden tot hart en vaatziekten, maar ook tot (indirecte) schade in andere organen, zoals in de nier. In dit proefschrift hebben we de compositie van de endotheliale glycocalyx in endotheelcellen bestudeerd. Vervolgens hebben we meer specifiek de rol van de glycocalyx in de filterfunctie van de nier onderzocht. Uiteindelijk hebben we gekeken naar glycocalyx schade bij patiënten met nierfalen.

In Hoofdstuk 2 hebben we de huidige technieken voor het detecteren van de glycocalyx beschreven. Dit zijn vooral visualisatietechnieken zoals elektronenmicroscopie en fluorescentiemicroscopie. In dit hoofdstuk beschrijven we ook SDF visualisatie van de microcirculatie en daaropvolgende schatting van veranderingen in de dikte van de glycocalyx. Dit gebeurt door het meten van de zijwaartse verplaatsing van rode bloedcellen, die gevisualiseerd worden doordat hemoglobine (in rode bloedcellen) het licht van de SDF camera absorberen. Wanneer de glycocalyx beschadigd is, kunnen rode bloedcellen dichter bij het endotheel komen en zich dus verder zijwaarts verplaatsen. Het grote voordeel van deze techniek is dat het mogelijk is om de glycocalyx non-invasief te meten zonder de laag uit de in vivo omgeving te halen. Dit maakt het een veelbelovende techniek voor studies naar de mogelijkheid tot het gebruiken van glycocalyx schade als vroege marker voor vasculaire schade in patiënten. Voor meer specifieke studies naar de compositie en functie van de glycocalyx zijn microscopie en specifieke kleuringen echter nog steeds de best mogelijke techniek. De glycocalyx is echter een instabiele en dynamische laag, waardoor het lastig is deze laag intact te houden buiten het lichaam. Ondanks deze uitdagingen hebben de specifieke kleuringen geleid tot inzichten in de compositie en functie van de verschillende componenten in de glycocalyx.

In hoofdstuk 3 hebben we deze compositie en functie van de glycocalyx *in vitro* bestudeerd. In eerdere studies is gebleken dat de glycocalyx dunner en minder functioneel is in cellen die *in vitro* (buiten het lichaam) gekweekt zijn. Deze cellen missen vele factoren vergeleken met de in vivo (in het lichaam) situatie, waarvan stromend bloed een van de meest cruciale

is. Eerder was al beschreven dat endotheel cellen die gekweekt worden in een omgeving waarbij medium over de cellen stroomt meer lijken op de cellen in bloedvaten. In dit hoofdstuk laten wij zien dat de glycocalyx in de cellen waarover medium stroomt dikker en dichter is dan in cellen waarbij dit niet is gebeurd. Verder laten we zien dat binnen de glycocalyx specifieke eiwitbindingsplaatsen in de heparan sulfaten veranderen. Deze veranderingen zorgen ervoor dat de endotheellaag minder inflammatoire cellen bindt na een inflammatoire stimulus. In dit hoofdstuk laten we dus zien dat stromend bloed ervoor zorgt dat zowel de cellen als de glycocalyx meer gezonde kenmerken krijgen. Als gevolg zou je kunnen speculeren dat vaten met een verstoorde bloedflow (bijvoorbeeld op plaatsen waar atherosclerose plaats vindt) niet alleen een ongezonde endotheelcel maar ook een beschadigde glycocalyx hebben.

In hoofdstuk 4 hebben we de rol van de glycocalyx in de filterfunctie van de nier bestudeerd. Meer specifiek hebben we gekeken naar de rol van een van de suikercomponenten van de glycocalyx: hyaluronan. Wij denken dat de glycocalyx een barrière vormt voor grote eiwitten, terwijl het water en kleinere moleculen doorlaat. Op deze manier zorgt de glycocalyx ervoor dat belangrijke eiwitten en cellen in het bloed behouden blijven. Hyaluronan heeft een belangrijke functie in deze barrière. Het is namelijk al langer bekend dat een gel-achtige laag van hyaluronan makkelijker kleine dan grote stoffen doorlaat. Om dit te onderzoeken hebben we muizen een maand lang een constant infuus van kleine hoeveelheden hyaluronidase, een enzym wat hyaluronan afbreekt, gegeven. Vervolgens hebben we gekeken naar het effect op de glycocalyx en het effect op de filtratie barrière in de nier. Ten eerste zagen we dat vooral de glycocalyx in de fenestrae (gaten in de endotheelcellen waardoor vloeistoffen de filtratie barrière kunnen passeren) verdwenen was na behandeling met hyaluronidase. Hoewel we geen verhoging van albumine terug konden vinden in de urine, zagen we wel degelijk dat albumine de filtratie barrière gepasseerd was. Dit geeft aan dat de verstoring van de glycocalyx door het afbreken van hyaluronan leidt tot een verslechtering van de filtratie barrière. Ook zagen we dat albumine voorbij de filtratie barrière gebonden was aan podocyten, wat samenging met een lichte verhoging van schademarkers aan deze podocyten. Dit wekt de suggestie dat podocyten beschadigd raken, mogelijk doordat relatief grote hoeveelheden albumine gebonden worden. Deze data impliceert dat beschadiging van glycocalyx het begin in de ontwikkelin van uiteindelijke nierschade kan zijn. Dit kan bijvoorbeeld zo zijn bij de ontwikkeling van nierfalen als gevolg van suikerziekte, een ziekte waarin enkele studies aangetoond hebben dat de glycocalyx beschadigd raakt.

Vervolgens hebben we naar glycocalyx-schade als marker voor (beginnende) vaatschade gekeken. In hoofdstuk 5 hebben we de glycocalyx-dikte gemeten met de eerder beschreven SDF camera in patiënten voor en na een niertransplantatie. Hier zagen we een vermindering van de dikte van de glycocalyx in patiënten met nierfalen vergeleken met gezonde controles. Na succesvolle niertransplantatie was de glycocalyx weer hersteld naar waardes zoals gemeten in gezonde controles. Na een minder succesvolle transplantatie was dit herstel niet te zien. De met de SDF gemeten glycocalyx-diktes



correleerden met circulerende glyocalyx afbraak-markers (syndecan, sTM), endotheel-activatiemarkers (Ang-2) en markers voor nierschade (GFR). Dit geeft duidelijk aan dat samen met endotheel activatie, de endotheliale glyocalyx ook beschadigd is in patiënten met nierfalen. Aangezien verwacht wordt dat schade aan de glyocalyx vooraf gaat aan vasculair en mogelijk ook renaal falen, is het meten van de endotheliale glyocalyx met een SDF camera een veelbelovende manier om op een non-invasieve manier de vasculaire (glyocalyx) status te monitoren. Hoewel meer studies nodig zijn, zou het een manier kunnen zijn om het risico op cardiovasculair- en mogelijk zelfs nierfalen te voorspellen.

Een studie met als uiteindelijke doel om uit te zoeken of dit inderdaad mogelijk is, is beschreven in hoofdstuk 6. De hier beschreven NEO studie, bestaat uit personen met een gemiddeld tot hoge BMI. Op basis hiervan hebben deze personen een hoger risico op cardiovasculair falen. Hoofdstuk 6 beschrijft de studie en de eerste basismetingen van de glyocalyx met SDF. Uiteindelijk worden deze patiënten vervolgd, zodat mogelijke complicaties op kunnen treden en gekeken kan worden naar de voorspellende waarde van de SDF metingen. Hoewel deze data nog niet beschikbaar is, vonden we wel een interessante correlatie tussen glyocalyx dikte en de perfusie van de gemeten vaten. Ondanks dat we nog geen vervolgmetingen hebben kunnen doen, zou de combinatie van dunnere glyocalyx en verslechterde perfusie al een hint kunnen zijn richting aangetaste microvaten. Toekomstige data moet uitwijzen of dit inderdaad zo is en of vervolgens de schattingen van de glyocalyx dikte aan de hand van metingen met de SDF camera gebruikt kunnen worden om cardiovasculair risico te voorspellen en zo preventief in te kunnen grijpen bij ogenschijnlijk gezonde personen.

Hoofdstuk 7 is een samenvatting en uitgebreide interpretatie van de data die in dit proefschrift beschreven is.



Curriculum Vitae

The author of this thesis was born on September 21, 1986, in Roosendaal, the Netherlands. After completing secondary education, VWO, in 2004, he started with the bachelor study Molecular Life Sciences in Maastricht. He continued with the master Clinical Molecular Sciences in Maastricht. During this master he completed two research projects. The first internship was at the department of tumor immunology, a project about haploidentical NK cells as a treatment for breast cancer. The second one was at the department of physiology, a project about the role for the endothelial glycocalyx in regulation of insulin sensitivity. In 2009, after he received his M.Sc. in Clinical Molecular Sciences, he started as PhD student in the department of Nephrology, Leiden University Medical Centre, under the supervision of dr. van den Berg and prof. A.J. Rabelink and the department of Physiology, Maastricht University, under the supervision of dr. H. Vink. This PhD project was funded by the Dutch kidney foundation and was titled: Role of the endothelial glycocalyx in renal glomerular and tubular function. The obtained data resulted in several publications in peer-reviewed international scientific journals and are shown in this thesis. In March 2014 he worked on a project to study the role of the glycocalyx in vascular drug adhesion. From December 2014 on he started the training to become a clinical chemist at LabWest in the Haga Ziekenhuis in the Hague, the Netherlands.

List of Publications

A Microscopic view on the Renal Endothelial Glycocalyx

Martijn J.C. Dane, Bernard M. van den Berg, Dae Hyun Lee, Margien G.S. Boels, Gesa Tiemeier, M. Cristina Avramut, Anton Jan van Zonneveld, Johan van der Vlag, Hans Vink, Ton J. Rabelink

American Journal of Physiology Renal Physiology, 2014

The Endothelial Glycocalyx: Scratching the Surface for Cardiovascular Disease in Kidney Failure.

Martijn J.C. Dane, Bernard M. van den Berg, Ton J. Rabelink

Commentary in Atherosclerosis, 2014

Deeper Penetration of Erythrocytes into the Endothelial Glycocalyx is Associated with Impaired Microvascular Perfusion.

Dae Hyun Lee, **Martijn J.C. Dane**, Bernard M. van den Berg, Margien G. S. Boels, Jurgen W. van Teeffelen, Renee de Mutsert, Martin den Heijer, Frits R. Rosendaal, Johan van der Vlag, Anton Jan van Zonneveld, Hans Vink, Ton J. Rabelink, for the NEO study group.

PlosOne, 2014

Association of Kidney Function with Changes in the Endothelial Surface Layer.

Martijn J.C. Dane, Meriem Khairoun, Dae Hyun Lee, Bernard M. van den Berg, Bart J.M. Eskens, Margien G.S. Boels, Jurgen W.G.E. van Teeffelen, Angelique L.W.M.M. Rops, Johan van der Vlag, Anton Jan van Zonneveld, Marlies E.J. Reinders, Hans Vink, Ton J. Rabelink
Clinical Journal of the American Society of Nephrology, 2013

The Endothelial Glycocalyx as a Potential Modifier of the Hemolytic Uremic Syndrome.

Boels MG, Lee DH, van den Berg BM, **Dane MJC**, van der Vlag J, Rabelink TJ.

European Journal of internal medicine, 2013

Glomerular Endothelial Surface Layer acts a Barrier against Albumin Filtration.

Martijn J.C. Dane, Bernard M. van den Berg, M. Cristina Avramut, Frank G.A. Faas, Johan van der Vlag, Angelique L.W.M.M. Rops, Raimond B.G. Ravelli, Bram J. Koster, Anton Jan van Zonneveld, Hans Vink, Ton J. Rabelink

American Journal of Pathology, 2013



Dankwoord

Er zijn vanzelfsprekend veel mensen die ik wil bedanken. Op verschillende manieren heeft iedereen binnen de afdelingen Nierziekten en het Eindhoven Laboratorium een bijdrage geleverd aan dit proefschrift. Daarnaast is de samenwerking met de Pathologie, MCB en de Nefrologie in Nijmegen erg fijn geweest. Zonder jullie was dit proefschrift op zijn minst veel dunner geweest.

Ton, allereerst wil ik jou bedanken voor alle hulp en begeleiding gedurende het glycolalyx-onderzoek in Leiden. Ik heb gedurende mijn tijd in het LUMC veel van je geleerd over onderzoeks-opzet, gestructureerd schrijven en organisatie. Bernard, jou wil ik natuurlijk bedanken voor de ‘bevrijding’ uit Maastricht. Ik heb geen seconde spijt gekregen van mijn keuze om mee naar Leiden te gaan. Bedankt voor de dagelijkse begeleiding, het doorzetten van onderzoek wanneer ik al vroegtijdig teleurgesteld afgehaakt was en het delen van jouw kennis over ongeveer alles.

Hans, de afgelopen 10-15 jaar zijn glycolalyx en Hans Vink bijna synoniemen geworden. De communicatie tussen Maastricht en Leiden was soms wat lastig, maar natuurlijk wil ik je heel erg bedanken voor alle uitleg en discussie. Anton-Jan, bedankt voor het feit dat Bernard en ik met ons onbekende onderwerp (‘glycolalyx, wat is dat?’) zo gastvrij opgenomen zijn in jouw onderzoeksgroep. Jurgen, door jouw enthousiasme ben ik begonnen met een onderzoeksstage naar de glycolalyx bij de afdeling fysiologie in Maastricht. Ik weet nog dat ik 10 minuutjes langs zou komen voor wat informatie en uiteindelijk na 30 minuten een MRI-scanner voor proefdieren aan de andere kant van het gebouw stond te bekijken. Jurgen, Bart, bedankt!

Het LUMC: ik kwam er voor mijn eerste werkdag zonder er ooit geweest te zijn. Hier kwam ik terecht in de glycolalyx-groep, toen bestaande uit.. Bernard. Later kwamen er enkele geweldige collega’s bij! Cristina, bedankt voor je hulp met alle EM plaatjes. Het zijn de mooiste figuren in mijn proefschrift. Wendy bedankt voor alle hulp in het laatste jaar. DaeHyun! I really enjoyed working with you! Thanks for the coffeebreaks: and discussing our latest progress (or fungus, SDF and cell culture). Margien bedankt voor alles: hulp, discussie en gezelligheid binnen en buiten het lab. Johan, Angelique, ondanks de afstand tot Nijmegen voelde het alsof jullie ook binnen de ‘glycolalyx-groep’ Leiden hoorden: bedankt!

In het LUMC begon ik in een afgelegen hok in het midden van het ziekenhuis, waar dag, nacht of frisse lucht niet leken te bestaan. Gelukkig werd er door de vele kamergenoten voor gezorgd dat het er altijd gezellig was. Er was altijd wel iemand om frustratie of vooruitgang mee te delen. Hierdoor voelde het altijd alsof ik naar het LUMC kwam voor de gezelligheid... en om te werken. De alhier opgedane kennis en kunde door Escape-the-Room en Sporcle zijn onmisbaar gebleken voor mijn verdere carrière. Coen: bedankt voor alle diepgaande discussies over cruciale randzaken. Ik zie je nog wel een keer in New York! Eric, als jij begint te praten, blijf je praten: altijd gezellig! Ik mis onze maandagochtend bespreking al. Roel, door jou heb ik geleerd dat er ook goede Rotterdammers zijn... Mooi om op C7 dagelijks jouw goede slechte humor mee te maken. Ruben, jij staat altijd

voor iedereen klaar. Altijd fijn om met jou de vorderingen in en om het onderzoek te bespreken. Ik zie je op de tennisbaan! Hetty, bedankt voor alle hulp in en om het lab! Ik zal de bloedplaatjes nooit meer vergeten... Meriem, Annemarie, Janine, Marina, Jac, Marko, Danielle, Ellen, Nicole, Taya, Carolien, ChunYu, Jonna, Jurrien, Carla; bedankt! Natuurlijk geldt dit ook voor de rest van de afdeling nierziekten en het Einthoven lab: bedankt voor voor alle hulp en de gezelligheid de afgelopen jaren.

Paranimfen! Ties, ik ken je ondertussen al 'even'. Mede door jou ben ik bij dit onderwerp terecht gekomen en mede door jou mag ik dus ook dit proefschrift verdedigen. Een betere paranimf kan er voor mij dus niet zijn! Margien: Jij bent een echte versterking binnen onze groep gebleken! Fijn dat je naast mij wilt staan tijdens mijn verdediging!

Wouter, Marissa, Ingrid, Remco, opa's en oma's: Bedankt voor de interesse in mijn onderzoek en de steun gedurende de laatste 'ongeduldige' maanden van het schrijven van dit proefschrift! Pap, mam: hoewel voor jullie het grootste deel van dit proefschrift onbegrijpelijk al zijn wil ik jullie het meest bedanken. Dit is een opstapeling van jullie hulp, steun en alles wat jullie de afgelopen 28 jaar voor mij gedaan hebben. Dank daarvoor!

Liefste Manon: Jij hebt me het hele promotietraject gesteund en was er altijd voor me. Bedankt voor je begrip, geduld en liefde.



